

A comparison of the pore-forming
subunits of the ATP-sensitive
potassium channel

Thesis submitted for the degree of
Doctor of Philosophy
at University of Leicester

by

Andrew James Chadburn BSc
Department of Cardiovascular Sciences
University of Leicester

September 2009

Abstract

Andrew Chadburn – A comparison of the pore-forming subunit of the ATP-sensitive potassium channel

K_{ir}6.1 and K_{ir}6.2 display several key differences in characteristics e.g. K_{ir}6.2 can open spontaneously upon removal of inhibitory nucleotides while K_{ir}6.1 cannot. Residues responsible for some of these disparate properties have been mapped to the N-terminus of K_{ir}6.0. Mutant cDNAs for these subunits were created where amino acid(s) were taken from one isoform and replaced with the corresponding residue(s) from the other. The whole cell and inside-out patch clamp techniques were used to assess the current density, spontaneous opening, ATP sensitivity and unitary conductance of these mutant channels. All mutants showed similar current density to their parent channels, suggesting similar expression. One mutant, which exchanged residues 15-17 of K_{ir}6.2 (TRL) for ARI, had significantly lower conductance than wild type, possibly due to allosteric modulation of the conduction pathway. Simultaneous mutation of a group of residues from K_{ir}6.2 (S37A, K39S, N41A and V44L) reduced relative activation, a measure of spontaneous opening. However, mutation of these residues individually had no effect, suggesting that they interact to affect spontaneous opening in wild type channels.

14-3-3 are a family of chaperone and scaffold proteins shown to interact with several ion channels both functionally and during expression. 14-3-3 ϵ and ζ have been implicated in expression of K_{ATP} channels. To try and address the poor expression of K_{ir}6.1-based channels, 14-3-3 ϵ and ζ were co-expressed with K_{ATP} channels. No effect was seen with any 14-3-3 isoforms co-expressed with K_{ir}6.1. However, 14-3-3 ϵ significantly increased current density of K_{ir}6.2/SUR2A channels. Co-expression of 14-3-3 ϵ and ζ attenuated this effect. The disparate effects of different combinations of these 14-3-3 isoforms suggest that their dimerisation may play a role in the effect seen here.

Acknowledgements

Firstly, I would like to thank my supervisors Dr Dave Lodwick and Prof Nick Standen, without whom this work would never have been possible. I would like to wish Nick all the best in his recovery. I would particularly like to thank Dave for his help during the writing of this thesis and for never getting too upset or taking it too personally when Walsall whoop Brighton at football. For her help during the bad experimental times I would like to thank Dr Nina Storey for all her advice. I would like to thank Dr Noel Davies for answering all those annoying technical questions I bothered him with and for taking the time to comment on some of my writing. Thanks to Dr Richard Rainbow also for answering my annoying questions. Thanks to anyone who helped me in the lab. Undoubtedly I'd forget someone if I tried to list them all so I won't. Thank you all.

Thanks to Dr Anna Parker for putting up with sharing a flat with me for 3 argument free years. It was fun. Thanks to Steve "acceptable in the 80s" Thomson and Dr Conor "YOU BUY GOLD" McCloskey for giving me a roof when the money ran out and for being great drinking buddies. Thanks to Marie Valente for being ginger and for buying me food, putting up with my hairiness and grumpiness while I've been writing, and for generally being lovely..... but mostly for being ginger. Big thanks to all of my friends, PhD students and post-docs alike, especially for buying me drinks during the last year while I've had no money. I'm sure I'll pay you back some day. I'd like to thank my family for supporting me and always being there during these difficult four years. Thanks to my Mum for being one last proof-reader. Finally, I'd like to thank the British Heart Foundation for their generous funding. I spent it wisely, honest.

Contents

Abstract.....	ii
Acknowledgements	iii
Contents.....	iv
Abbreviations.....	vii
1 Introduction	2
1.1 Cells and their membranes	2
1.1.1 Membrane potentials	2
1.1.2 The resting membrane potential and its development.....	4
1.2 Ion channels	5
1.2.1 Selectivity	6
1.2.2 Sodium channels	6
1.2.3 Calcium channels.....	7
1.2.4 Chloride channels.....	7
1.3 The potassium channel family	8
1.3.1 Generalised potassium channel structure	9
1.3.2 Voltage-gated potassium channels.....	9
1.3.3 Calcium-activated potassium channels (K_{Ca}).....	10
1.3.4 Two pore potassium channels	10
1.3.5 Inwardly rectifying potassium channels (K_{ir}).....	11
1.4 ATP-sensitive potassium channel - K_{ATP}	12
1.4.1 Identification and structure	12
1.4.2 Assembly and trafficking	16
1.4.3 Physiological roles and distribution	18
1.4.3.1 K_{ATP} channels in the brain	19
1.4.3.2 K_{ATP} channels in the cardiovascular system.....	20
1.4.3.3 K_{ATP} channels in the pancreas.....	21
1.5 Properties of K_{ATP} channels	21
1.5.1 Biophysical properties.....	22
1.5.2 Regulation by endogenous molecules	25

1.5.2.1	Inhibition by ATP	25
1.5.2.2	Stimulation by nucleotide diphosphates.....	27
1.5.2.3	Activation by PIP ₂	29
1.5.3	Regulation by other proteins	30
1.5.4	Pharmacological regulation	31
1.6	K _{ATP} channel subunit knockouts	34
1.6.1	K _{ir} 6.1 ^{-/-}	34
1.6.2	K _{ir} 6.2 ^{-/-}	35
1.6.3	SUR1 ^{-/-}	36
1.6.4	SUR2 ^{-/-}	37
1.7	Aims of this study	37
2	Materials and methods.....	41
2.1	Molecular biology.....	41
2.1.1	Overlap polymerase chain reaction	41
2.1.2	Cloning Into expression vectors	46
2.1.3	Transforming Escherichia coli	47
2.1.4	Media	48
2.1.5	Agarose gel electrophoresis.....	49
2.2	Tissue culture	50
2.2.1	Maintenance of cell lines	51
2.2.2	Transfections.....	52
2.3	Electrophysiology	52
2.3.1	Patch clamp.....	52
2.3.2	Pulling electrodes.....	54
2.3.3	Whole cell patch clamp	54
2.3.3.1	Inside-out patch clamp.....	55
2.3.3.2	Patch clamp solutions.....	56
2.3.3.3	Patch clamp apparatus	57
2.3.4	Analysis.....	57
3	Characterisation of wild type K _{ATP} channels	62
3.1	Introduction	62
3.2	Results and discussion.....	63

3.2.1	Whole cell recordings.....	63
3.2.2	Single channel conductance of wild type channels	70
3.2.3	ATP sensitivity of $K_{ir}6.2/SUR2A$	71
3.2.4	Conclusion	73
4	Construction and characterisation of mutant Kir6.0 subunits	75
4.1	Introduction	75
4.2	Production of mutant cDNA.....	78
4.2.1	Overlap PCR to produce mutant $K_{ir}6.0$ cDNA.....	79
4.2.2	Cloning mutant cDNA into Xenopus oocyte expression vector	86
4.2.3	Cloning mutant cDNA into mammalian expression vector.....	87
4.3	Characterisation of mutant channels.....	95
4.3.1	Whole cell recordings.....	95
4.3.2	Single channel current-voltage relationships	100
4.3.3	Spontaneous opening in the absence of intracellular ATP	103
4.3.4	ATP sensitivity	107
4.4	Discussion.....	110
5	The effect of 14-3-3 on K_{ATP} channels.....	129
5.1	Introduction	129
5.2	The effect of 14-3-3 on whole cell K_{ATP} currents.....	131
5.3	Discussion.....	135
6	Summary and Overall Discussion.....	140
6.1	Characterisation of Wild Type K_{ATP} Channels.....	140
6.2	Construction and Characterisation of Mutant $K_{ir}6.0$ Subunits	142
6.3	The Effect of 14-3-3 on K_{ATP} Channels.....	147
	Bibliography	149

Abbreviations

Å	angstrom
ABC protein	ATP binding cassette protein
ADP	adenosine diphosphate
AMP	adenosine monophosphate
ANOVA	analysis of variance
ATP	adenosine triphosphate
BNC1	brain sodium channel 1
bp	base pairs
Ca _v	voltage-gated calcium channel
cDNA	complementary DNA
CFTR	cystic fibrosis transmembrane conductor
CHO	Chinese hamster ovary
CIC	voltage-gated chloride channel
CMV	cytomegalovirus
COPI	coatamer protein 1
C-terminus	carboxy terminus
DNA	deoxyribonucleic acid
EDTA	ethylenediaminetetraacetic acid
EGFP	enhanced green fluorescent protein
EGTA	ethyleneglycoltetraacetic acid
E _k	potassium equilibrium potential
Epac	exchange protein activated by cAMP
ER	endoplasmic reticulum
EtBr	ethidium bromide
GABA _A	γ-aminobutyric acid _A receptor
GIRK	G-protein activated inwardly rectifying potassium channel
GTP	guanosine triphosphate
HEPES	4-(2-hydroxyethyl)-1-piperazineethanesulfonic acid
hERG	human ether-a-go-go related gene
IC ₅₀	concentration that causes 50% inhibition
IPC	ischemic preconditioning
K _{2P}	two pore potassium channel
K _{ATP}	ATP-sensitive potassium channel
kb	kilo-base pairs
K _{Ca}	calcium-activated potassium channel
KCO	potassium channel opener
K _{ir}	inwardly rectifying potassium channel

K _v	voltage-gated potassium channel
LB	Luria Bertani medium
mRNA	messenger ribonucleic acid
mV	millivolts
Na _x	uncharacterised sodium channel
Na _v	voltage-gated sodium channel
NBD	nucleotide binding domain
N-terminus	amino terminus
NTP	nucleotide triphosphate
Ntp	N-terminal peptide
P1075	N-cyano-N'-(1,1-dimethylpropyl)-N''-3-pyridylguanidine
PBS	phosphate buffered saline
PCR	polymerase chain reaction
PHHI	persistent hyperinsulinaemic hypoglycaemia of infancy
PIP ₂	phosphatidylinositol-4, 5-bisphosphate
PKA	cAMP activated protein kinase
PKC	calcium activated protein kinase
P-loop	pore loop
PNU37883A	N-Cyclohexyl-N'-tricyclo[3.3.1.1 ^{3,7}]dec-1-yl-4-morpholine carboximidamide
P _o	open probability
RNA	ribonucleic acid
ROMK	renal outer medullary potassium channel
r.p.m.	revolutions per minute
SAP	shrimp alkaline phosphatase
SDS-PAGE	sodium dodecyl sulphate polyacrylamide gel electrophoresis
s.e.m.	standard error of the mean
Slob	slowpoke binding protein
SNARE	soluble NSF attachment protein receptor
SUR	sulphonylurea receptor
TAE (buffer)	Tris, acetic acid and EDTA buffer
TASK	TWIK-related acid sensitive potassium channel
TMD	transmembrane domain
Tris	tris(hydroxymethyl)aminomethane
UDP	uridine diphosphate
UV	ultraviolet

Chapter One

Introduction

1 Introduction

1.1 Cells and their membranes

The cell as we know it consists of a number of organelles, which organelles depends on its origin, surrounded by a lipid bilayer. This bilayer forms the cell membrane and provides a means of containing the important organelles of the cell as well as forming a barrier excluding entry of unwanted entities. The structure of the lipid bilayer, hydrophilic heads facing outwards and hydrophobic tails facing inwards producing a water-free and very hydrophobic “internal” environment, is such that as well as limiting entry of unwanted hydrophilic species it also prevents entry of entities necessary for cellular functions e.g. calcium ions in muscle contraction. Mechanisms have therefore evolved to allow the transport, or regulated diffusion, of hydrophilic species across the membrane. These fall into two categories – transporter proteins and ion channels. As an ion channel is being studied here, the focus of this introduction will reflect that fact. However, it is impossible to talk about ion channels and their importance in cellular processes without mentioning transporters (see 1.1.2).

1.1.1 *Membrane potentials*

Cell membrane potential is determined by the difference in voltage inside the cell relative to that outside (given an arbitrary value of 0 mV). When a cell is inactive its membrane potential will be set by the concentration of ions inside and outside the cell and the permeability of the membrane to these ions, which in most cases is very low. This value is known as the resting membrane potential. Consider a cell membrane only

permeable to potassium ions – their concentration inside and outside the cell, physiologically, is approximately 155 mM and 4 mM, respectively (Hille, 2001). Diffusion will drive potassium out of the cell but in doing so the inside becomes negatively charged i.e. attracts the positively charged potassium ions back into the cell. This interplay of diffusion and charge caused by a difference in concentration of ions across the membrane creates what is known as an electrochemical gradient. The potential at which the movement of ions out of the cell due to diffusion equals the movement of ions into the cell due to the potential difference is known as the equilibrium potential. The equilibrium potential (E_x) for an ion (X) can be calculated using the Nernst equation:

$$E_x = \frac{RT}{zF} \ln \frac{[X]_o}{[X]_i}$$

Where $[X]_{o/i}$ is the concentration of X outside or inside the cell, R is the universal gas constant ($8.314 \text{ J K}^{-1} \text{ mol}^{-1}$), T is the temperature in Kelvin, z is the charge of the ion and F is the Faraday constant (96500 C mol^{-1}). For example, the equilibrium potential for potassium (E_K) is -98 mV at 37°C. An understanding of equilibrium potentials allows us to know what will happen under certain conditions when an ion channel opens e.g. whether currents will be inwards or outwards; and is necessary to know what voltage is needed to give an appropriate driving force to create recordable currents. The concentrations of ions (in mM) inside and outside the cell are: Na^+ - 12 and 145, Ca^{2+} - 0.1 and 1.5, Cl^- - 4.2 and 123; giving equilibrium potentials of +67 mV, +129 mV and -90 mV, respectively, at 37°C (Hille, 2001). Equilibrium potentials vary by cell type as the concentration of ions across the membrane varies.

1.1.2 The resting membrane potential and its development

In a simplified version of a cell we can assess the influence of one ion at a time and its effect on membrane potential, as above with potassium. In this case the resting membrane potential is equal to the equilibrium potential for that ion. However, in reality this is not the case. While potassium permeability accounts for much of the resting membrane potential, slight permeability to other ions drives the resting membrane potential slightly more positive e.g. ~ -70 mV in neurons.

While the resting membrane potential of a cell is controlled by the permeability of the membrane to different ions, which is in turn controlled by the fact that the concentration of ions differs across the membrane, this does not come about of its own accord. The concentration of all ions inside and outside the cell is created by transporters. The fact that this is usually against the concentration gradient means that the process requires energy. This is where a transporter protein differs from an ion channel. Ion channels allow the passage of ions across the membrane simply by diffusion, and thus require no energy, but allow it to occur in a regulated fashion. Transporters bind ions and carry them across the membrane by conformational changes of the protein. The energy to create this conformational change sometimes comes from ATP hydrolysis and other times comes from the facilitated transport of an ion down its concentration gradient, usually sodium. However, in some instances transporters simply provide an alternative method for passing ions down their concentration gradient and no energy is required. The sodium potassium ATPase uses ATP hydrolysis to drive the transport of sodium out of, and potassium into, the cell. The concentration gradients for sodium and potassium created by this pump are

essential in establishing the resting membrane potential of a cell. In the case of sodium, this gradient can also be used to drive transport of other species, including molecules like sugars, across the membrane.

1.2 Ion channels

Ion channels permit the controlled flux of charged particles through the membrane, a process that would not occur in their absence. Opening an ion channel dramatically increases the permeability of the membrane to that ion leading to a rapid flow of ions down their electrochemical gradient until the channel closes. When a channel selective for one ion opens, and if only that channel opens, the membrane potential of the cell moves towards the equilibrium potential for that ion. Ion channels share a common minimum architecture – a hydrophilic, membrane spanning pore at the core of the protein that comprises the conduction pathway for ions across the membrane. The main ions that permeate the membrane are sodium, calcium, chloride and potassium. Ion channels are first categorised based on the ion to which they are selective. They are then further characterised according to other properties such as what controls their gating e.g. voltage- or ligand-gated; and their gating characteristics e.g. inwardly rectifying channels or fast/ slow delayed rectifier channels. There are several examples of non-selective channels e.g. the nicotinic acetylcholine receptor, a non-selective cation channel. However, for the purposes of this brief introduction to the different ion channels I will concentrate on selective ion channels. N.B. potassium channels will be described in greater detail later (see 1.3) so they will be omitted here.

1.2.1 Selectivity

An important feature of ion channels is their ability to distinguish between ions. Each ion channel listed below possesses a structural motif that endows it with selectivity for one ion over the others. Different channels can do this to varying degrees – potassium channels are in excess of 10000 times more selective for potassium ions over sodium ions (Doyle *et al.*, 1998). However, sodium channels are much less selective with a permeability for potassium that is ~10% of that for sodium (Hille, 2001). Chloride channels are less selective for passage of a single ion than many other ion channels, being permeable to HCO_3^- and NO_3^- amongst others (Suzuki *et al.*, 2006), to the point where they can be broadly described as anion channels just as easily as they can chloride channels (Hille, 2001).

1.2.2 Sodium channels

Sodium channels are one of the likely causes of a change in membrane potential towards positive potential e.g. the upstroke of an action potential. As a result, sodium channels are primarily found in excitable cells. Nine voltage-gated sodium channels have been cloned and identified, $\text{Na}_v1.1$ - $\text{Na}_v1.9$ with one further channel not cloned and characterised as yet and therefore referred to as simply Na_x (Goldin, 2001). The high sequence similarity suggests that they are all part of the same subfamily, hence being named $\text{Na}_v1.x$ (Goldin, 2001). Voltage-gated sodium channels are localised to brain, skeletal muscle and heart where their primary function is initiation of the action potential (Catterall *et al.*, 2005a). While the majority of sodium channels are voltage-

gated, ligand-gated sodium channels do exist. An example of a ligand-gated sodium channel is the brain sodium channel 1 (BNC1; Price *et al.*, 1996).

1.2.3 Calcium channels

Unlike sodium, whose entry into the cell produces a sharp depolarising effect but has very little direct impact on cellular processes, calcium is a second messenger in its own right and its influx triggers a wide range of processes including muscle contraction and neurotransmitter release. Ligand-gated calcium channels are more abundant than their sodium channel counterparts. Examples include the ryanodine receptor, involved in calcium induced calcium release from intracellular stores. Voltage-gated calcium channels are split into three subfamilies Ca_v1 , Ca_v2 and Ca_v3 based on sequence homology (Catterall *et al.*, 2005b). The physiological roles of calcium channels are far more diverse than sodium channels including excitation-contraction coupling in skeletal muscle ($Ca_v1.1$), neurotransmitter release in nerve terminals ($Ca_v2.1$) and pacemaking in the heart ($Ca_v3.1$; Catterall *et al.*, 2005b).

1.2.4 Chloride channels

As the equilibrium potential for chloride is negative, chloride flux would be expected to have an inhibitory influence on the excitability of the cell. However, the presence of chloride transporters in some tissues increases the intracellular concentration of chloride so that its equilibrium potential is less negative, so that when a chloride channel is opened it can raise the membrane potential and even elicit an action potential (Olsen & Sieghart, 2008). Chloride channels include the ionotropic

γ -aminobutyric acid_A (GABA_A) and glycine receptors, the cystic fibrosis transmembrane conductors (CFTRs) and the voltage-gated chloride channels (ClCs; Suzuki *et al.*, 2006). They are involved in inhibitory post-synaptic transmission (glycine and GABA_A receptors; Olsen & Sieghart, 2008) and control of cell volume (Suzuki *et al.*, 2006).

1.3 The potassium channel family

Potassium channels are a structurally and functionally diverse class of ion channel. Opening of potassium channels is generally involved in hyperpolarisation of cell membranes as E_k is more negative than resting membrane potential and therefore, more importantly, much more negative than the threshold for action potential firing. This chapter will give a much more detailed view of the potassium channel than has been given for the other common ion channels. Potassium channels are highly selective for potassium over smaller cations like sodium and lithium (>10000 times more selective) but retain the ability to pass 10^8 ions per second (Doyle *et al.*, 1998). Potassium channels can be grouped based on their proposed structures into those that contain six-, four- and two-transmembrane domains. Structurally similar channels tend to have similar characteristics but those that do not are further separated by sequence homology. All potassium channels, as well as other channels, coordinate four loops to line part of the conducting pore (MacKinnon, 1991). Potassium channels do this in a variety of ways, as you will see below. Many potassium channels also associate with accessory subunits that do not contribute to the ion conduction pathway e.g. MinK associates with hERG (McDonald *et al.*, 1997). Below are details of the different types of potassium channel α subunits i.e. those that contain the pore of the channel.

1.3.1 Generalised potassium channel structure

The *Streptomyces lividans* potassium channels KcsA was the first natural ion channel to be crystallised and have its structure elucidated (Doyle *et al.*, 1998). This gave great insight into many important concepts of ion conduction e.g. how selectivity is achieved and how ions pass through the pore. Since that original study, a number of structures for other potassium channels have been obtained covering a wider range of the subtypes of this family (Jiang *et al.*, 2002a, Jiang *et al.*, 2003, Kuo *et al.*, 2003). The minimum structural requirements of potassium channel subunits are two transmembrane domains and a pore loop (P-loop), as identified in KcsA but also present in the calcium-gated potassium channel MthK, the voltage-gated KvAP and the bacterial inwardly rectifying KirBac1.1 (Doyle *et al.*, 1998, Jiang *et al.*, 2002a, Jiang *et al.*, 2003, Kuo *et al.*, 2003). The exception being the two pore potassium channels where one subunit contains two sets of helices and P-loops as if it were two subunits fused together (see 1.3.4). Four additional alpha helices present in KvAP provide the voltage sensor for this channel (Jiang *et al.*, 2003). All potassium channels share a consensus motif within the P-loop that accounts for their selectivity for potassium ions over smaller cations, -TXXTXGYGD- (Hille, 2001). The only exception is a conservative substitution of GFG for GYG in the Kir6 subfamily.

1.3.2 Voltage-gated potassium channels

Voltage-gated potassium channels make up over half of the known potassium channels (Gutman *et al.*, 2005). These include Kv1- Kv12 (Kv10, Kv11 and Kv12 were formerly widely known as eag, erg and elk respectively; Gutman *et al.*, 2005). Kv channels have

six transmembrane domains with the last two, S5 and S6, contributing to the pore in a similar fashion to KcsA. The additional helices form the voltage sensor with S4 being particularly important in this respect. As expected, the role of K_v channels is most frequently to control the excitability of cells. Different isoforms often have the same role of hyperpolarising cells but in different tissues (Gutman *et al.*, 2005).

1.3.3 Calcium-activated potassium channels (K_{Ca})

K_{Ca} channels also have six transmembrane domains. There are three subtypes of K_{Ca} based on channel conductance – small (SK_{Ca}), intermediate (IK_{Ca}) and “big” conductance (BK_{Ca}) channels. Conductance of these channels ranges from 9 pS in SK_{Ca} channels up to 260 pS in BK_{Ca} channels (Wei *et al.*, 2005). BK_{Ca} channels differ slightly from the others in that they have seven transmembrane domains. BK_{Ca} channels are voltage sensitive but this sensitivity can be regulated by calcium.

1.3.4 Two pore potassium channels

Sometimes called leak channels due to their activity at resting membrane potentials, this group of channels is unique amongst potassium channels. This is because rather than being formed by a tetramer of pore-forming subunits, they are formed by dimerisation of subunits with each subunit consisting of four transmembrane domains with two P-loops contributing towards half of the pore structure. As a result of this unique composition they are more commonly known as two-pore channels (K_{2P}). Under physiological potassium concentrations they are outwardly rectifying channels i.e. they pass little or no current inwards (Goldstein *et al.*, 2001). Though many genes

encoding K_{2P} channels have been identified and they have been localised to a variety of tissues, few physiological roles have been attributed to these channels. One of the few specific roles identified is in cell volume regulation (Goldstein *et al.*, 2005).

1.3.5 Inwardly rectifying potassium channels (K_{ir})

Inwardly rectifying potassium channels (K_{ir}) are two transmembrane domain proteins. As the name implies, these channels are inwardly rectifying i.e. they pass little current at membrane potentials positive to E_k . This means that they are only active at hyperpolarised membrane potentials. Given that the membrane potential of a cell is very unlikely to reach values negative to E_k , it is the small amount of outward current that they can pass at more positive potentials that allows K_{ir} channels to contribute physiologically. The physiological contribution of K_{ir} usually involves stabilisation of the resting membrane potential but without exerting an influence during depolarisation. Rectification in these channels is caused by voltage sensitive blocking of the pore by intracellular magnesium ions (Vandenberg, 1987) or polyamines such as spermine (Lopatin *et al.*, 1994). Strong rectification tends to arise as a result of polyamine block whereas mild rectification is usually brought about by magnesium ions blocking the pore (Hille, 2001). There are seven subtypes of K_{ir} (K_{ir1} - K_{ir7}) with a diverse array of characteristics. Their activity can be affected by intracellular pH as in the case of K_{ir1} (Shuck *et al.*, 1997). Heteromultimers of K_{ir4} and K_{ir5} are sensitive to changes in intracellular pH as well as CO_2 (Yang *et al.*, 2000). K_{ir} channels can even be regulated by G-proteins – $G_{\beta\gamma}$ subunits activate the K_{ir3} subclass (Wickman *et al.*, 1994). Most relevant here is the K_{ir6} isoform, a weak inwardly rectifying potassium channel that it is regulated by nucleotides and forms the ATP-sensitive potassium channel (K_{ATP} ; Inagaki

et al., 1995a, Inagaki *et al.*, 1995b). The remainder of this introduction will concentrate on the K_{ATP} channel.

1.4 ATP-sensitive potassium channel - K_{ATP}

The ATP-sensitive potassium channel (K_{ATP}) was first identified in 1983 by Noma (Noma, 1983) who demonstrated the presence of a potassium channel in the heart whose activity was inhibited by intracellular application of ATP. K_{ATP} channels have since been found to be expressed in a variety of tissues, most notably pancreatic β -cells (Ashcroft *et al.*, 1984), brain (Ashford *et al.*, 1988), and skeletal (Spruce *et al.*, 1985) and vascular smooth (Standen *et al.*, 1989) muscle. By virtue of their sensitivity to ATP and ADP (Dunne & Petersen, 1986), K_{ATP} channels provide a link between the metabolic state of a cell and its electrical excitability. As far back as 1973 it was known that sulphonylurea drugs like glibenclamide affect insulin release (Ashcroft *et al.*, 1973). Eventually this effect was attributed to K_{ATP} channels (Sturgess *et al.*, 1985), however it was some time before the sulphonylurea receptor (SUR) was identified as a separate entity to the K_{ATP} channel i.e. that SUR expression produced no currents (Aguilar-Bryan *et al.*, 1995). *N.B. $K_{ir}6.0$ will be used when referring to both $K_{ir}6.1$ and $K_{ir}6.2$ at the same time.*

1.4.1 Identification and structure

The discovery of the inwardly rectifying potassium channels, firstly ROMK ($K_{ir}1.1$; Ho *et al.*, 1993) but including GIRK ($K_{ir}3.1$; Kubo *et al.*, 1993), started the race to discover new channels in this emerging class. Using a GIRK cDNA fragment as bait for a screen

of a pancreatic β -cell cDNA library, Inagaki and colleagues cloned the first K_{ATP} channel subunit – the ubiquitously expressed $K_{ir}6.1$ (Inagaki *et al.*, 1995a). However, $K_{ir}6.1$ was not present in a β -cell line. Using $K_{ir}6.1$ cDNA as a probe quickly lead to identification of another K_{ATP} channel subunit, $K_{ir}6.2$ (Inagaki *et al.*, 1995b, Sakura *et al.*, 1995)¹. $K_{ir}6.1$ and $K_{ir}6.2$ show ~70% identity (Inagaki *et al.*, 1995b) and based on homology with other inwardly rectifying potassium channels whose structures have been determined, namely $K_{ir}3.1$ (Nishida & MacKinnon, 2002) and $K_{ir}Bac1.1$ (Kuo *et al.*, 2003), $K_{ir}6.0$ is assumed to have intracellular N- and C- termini and two transmembrane domains separated by a pore-forming loop (P-loop). The potassium selectivity consensus sequence in the selectivity filter of $K_{ir}6.0$ contains GFG rather than GYG (Inagaki *et al.*, 1995a) but selectivity is unaffected. See figure 1.1 for the structure of $K_{ir}6.0$. Iodinated glyburide was used to purify SUR allowing its N-terminus to be sequenced. cDNA encoding this N-terminal peptide was used to screen phage libraries from two insulin secreting cell lines. This lead to the cloning of SUR1 (Aguilar-Bryan *et al.*, 1995). Shortly afterwards, the almost identical SUR2A (Chutkow *et al.*, 1996), and SUR2B (Isomoto *et al.*, 1996) were identified and cloned. SUR2A and SUR2B are splice variants sharing 97% homology with the divergence occurring at the C-terminus of the protein (Isomoto *et al.*, 1996) while SUR2A shares ~86% identity with SUR1 (Chutkow *et al.*, 1996). SUR is a member of the ATP-binding cassette (ABC) protein superfamily (Aguilar-Bryan *et al.*, 1995). Unlike other members of this family, SUR has no transport role and only achieves this function when associated with $K_{ir}6.0$. Structurally SUR resembles other ABC proteins with a core consisting of two bundles of

¹ It should be noted that a third isoform, $K_{ir}6.3$, has recently been discovered in zebrafish (Zhang *et al.*, 2006), however as this isoform does not appear outside of zebrafish I shall only mention it in passing.

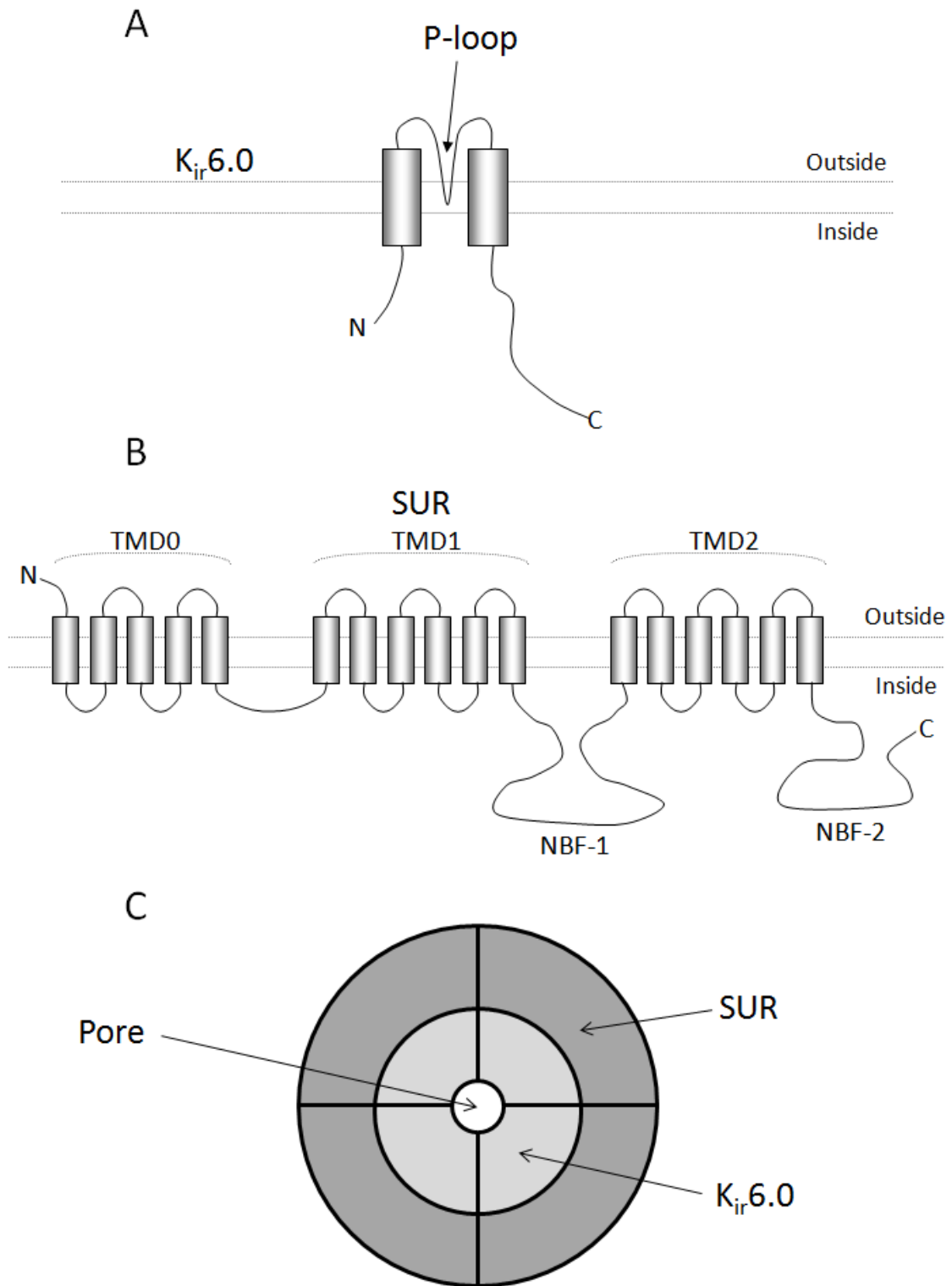


Figure 1.1 - Secondary structure of K_{ATP} channel subunits

A, structure of pore-forming subunit – $K_{ir}6.0$; including the pore-loop (P-loop).

B, structure of sulphonylurea receptor (SUR) including transmembrane domains (TMD) and nucleotide binding folds (NBF).

C, topology of the assembled hetero-octamer viewed from directly above. Four SUR subunits surround four $K_{ir}6.0$ subunits, which combine to form the pore.

six transmembrane domains (TMD1 and 2; Tusnady *et al.*, 1997). C-terminal to each TMD is an intracellular nucleotide binding domain (NBD1 and 2) containing Walker A and B motifs (Tusnady *et al.*, 1997). However, SUR has an additional N-terminal bundle of five transmembrane domains (TMD0) connected to the core via an intracellular linker (L0; Conti *et al.*, 2001, Raab-Graham *et al.*, 1999, Tusnady *et al.*, 1997). The structure of SUR can be seen in figure 1.1.

Once the subunits that comprise K_{ATP} were identified, the structure of the channel could be more easily studied. Expression of either $K_{ir}6.2$ or SUR1 alone produced no currents, however, co-expressing these subunits was shown to reconstitute a K_{ATP} current resembling the β -cell K_{ATP} current (Inagaki *et al.*, 1995b). This showed that the K_{ATP} channel is a multimer of $K_{ir}6.0$ and SUR but shed no light on the proportions required to reconstitute the channel. It was proposed that the channel is formed by a heterooctamer of four $K_{ir}6.2$ and four SUR1 subunits based on the molecular mass of the channel complex determined by SDS-PAGE (Clement *et al.*, 1997). Covalently linking $K_{ir}6.2$ and SUR1 showed that the subunits combine in a 1:1 ratio (Clement *et al.*, 1997, Inagaki *et al.*, 1997, Shyng & Nichols, 1997). Also, co-expression of mutant $K_{ir}6.2$ subunits with stronger rectification (N160D) and wild type $K_{ir}6.2$ produced a population of channels showing varying degrees of rectification best explained by the hypothesis that different combinations of wild type and mutant $K_{ir}6.2$ subunits produced different rectification characteristics. There are five sub-populations suggesting that the channel contains four $K_{ir}6.2$ subunits, thus confirming that K_{ATP} is a heterooctamers – $(K_{ir}6.0)_4(SUR)_4$, (Clement *et al.*, 1997, Shyng & Nichols, 1997).

1.4.2 Assembly and trafficking

It has been demonstrated that all combinations of K_{ir}6.0 and SUR can form functional channels (Ammala *et al.*, 1996, Inagaki *et al.*, 1995b, Inagaki *et al.*, 1996, Isomoto *et al.*, 1996, Kondo *et al.*, 1998, Yamada *et al.*, 1997) but given that K_{ATP} is formed by eight subunits it is possible that hybrid channels could form containing multiple isoforms within one functional channel. It is possible for K_{ir}6.1 and K_{ir}6.2 to combine to form a hybrid channel (Cui *et al.*, 2001). However, SUR appears to be less promiscuous. There have been no reports of channels forming containing multiple SUR isoforms.

Interactions between K_{ir}6.0 and SUR are important during assembly of K_{ATP} channels. K_{ir}2.1 does not associate with SUR and this provides a very useful tool for investigating assembly of K_{ATP} channels. Using chimeras of K_{ir}6.2 and K_{ir}2.1 the regions of K_{ir}6.2 involved in assembly with SUR have been identified. The C-terminal 182 amino acids (Giblin *et al.*, 1999) and the first transmembrane helix (M1; Schwappach *et al.*, 2000) of K_{ir}6.2 were sufficient to confer SUR interaction onto K_{ir}2.1. The N-terminus of SUR1 i.e. TMD0 and to some extent L0, has been shown to mediate association with K_{ir}6.2 (Babenko & Bryan, 2003, Chan *et al.*, 2003). Also, a C-terminal peptide from SUR2A corresponding to the Walker A motif of NBD2 has been shown to interact with K_{ir}6.1 and K_{ir}6.2 and cause a reduction in surface expression of a number of K_{ATP} channel isoforms when expressed alongside them (Rainbow *et al.*, 2004).

Neither K_{ir}6.0 nor SUR produces currents when expressed alone, however, their co-expression generates recognisable K_{ATP} currents. Interestingly, removal of the C-terminal 26 or 36 amino acids (denoted K_{ir}6.2ΔC26 or 36) of K_{ir}6.2 reconstitutes

currents in the absence of SUR (Tucker *et al.*, 1997). The ability of these channels to form functional homotetramers without SUR was later shown to be a result of removal of an arginine-based endoplasmic reticulum (ER) retention signal, RKR (Zerangue *et al.*, 1999). The RKR motif is present in both K_{ir}6.0 and SUR, where it is present in the intracellular loop linking the 11th transmembrane helix with NBD1. Mutating RKR in SUR allows it to reach the surface in the absence of K_{ir}6.0 (Zerangue *et al.*, 1999). During normal assembly of K_{ATP} channels, SUR masks the RKR motifs present on K_{ir}6.0 but even in fully assembled channels that exit the ER and reach the membrane the RKR motifs of SUR are partially exposed. When K_{ir}6.2 and SUR are fused and the RKR motif of SUR mutated, surface expression is increased compared to when all RKR signals are left intact to a level almost as high as when RKR is absent in both subunits (Zerangue *et al.*, 1999). This RKR-based ER retention mechanism serves to prevent partially assembled channels from reaching the membrane. If expression were left unchecked, channels with unwanted properties e.g. insensitivity to metabolic inhibition, would be able to reach the membrane (Zerangue *et al.*, 1999) and this could have a severely detrimental effect on the cell. This shows that assembly and trafficking of K_{ATP} channels are inextricably linked.

It has been suggested that ER retention is mediated by the coatamer I (COPI) vesicle coat complex which binds to the RKR motif of K_{ir}6.2. Mutating RKR to KKK in a K_{ir}6.2 C-terminal fragment abolishes COPI binding (Yuan *et al.*, 2003). It is believed that competition for binding sites on K_{ir}6.2 between COPI and the chaperone protein 14-3-3 regulates ER exit of the K_{ATP} channel complex (Heusser *et al.*, 2006, Yuan *et al.*, 2003). While the RKR motif is important during 14-3-3 binding, it is believed that its binding

site is separate to RKR as removal of the final ten amino acids of a C-terminal K_{ir}6.2 peptide prevents association with 14-3-3 but leaves RKR intact (Heusser *et al.*, 2006). There is no evidence of either COPI or 14-3-3 binding directly to SUR.

Glycosylation of SUR has been shown to promote expression of the fully assembled K_{ATP} complex (Conti *et al.*, 2002). Mutation of two asparagine residues to glutamine in SUR1 to prevent N-linked glycosylation was shown to reduce K_{ATP} current when co-expressed with K_{ir}6.2 by increasing ER retention of the mutant channel complex (Conti *et al.*, 2002).

A study by Crane and Aguilar-Bryan has shown that the turnover of each K_{ATP} subunit is markedly different when expressed alone (Crane & Aguilar-Bryan, 2004). K_{ir}6.2 shows a biphasic turnover where ~60% is lost very quickly, $t_{1/2} \sim 36$ minutes, but the remainder is much longer-lived, $t_{1/2} \sim 26$ hours. While SUR1 expressed alone has a long half life, ~25.5 hours. When expressed together, K_{ir}6.2 and SUR1 associate very quickly and the short-lived K_{ir}6.2 entity is lost. Associated K_{ir}6.2 and SUR1 have a half life of ~ 7 hours (Crane & Aguilar-Bryan, 2004). The disappearance of the short-lived form of K_{ir}6.2 when co-expressed with SUR1 suggests that SUR1 can associate with K_{ir}6.2 monomers and protect them from degradation.

1.4.3 Physiological roles and distribution

K_{ATP} channels are found in a wide range of tissues and often differ in their characteristics depending on the tissue examined. Cloning of the K_{ir}6.0 and SUR subunits and their subsequent heterologous expression shed light on this

phenomenon. It was shown that different combinations of $K_{ir}6.0$ and SUR confer different properties on the K_{ATP} channel. Based on drug and nucleotide sensitivity as well as other properties like unitary conductance, the subunit combinations responsible for tissue specific K_{ATP} channels have been identified. For example, $K_{ir}6.2/SUR1$ comprises the β -cell channel (Inagaki *et al.*, 1995b), $K_{ir}6.2/SUR2A$ is thought to be the cardiac channel (Inagaki *et al.*, 1996) and $K_{ir}6.1/SUR2B$ constitutes the vascular smooth muscle channel (Yamada *et al.*, 1997). Below I will concentrate on a few regions where K_{ATP} is abundant and its role in each.

1.4.3.1 K_{ATP} channels in the brain

K_{ATP} channels have been identified in various regions of the brain including the substantia nigra (Amoroso *et al.*, 1990), neocortex (Luhmann & Heinemann, 1992), hippocampus (Margaill *et al.*, 1992) and hypothalamus (Ashford *et al.*, 1990). The following is an example of one the many possible roles of K_{ATP} channels in the brain. K_{ATP} channels are particularly abundant in the hypothalamus where its function is reasonably well studied. The hypothalamus plays a crucial role in glucose homeostasis by controlling the release of regulatory molecules like glucagon and catecholamines via the autonomic nervous system (Taborsky *et al.*, 1998). Contained within this region of the brain are a subset of neurons that increase or decrease their firing rate in response to elevated glucose, named glucose responsive and glucose sensitive neurons respectively (Oomura *et al.*, 1974, Panksepp & Reilly, 1975). Though the precise mechanism of glucose sensing in the hypothalamus is unclear, $K_{ir}6.2$ null mice highlighted some involvement of K_{ATP} channels in this process (Miki *et al.*, 1998a, Miki *et al.*, 2001b). It is suggested that insulin-induced lowering of blood glucose is sensed

in the hypothalamus by glucose responsive neurons, this stimulates autonomic input to pancreatic α -cells and causes glucagon secretion (Seino & Miki, 2003).

1.4.3.2 K_{ATP} channels in the cardiovascular system

K_{ATP} channels are known to exist in the heart and vascular smooth muscle. The role of K_{ATP} channels in the heart is somewhat unclear despite its presence being in no doubt. Upon discovering the ATP-sensitive potassium current in the heart, Noma suggested that its role was likely to be cardioprotective by virtue of hyperpolarisation of the cell and the energy saving that results (Noma, 1983). Ischemic preconditioning (IPC) is a phenomenon where brief periods of ischemia prior to a major ischemic insult provide protection for the heart (Murry *et al.*, 1986). IPC was suggested to involve K_{ATP} channels because K_{ATP} channel blockers can prevent the beneficial effects of IPC and K_{ATP} channel openers can mimic it (Gross & Auchampach, 1992). This finding seems to confirm the original hypothesis for the role of cardiac K_{ATP} channels being cardioprotective. However, more recent studies have suggested that it is a mitochondrial K_{ATP} channel that is responsible for IPC (Garlid *et al.*, 1997).

Vascular smooth muscle K_{ATP} channels are thought to regulate vascular tone. Opening of potassium channels in vascular smooth muscle causes hyperpolarisation and reduced calcium entry leading to vasodilation. The involvement of K_{ATP} channels in this process appears to be through activation via PKA or inhibition via PKC (Quayle *et al.*, 1997). This process is thought to be initiated by a number of substances including calcitonin gene-related peptide (Miyoshi & Nakaya, 1995) and adenosine (Mutafova-Yambolieva & Keef, 1997). As well as causing vasodilation in response to a stimulus

such as hypoxia (Daut *et al.*, 1990), vascular K_{ATP} channels play some part in setting the basal vascular tone in the absence of stimulation (Imamura *et al.*, 1992).

1.4.3.3 K_{ATP} channels in the pancreas

Perhaps the best characterised role of the K_{ATP} channel is in the pancreas (see Mislner *et al.*, 1992 for review). In support of this, mutations in genes encoding $K_{ir}6.2$ and SUR1 have been shown to be responsible for persistent hyperinsulinaemic hypoglycaemia of infancy (PHHI; Nestorowicz *et al.*, 1997, Thomas *et al.*, 1995, Thomas *et al.*, 1996). When blood glucose levels rise e.g. after a meal, glucose uptake into pancreatic β -cells increases. Increased glucose uptake leads to increased glycolysis, the result of which being elevated intracellular concentrations of ATP. The increased ATP concentration, or more specifically the increased ATP: ADP ratio, leads to inhibition of β -cell K_{ATP} channels. As the K_{ATP} channel is exerting a hyperpolarising effect on the cell its closure leads to depolarisation and opening of voltage-gated calcium channels. The subsequent influx of calcium ions leads to calcium mediated exocytosis of insulin containing vesicles and the release of insulin into the bloodstream.

1.5 Properties of K_{ATP} channels

Once the fully and correctly assembled K_{ATP} complex has left the ER and been inserted into the plasma membrane it has a number of characteristics that separate it from other potassium channels. Most importantly, it is sensitive to inhibition by intracellular ATP (Noma, 1983). Almost paradoxically, the channel can also be activated by nucleotides, including ATP, but only in the presence of magnesium (Findlay, 1987,

Gribble *et al.*, 1998a). Phosphatidylinositol-4, 5-bisphosphate (PIP₂) activates many inwardly rectifying potassium channels, K_{ATP} is no exception. PIP₂ activates K_{ATP} channels and is thought to antagonise inhibition by ATP as a result (Ribalet *et al.*, 2000, Shyng & Nichols, 1998). K_{ATP} channels can also be regulated by a number of pharmacological agents including sulphonylureas and potassium channel openers (KCOs). This section will describe the characteristics of K_{ATP} channels in more detail.

1.5.1 Biophysical properties

A minimum description of K_{ATP} channel activity is that it cycles between three states – a short-lived burst or open state, a shorter-lived intraburst closed state that punctuates bursts of openings and a long-lived interburst closed state, sometimes called O, C_f and C_s (figure 1.2). C_f and C_s are used to distinguish between the closed state that occurs during fast flickering observed during a burst of opening in single channel recordings between the open and closed states (examples can be seen in figure 1.2), and the long periods of inactivity that occur between bursts, respectively. Intraburst closures are voltage sensitive and ligand insensitive and the gate is believed to lie in the selectivity filter (Proks *et al.*, 2001). Interburst closures are controlled by a different gate which is ligand sensitive. By inference from the bacterial MthK potassium channel, this is thought to be a hinged gate lying at the bundle crossing of the M2, inner, helices (Jiang *et al.*, 2002b). The mechanism by which this gate closes is rather controversial, some believe it is the result of concerted closure of each gate i.e. virtually a single gate (Drain *et al.*, 2004), while others claim that each subunit contributes and closes its own gate and closure of any one is sufficient to close the channel (Enkvetchakul & Nichols, 2003).

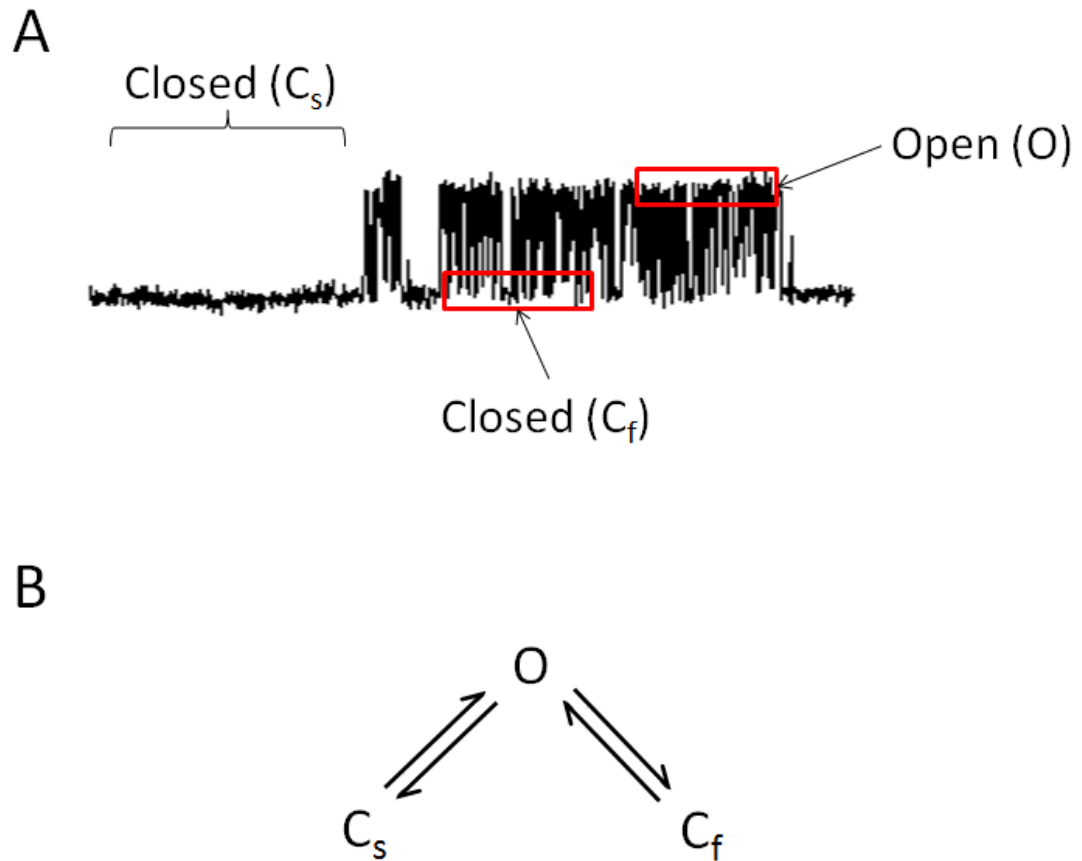


Figure 1.2 - Biophysical properties of the K_{ATP} channel

A, single channel current recorded from the IRD mutant, which displays the same bursting characteristics as wild type K_{ATP} channels, and SUR2A. The intraburst closed state (C_f) punctuates bursts of openings (O). Bursts are separated by relatively long closures of the channel (C_s).

B, state diagram to represent K_{ATP} channel bursting properties.

K_{ATP} channels that contain $K_{ir}6.2$ open spontaneously upon removal of ATP (Cook & Hales, 1984, Trube & Hescheler, 1984), however those containing $K_{ir}6.1$ do not (Beech *et al.*, 1993). Kondo and colleagues demonstrated that it was possible to reverse this phenomenon by constructing chimeric $K_{ir}6.0$. They showed that regions of the N- and C-termini of the pore forming subunit (residues 37-45 and 243-248, respectively, in $K_{ir}6.2$ and their equivalents in $K_{ir}6.1$) were “structural prerequisites” for spontaneous bursting (Kondo *et al.*, 1998). A separate study has been able to produce $K_{ir}6.1$ -containing channels that spontaneously open by deleting residues 2-5 of the subunit (Babenko & Bryan, 2001). When this mutant subunit was co-expressed with SUR1 it produced K_{ATP} channels with a P_o of ≈ 0.01 in the absence of nucleotides. However, a similar effect was seen for the equivalent $K_{ir}6.2$ channel suggesting that the deleted region is not necessarily involved in controlling spontaneous opening, certainly not with respect to the difference between the two $K_{ir}6.0$ isoforms, given the high amino acid sequence similarity in this region.

Single channel conductance of K_{ATP} channels varies by tissue. Recombinant channels have reconstituted a similar scenario where channels containing $K_{ir}6.1$ have a lower conductance than those containing $K_{ir}6.2$. The difference in conductance between tissue specific K_{ATP} channels helped to clarify which subunit combinations were likely to be responsible for which population of channels, particularly in identifying the vascular smooth muscle isoform as containing $K_{ir}6.1$ (Yamada *et al.*, 1997). SUR makes no contribution to determining conductance so other characteristic differences were used to identify tissue specific SUR subunits.

1.5.2 Regulation by endogenous molecules

The activity of native K_{ATP} channels is finely tuned by a complex symphony of inhibitory and stimulatory effects of several endogenous molecules. The importance of inhibition by ATP cannot be understated especially due its pivotal role in the discovery of the K_{ATP} channel (Noma, 1983). But similarly, the stimulatory effect of other nucleotides and PIP_2 play a key role as open K_{ATP} channels are as important as closed ones. It has been suggested that, under normal circumstances, the un-liganded channel i.e. ATP and PIP_2 free, is unstable and that ATP and PIP_2 binding is mutually exclusive (Enkvetchakul & Nichols, 2003). Therefore, the channel will exist bound to one or the other.

1.5.2.1 Inhibition by ATP

When SUR was cloned it was believed to be responsible for the nucleotide sensitivity of K_{ATP} channels by virtue of the nucleotide binding folds and the finding that ATP sensitivity differs between channels formed from $K_{ir6.2}$ with SUR1 and SUR2A (Inagaki *et al.*, 1996). Though some believed this not to be the case it was not until the expression of $K_{ir6.2\Delta C}$ in the absence of SUR that the argument was convincingly swung one way or the other. These homotetramers retained ATP sensitivity despite the lack of SUR (Tucker *et al.*, 1997) suggesting that the inhibitory ATP binding site is located on $K_{ir6.0}$.

Inhibition of K_{ATP} channels by ATP is state dependent where ATP binds more readily to the closed state of the channel (Alekseev *et al.*, 1998, Trapp *et al.*, 1998). This means that a change in open probability (P_o) will affect ATP sensitivity. Therefore, the ATP

binding site can be identified if mutation of $K_{ir}6.0$ alters ATP sensitivity without affecting P_o . As inhibition of K_{ATP} channels occurs in response to intracellular ATP, the search for its binding site focussed on the intracellular N- and C-termini of $K_{ir}6.0$. Initial studies implicated two positively charged residues in ATP binding, R50 and K185 in $K_{ir}6.2$ (Tucker *et al.*, 1998). The charge of these residues, particularly K185, was shown to be important in ATP binding where replacement of K185 with another positive residue had little effect on ATP binding (Reimann *et al.*, 1999). Following this finding, systematic mutation of all of the positive residues in the N- and C-termini of $K_{ir}6.2$ identified more residues that affect ATP binding, including R201 (Shyng *et al.*, 2000). The assumption was that electrostatic interaction between these positively charged amino acids and the negatively charged phosphate groups of ATP accounted for ATP binding. By studying the effect of different numbers of phosphate groups i.e. adenosine, AMP, ADP and ATP; on ATP sensitivity it has been suggested that specific residues interact with certain phosphate groups to accommodate ATP in $K_{ir}6.2$. R50 and K185 interact with the β -phosphate and R201 interacts with the α -phosphate (Dabrowski *et al.*, 2004, Ribalet *et al.*, 2003, Trapp *et al.*, 2003). The γ -phosphate is believed to lie mostly outside the binding site (Dabrowski *et al.*, 2004). Molecular modelling of $K_{ir}6.2$ has shed more light on the subject and seems to confirm these suggestions with the addition that, rather than β -phosphate, R50 coordinates the γ -phosphate (Antcliff *et al.*, 2005). In this model of $K_{ir}6.2$ the ATP binding site is a long, thin pocket approximately 17 Å x 10 Å x 8 Å with 17 residues within 4.5 Å of the ATP molecule. Each subunit of the $K_{ir}6.2$ tetramer contributes an ATP binding site where the main binding pocket is thought to lie at the interface of the N- and C-termini of the same subunit. However, R50 seems to be contributed by an adjacent subunit. Though

the residues that directly contribute to the ATP binding site are reasonably well characterised, there are still some residues that have been shown to affect ATP sensitivity including K47 and R54 (Cukras *et al.*, 2002a), and R192 (Shyng *et al.*, 2000). These residues may have an allosteric effect on ATP binding, however, the involvement of K47 and R54 is clouded by studies where no effect was found by mutations in the N-terminus other than to R50 (Ribalet *et al.*, 2003, Tucker *et al.*, 1998). It has also been suggested that different residues are responsible for the different characteristics of ATP inhibition. Binding of the β -phosphate of ATP to R50, R182 and K185 is thought to destabilise the open state of the channel and promote transition to the closed state followed by R201 interaction with the α -phosphate, which stabilises the channel in the closed state (Ribalet *et al.*, 2003).

1.5.2.2 Stimulation by nucleotide diphosphates

Stimulation of K_{ATP} channels by Mg-nucleotides involves the SUR subunit (Nichols *et al.*, 1996). A mutation found to cause PPHI abolished the stimulatory effect of MgADP. This mutation is located in NBD2 of SUR suggesting that this domain is important in binding MgADP (Nichols *et al.*, 1996). Nucleotides bind to both NBDs of SUR. NBD1 is a magnesium-independent, high affinity binding site whereas NBD2 is magnesium-dependent and low affinity (Gribble *et al.*, 1997a, Ueda *et al.*, 1997). This suggests that NBD2 is responsible for the stimulation by ADP as this effect is also magnesium-dependent (Gribble *et al.*, 1997a)). It has been demonstrated that specific residues are involved in the potentiatory effect of MgADP. Mutations in the Walker A and B motifs of both NBDs abolish the stimulatory effect of MgADP suggesting that binding of nucleotides to NBD1 may also play a part in the stimulation affected by NBD2 Gribble

et al., 1997a, Gribble *et al.*, 1997b, Shyng *et al.*, 1997b). Ueda *et al.* have suggested that stimulation of K_{ATP} channels is achieved by cooperative binding of nucleotides to both NBDs of SUR (Ueda *et al.*, 1999). They showed that when SUR was pre-incubated with the photoaffinity ATP analogue 8-azido- $[\alpha\text{-}^{32}\text{P}]\text{ATP}$ this interaction was stabilised by subsequent incubation with MgATP/MgADP. It is believed that either binding of MgADP directly to or binding and hydrolysis of MgATP at NBD2 causes a conformational change in NBD2 which produces a conformational change in NBD1 stabilising bound ATP (Ueda *et al.*, 1999).

Studies using an analogue of ATP with a radioactive group at different positions (8-azido- $[\alpha/\gamma\text{-}^{32}\text{P}]\text{ATP}$) showed that NBD2 possesses some ATPase activity but NBD1 has little or no activity (Matsuo *et al.*, 1999, Matsuo *et al.*, 2000). It has been suggested that a difference in some properties between SUR isoforms is responsible for the different regulation of K_{ATP} subtypes (Matsuo *et al.*, 2000). NBD2 of SUR1 shows higher ATP hydrolysis (measured in-vitro) than that of SUR2A. This difference is suggested to cause greater stimulation in response to MgADP in channels containing SUR1 (Masia *et al.*, 2005). In a model of the activation of K_{ATP} channels by nucleotides through SUR by Matsuo *et al.*, stimulation requires MgATP at NBD1 and MgADP at NBD2 (Matsuo *et al.*, 2005). The correct state of NBD1 can only be reached by MgATP binding directly; however, MgADP can reach NBD2 by two paths – binding directly or hydrolysis of MgATP.

1.5.2.3 Activation by PIP₂

Most inwardly rectifying potassium channels are sensitive to activation by PIP₂. For K_{ATP} channels, PIP₂ increases the open probability by prolonging open times and shortening closed times (Fan & Makielski, 1999). PIP₂ also reduced the ATP sensitivity of K_{ATP} channels. It is thought that this is brought about by direct competition between PIP₂ and ATP for binding to the channel (MacGregor *et al.*, 2002) and indirectly as a result of the increase in P_o that PIP₂ induces (Trapp *et al.*, 1998). As with inhibition by ATP, when K_{ir}6.2ΔC is expressed without SUR it retains sensitivity to PIP₂, thus PIP₂ binds to K_{ir}6.0 (Baukrowitz *et al.*, 1998). To further support this, PIP₂ has been shown to directly bind to purified recombinant K_{ir}6.2 (Wang *et al.*, 2002). Regions of both the N- and C-termini contribute to the PIP₂ binding site (Cukras *et al.*, 2002b, Fan & Makielski, 1997, Schulze *et al.*, 2003, Shyng *et al.*, 2000). The same molecular model used to identify the ATP binding site (Antcliff *et al.*, 2005) was used to establish the residues of K_{ir}6.2 that interact with PIP₂ (Haider *et al.*, 2007). K_{ir}6.2 contains one PIP₂ binding site per subunit of the tetramer and like the ATP binding site, the main part of the PIP₂ site is formed by residues from one subunit but with an additional interaction (R54) contributed by the neighbouring subunit. Eight residues lie within 4.5 Å of the PIP₂ molecule in this model, including R54, R176, R177, R301 for which previous evidence exists for their involvement in PIP₂ sensitivity (Fan & Makielski, 1997, Schulze *et al.*, 2003, Shyng *et al.*, 2000). Though PIP₂ and ATP compete for binding to K_{ir}6.2 the model suggests they do not share a binding site. However, a number of residues, K39, E179 and R301; are predicted to be involved in the interaction with both ligands (Antcliff *et al.*, 2005, Haider *et al.*, 2007). From simulations of dual interactions with

ATP and PIP₂ in this model, an indirect effect on R50 serves to be the initiating event in the destabilisation of the interactions between ATP and the three main residues that contact it i.e. R50, K185 and R201 (Haider *et al.*, 2007).

1.5.3 Regulation by other proteins

Phosphorylation of the K_{ATP} channel complex constitutes a major regulatory mechanism outside of its interaction with endogenous molecules. A number of studies have shown that the cAMP-activated protein kinase (PKA) has a stimulatory effect on K_{ATP} channels via the adenosine A₂ receptor and adenylyl cyclase activation (Kleppisch & Nelson, 1995, Quayle *et al.*, 1994). Phosphorylation of K_{ir}6.2 at S372 causes increased channel activity while phosphorylation of SUR1 at S1571 leads to altered gating properties i.e. decreasing burst duration, interburst interval and P_o; as well as increasing surface density of the channel (Beguin *et al.*, 1999). Regulation of the vascular smooth muscle isoform of the K_{ATP} channel by phosphorylation is widely studied as it represents a likely physiological mechanism of controlling vascular tone. Phosphorylation of K_{ir}6.1 on S385 and SUR2B at T633 and S1465 activates the channel (Quinn *et al.*, 2004) as does phosphorylation of S1387 in SUR2B (Shi *et al.*, 2007). Calcium activated protein kinase (PKC) was originally thought to oppose the effects of PKA on K_{ATP} channels and cause inhibition but the picture that has emerged is less clear cut. Early studies demonstrated that phosphorylation of various smooth muscle isoforms of K_{ATP} channels by PKC caused a reduction in channel activity (Bonev & Nelson, 1993, Light *et al.*, 1995) and evidence to support an inhibitory role continued to emerge (Hayabuchi *et al.*, 2001, Kubo *et al.*, 1997, Mauerer *et al.*, 1998, Park *et al.*, 2005, Sampson *et al.*, 2007). However, PKC has been shown to activate cardiac K_{ATP}

channels and this effect seems to be caused by a reduction in ATP sensitivity (Hu *et al.*, 1996, Hu *et al.*, 1999, Light *et al.*, 1996). Light *et al.* showed that the stimulatory effect of PKC was the result of phosphorylation of T180 in K_{ir}6.2 (Light *et al.*, 2000). It has been suggested that the differential effects of PKC are subunit specific where phosphorylation of K_{ir}6.1 causes inhibition but its effect on K_{ir}6.2 is stimulatory. In support of this, recombinant channels composed of K_{ir}6.1 and SUR2B were inhibited by PKC but those comprising K_{ir}6.2, or a hybrid of the two isoforms, and SUR2B were stimulated by PKC (Thorneloe *et al.*, 2002). This effect has been used to identify four residues in K_{ir}6.1 whose mutation reduces the effect of PKC on the channel (Shi *et al.*, 2008).

Other proteins that have been shown to influence K_{ATP} channel activity include the SNARE complex protein syntaxin-1A which reduces P_o via the NBDs of SUR1 and SUR2A, presumably by affecting stimulation by MgADP and MgATP (Cui *et al.*, 2004, Kang *et al.*, 2004, Pasyk *et al.*, 2004). A very recently identified modulator of K_{ATP} channel activity is the exchange protein activated by cAMP (Epac) that has been shown to inhibit pancreatic and vascular K_{ATP} channel by increasing their sensitivity to ATP (Kang *et al.*, 2008, Purves *et al.*, 2009). This effect is suggested to be via activation of protein phosphatase-2B in a calcium dependent manner (Purves *et al.*, 2009).

1.5.4 Pharmacological regulation

K_{ATP} channels can also be affected by pharmacological manipulation. Pharmacological agents can both open and inhibit K_{ATP} channels and sensitivity to these drugs is usually conferred by SUR (Aguilar-Bryan *et al.*, 1995, Koster *et al.*, 1999a). Potassium channel

openers (KCOs) are a diverse family of compounds and despite their name, early members of this group were limited to opening K_{ATP} channels. Common KCOs include pinacidil, cromakalim and diazoxide. With the exception of diazoxide, which opens the β -cell K_{ATP} channel i.e. binds to SUR1, all other KCOs show specificity for SUR2A/B. Knowing this, chimeras of SUR2 and SUR1 were created to identify the regions responsible for KCO binding in SUR2. L1249 and T1253 in SUR2A (corresponding to residues 1253 and 1257 respectively in humans, as rat SUR was used) were shown to be the likely binding site for KCOs (Moreau *et al.*, 2000), except diazoxide.

The majority of K_{ATP} channel blockers fall into the class of sulphonylurea drugs. Due to their interaction with the pancreatic K_{ATP} channel they are often used to treat diabetes. Sulphonylureas are thought to have a high affinity binding site on SUR and a low affinity site on $K_{ir}6.2$ (Gribble *et al.*, 1998b). Binding of sulphonylureas to SUR is isoform specific in some cases. Two classic sulphonylureas are glibenclamide and tolbutamide. Tolbutamide displays specificity for the β -cell subtype over the cardiac channel. This suggests that SUR1 confers high affinity binding of tolbutamide. However, glibenclamide binds to β -cell and cardiac channels with similar high affinity (Gribble *et al.*, 1998b). This selectivity is thought to be due to SUR having two binding sites for sulphonylureas where SUR1 contains both binding sites but SUR2 only contains one. The regions of the K_{ATP} channel that are thought to contain the binding sites of both tolbutamide and glibenclamide have been identified. In the case of glibenclamide, the binding site is known to be bipartite where the linkers between H5 and H6 (L0) and H15 and H16 (TMD2) of SUR1 have been shown to combine to form a high affinity binding site (Mikhailov *et al.*, 2001). Work to identify the tolbutamide

binding site found that a similar region in the C-terminus of SUR1 is responsible for the high affinity aspect of tolbutamide binding (Ashfield *et al.*, 1999). It has been postulated that the binding site found in L0 interacts with the sulphonylurea moiety of these drugs while the second site in TMD2 binds the benzamido moiety (Ashfield *et al.*, 1999, Gribble *et al.*, 1998b). It is thought that selectivity of some sulphonylureas for SUR1 occurs because SUR2A and SUR2B do not contain the second binding site in TMD2 i.e. they only contain the benzamido binding site (Bryan *et al.*, 2004). A serine residue in the H15-H16 linker (S1238) has been shown to be particularly important for high affinity binding of both glibenclamide and tolbutamide to SUR1. When this residue is mutated to tyrosine (the corresponding residue in SUR2A) there is a reduction in tolbutamide inhibition as if high affinity binding has been lost and only low affinity binding remains (Ashfield *et al.*, 1999). High affinity binding of glibenclamide to SUR2B can be achieved if Y1206 is mutated to serine (corresponding to S1238 in SUR1; Hambrock *et al.*, 2001). There is evidence to suggest that the inhibitory effect of sulphonylureas on K_{ATP} channels is transmitted from SUR to the pore via the N-terminus of $K_{ir}6.0$. Tolbutamide block of K_{ATP} channels is attenuated by N-terminal truncations of $K_{ir}6.2$ (Babenko *et al.*, 1999c).

A number of non-sulphonylurea drugs have been shown to inhibit K_{ATP} channels. A very interesting example is the morpholinoguanidine drug PNU-37883A that appears to be selective for the vascular smooth muscle K_{ATP} channel. Evidence supporting this claim comes from studies in native tissues (Meisheri *et al.*, 1993, Wellman *et al.*, 1999) as well as using recombinant channels (Kovalev *et al.*, 2004, Surah-Narwal *et al.*, 1999). It is believed that $K_{ir}6.1$ confers sensitivity to PNU-37883A but that the SUR subunit may

have some effect on its inhibition (Kovalev *et al.*, 2004). The C-terminus of $K_{ir}6.1$ has been shown to be important in the interaction between PNU-37883A and the channel either by providing the structure to which the drug binds or by participating in the transduction of the response following binding (Kovalev *et al.*, 2004).

1.6 K_{ATP} channel subunit knockouts

Creating an animal void of the gene encoding a protein of interest or creating a dominant negative version of the protein is an extremely useful tool for investigating the importance of that protein in the physiological setting. These animals are said to be “knockouts”. Tissue specific and inducible knockouts can be created if removal of a gene is so detrimental to development that animals do not live long enough to study the effects on adult subjects or if the effect of the knockout in a specific organ is being studied. The only downside is that it is impossible to know if any other proteins compensate for the removed protein. Knockouts have been created for all of the K_{ATP} channel subunits.

1.6.1 $K_{ir}6.1^{-/-}$

When the first $K_{ir}6.1$ null mice were reported, lack of $K_{ir}6.1$ caused a sudden death phenotype similar to Prinzmetal angina in humans (Miki *et al.*, 2002). Sudden death was specifically caused by spontaneous ST elevation due to myocardial ischemia followed by atrioventricular block. Recent knockouts of $K_{ir}6.1$ have highlighted the importance of the vascular K_{ATP} channel during immune responses. Mice lacking $K_{ir}6.1$ died shortly after being subjected to several normally innocuous stimuli (Crocker *et al.*,

2007, Kane *et al.*, 2006). The vascular K_{ATP} channel was suggested to oppose cytokine induced vasoconstriction and importantly maintain sufficient coronary blood flow thus in its absence insufficient myocardial perfusion caused death. It is obvious from these studies that the vascular K_{ATP} channel, particularly in the coronary circulation, is vitally important under conditions of stress.

1.6.2 $K_{ir6.2}^{-/-}$

Mice lacking $K_{ir6.2}$ have been useful in investigating the role of K_{ATP} channels in the pancreas and heart. The findings of the initial $K_{ir6.2}$ knockout concentrated on its role in the pancreas (Miki *et al.*, 1998b). These mice had elevated resting membrane potential and calcium in pancreatic β -cells. They also displayed no glucose or tolbutamide induced calcium or insulin increases suggesting that K_{ATP} channels are involved in these processes. Despite having severely altered β -cells, these mice were only mildly intolerant to glucose and had an increased glucose-lowering response to insulin, which probably served as the compensatory mechanism saving them from severe glucose intolerance. Subsequent $K_{ir6.2}$ knockouts, including targeted removal of β -cell $K_{ir6.2}$, highlighted the importance of the channel in establishing normal β -cell architecture and in cell survival (Miki *et al.*, 2001a). The effect of $K_{ir6.2}$ deficiency on the heart has shown that the cardiac K_{ATP} channel is responsible for shortening of the action potential duration in response to ischemia but not for the potassium accumulation that accompanies it (Yamada *et al.*, 2006).

1.6.3 *SUR1*^{-/-}

Initial studies in SUR1 deficient mice placed most of the resulting phenotypic changes in the pancreas. Animals were normoglycaemic unless stressed but showed elevated and fluctuating membrane potential as a result of spontaneous action potential firing (Seghers *et al.*, 2000). This seemed to be as a result of altered calcium permeability as the effect could be reversed by a calcium channel blocker. Unlike *K_{ir}6.2* null mice, SUR1 knockouts had nearly normal islet histology and no change to apoptosis with the only change being the presence of α -cells in the β -cell mass but this was also present in *K_{ir}6.2*^{-/-} animals (Miki *et al.*, 1998b, Seghers *et al.*, 2000). Another divergence from mice lacking *K_{ir}6.2* is that SUR1 null mice display fasting hypoglycaemia but they show similar mild glucose intolerance. SUR1^{-/-} mice show normal insulin secretion following feeding but impaired glucose induced insulin secretion similar to *K_{ir}6.2* knockouts (Miki *et al.*, 1998b, Seghers *et al.*, 2000, Shiota *et al.*, 2002). Normal insulin secretion in response to feeding has been suggested to be a result of cholinergic stimulation of β -cells serving to compensate for the loss of *K_{ATP}* channels (Shiota *et al.*, 2002). SUR1 knockouts have also been shown to lack cAMP-induced PKA-independent insulin secretion (Eliasson *et al.*, 2003). They also show decreased secretion of glucagon from α -cells caused by reduced electrical activity which suggests that an SUR1-dependent but *K_{ATP}* channel-independent mechanism plays a role in control of excitability of α -cells (Gromada *et al.*, 2004). A recent SUR1 knockout study has shown surprising evidence for the role of SUR1 in the heart, specifically in the atria (Flagg *et al.*, 2008).

1.6.4 *SUR2*^{-/-}

A novel role for skeletal muscle K_{ATP} channels in insulin stimulated glucose uptake was identified by *SUR2* knockout mice (Chutkow *et al.*, 2001). This effect was unexpected but suggested a possible new treatment for diabetes. In a similar phenotype to *K_{ir}6.1* null mice, *SUR2*^{-/-} produced a dramatic cardiovascular effect. These animals displayed significantly increased resting blood pressure and a tendency toward sudden death. This effect was thought to be caused by a calcium mediated episodic coronary artery vasospasm (Chutkow *et al.*, 2002). The fact that both *K_{ir}6.1*^{-/-} and *SUR2*^{-/-} mice displayed a similar vasospastic phenotype lead to the assumption that the vascular K_{ATP} channel, widely accepted to consist of *K_{ir}6.1/SUR2B* (Yamada *et al.*, 1997), was responsible. However, reconstitution of vascular K_{ATP} channels by crossbreeding *SUR2*^{-/-} with mice expressing *SUR2B* targeted to smooth muscle did not restore normal function (Kakkar *et al.*, 2006). This suggests that loss of a vascular smooth muscle extrinsic *K_{ir}6.1/SUR2B* channel is responsible for the coronary vasospasm phenotype.

1.7 Aims of this study

K_{ATP} channels composed of *K_{ir}6.1* differ in many characteristic ways to channels containing *K_{ir}6.2*. The main aim of this study is to investigate the difference in characteristics between the vascular and the cardiac K_{ATP} channels controlled by their pore forming subunit. I will concentrate on the role of the N-terminus in affecting these differences. Several regions of the N-terminus of *K_{ir}6.0* have been identified as candidates for controlling some of the differential properties of *K_{ir}6.1* and *K_{ir}6.2* and I have created mutant subunits exchanging these regions between the two isoforms to

test the effect on channel function. Briefly, two arginine residues have been shown to influence P_o (Cukras *et al.*, 2002a) however these residues are conserved so I have mutated the amino acids flanking these important residues to assess whether the tertiary environment affects the ability of the arginines to affect P_o . A stretch of ten amino acids, position 20-30, has been shown to affect the ATP sensitivity of the channel as a result of a change in open state stability (Koster *et al.*, 1999b). I have exchanged a highly divergent region of 4 or 5 amino acids, within this ten residues section, between the pore-forming subunits in an attempt to identify the residues responsible for the effect of the altered ATP sensitivity and open state stability. My final set of mutants were selected based on the finding that short regions in the N- and C- termini of $K_{ir}6.0$ were responsible for the different spontaneous opening characteristics of $K_{ir}6.1$ and $K_{ir}6.2$ (Kondo *et al.*, 1998). I have created four point mutations exchanging the only different residues in the N-terminal region identified to assess if any individual amino acids are responsible for the N-terminal influence on spontaneous opening.

During my investigation I experienced some difficulty in expressing $K_{ir}6.1$, and any mutants of $K_{ir}6.1$, with SUR2A. I have attempted to improve the expression of these channels in the cells used here and also assessed the influence of the 14-3-3 family of proteins on expression of K_{ATP} channels.

Given the possible influence of the N-terminus of $K_{ir}6.0$ on P_o and in transducing effects between SUR and the pore, knowledge of how these events might occur would be useful in understanding how to manipulate them. Also, a better understanding of the factors affecting K_{ATP} channel expression could be useful in the experimental

setting to improve transient expression of well-known problem subunit combinations

i.e. Kir6.1 and SUR2A/B.

Chapter Two

Material and methods

2 Materials and methods

2.1 Molecular biology

Molecular biology has become an indispensable tool in scientific research. This study has used molecular biology techniques to manipulate DNA to produce mutated cDNAs for K_{ATP} subunits and their subsequent expression. Here I will outline the methods used in this study. A flow diagram describing the generalised cloning process that was used here can be seen in figure 2.1.

2.1.1 *Overlap polymerase chain reaction*

Overlap polymerase chain reaction (PCR) was used to mutate residues in the N-terminus of $K_{ir}6.1$ to the corresponding residues in $K_{ir}6.2$, or vice versa. The latter stages of this technique involved digesting the PCR products with restriction enzymes to allow their insertion into an appropriate expression vector. Therefore, it was essential to select one restriction site upstream and another downstream of the sequence of interest (these will subsequently be referred to as the 'upstream' and 'downstream' restriction sites, respectively). Thus, two short oligonucleotides were designed that would encompass the upstream and downstream restriction sites in their PCR products (primers 1 and 4 in fig 2.2). These oligonucleotides acted as primers for the thermostable polymerase to bind in the PCR. Additional overlapping oligonucleotides (primers 2 and 3 in fig 2.2) were designed for each mutant being created. These primers contained point mutations to alter the $K_{ir}6.0$ sequence as required and a silent mutation to either remove or insert a restriction site into the DNA

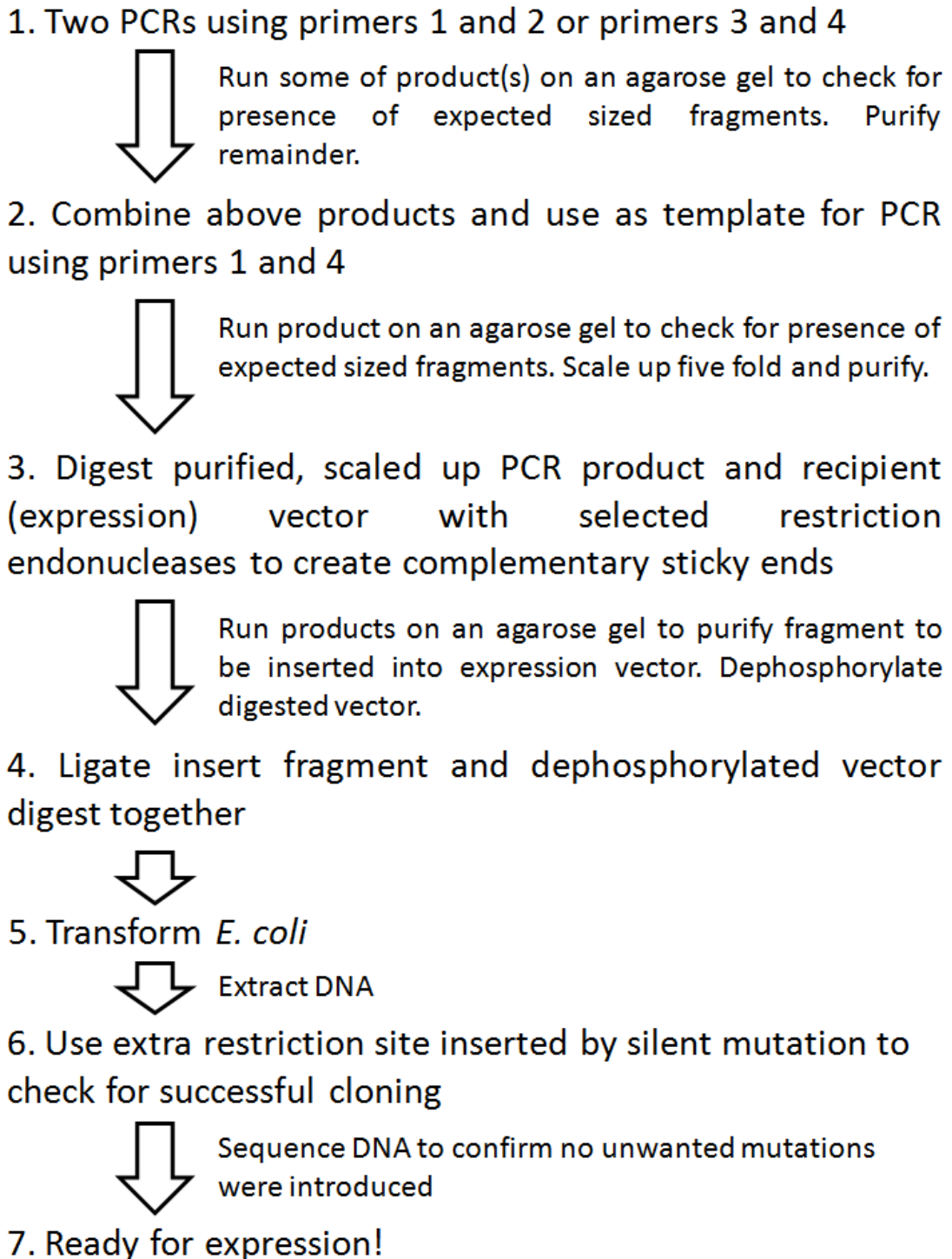


Figure 2.1 - A generalised cloning process

Generalised cloning process exemplifying the procedure used to create all of the mutants discussed here. In the case of the mutants created here an additional “sub-cloning” step was necessary to transfer the cDNA between two vectors as the template for PCR was not the same as the required expression vector. This involved repeating step 3-7 once the first clone was created but replacing “PCR product” in step 3 with “cDNA”.

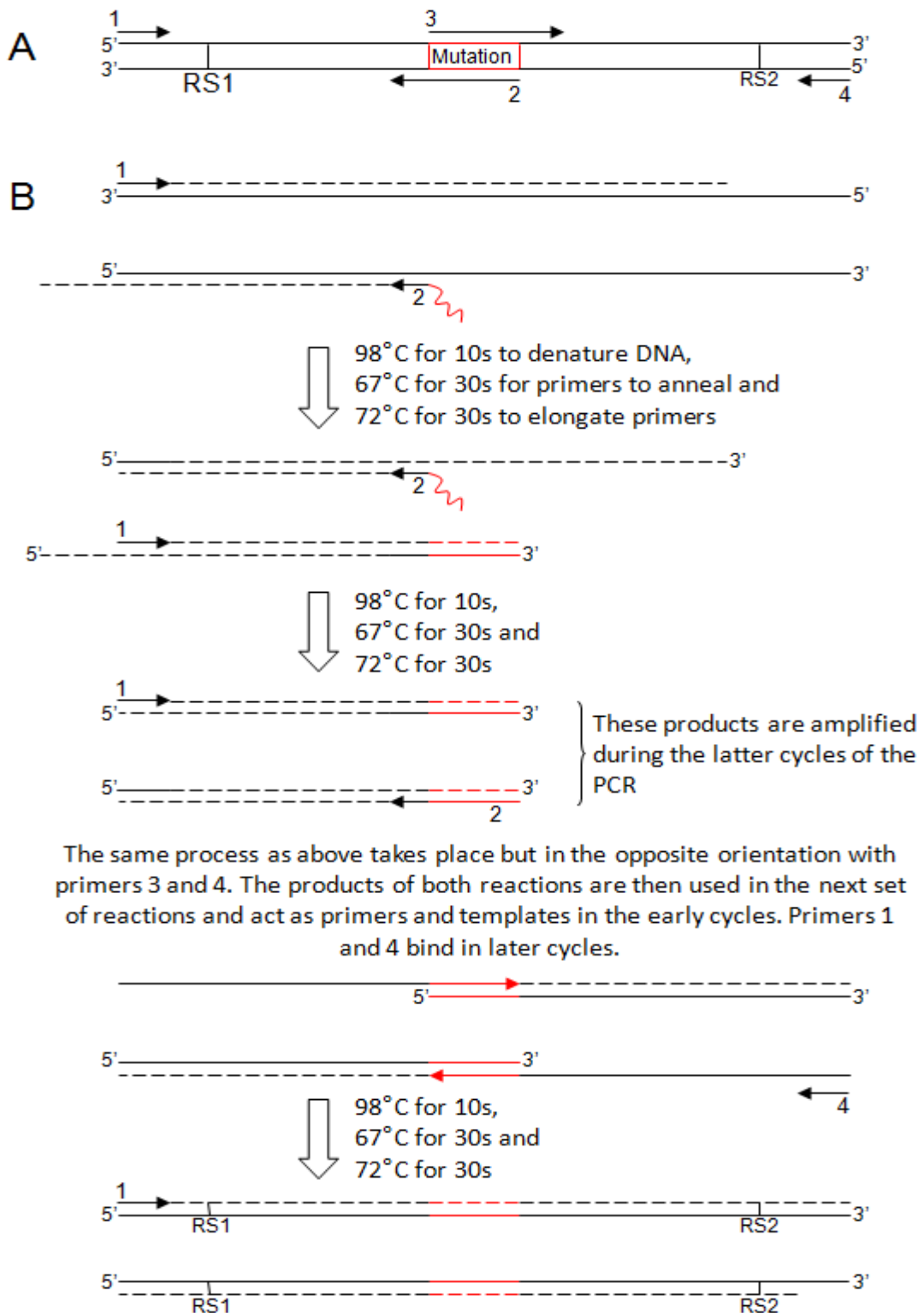


Figure 2.2 - Overview of overlap PCR

A, representation of the PCR primer locations and cloning strategy. RS1 and RS2 are the restriction sites being used to clone the PCR product into the vector.

B, schematic of overlap PCR. Arrowheads represent the 3' end of an oligonucleotide acting as a primer. All lines with 5' and 3' ends represent a template strand during a specific stage of the reaction. Dashed lines represent sequence created during reaction. Mutation being introduced is shown in red throughout.

but leave the coding sequence unaffected. This silent mutation allowed a digest to be carried out on the final DNA preparation to assess whether the mutated DNA was present. The overlapping primers constituted of complementary, mutated sequences as well as sequence that acted as a primer in the first cycle of the PCR. The mutated part of the primer did not participate in the early cycles of the PCR as the difference in sequence compared to the template prevented it from annealing. Following their design, the mutated sequences of the primers were checked against codon usage tables to ensure that no rare codons were used as this may have compromised expression of the protein due to ribosomal stalling during translation. The primers were designed using Oligo version 2 (NAR; Rychlik & Rhoads, 1989) to calculate the appropriate length of 'upstream' and 'downstream' sequence required to give an annealing temperature of ~64°C. In the case of primers 2 and 3, the end of the primer that bound in the first PCR cycle was selected for an annealing temperature of 64°C. The mutated end of the primer was then lengthened to ensure an overlap of 20 base pairs for all cycles from the second onwards. Oligonucleotides were purchased from MWG Biotech. The principle of overlap PCR is summed up in figure 2.2.

First, reactions were set up with the following concentrations and made up to a final volume of 20 µl with PCR grade water:

4 µl	5x Phusion buffer
0.4 µl	10 mM dNTPs (to give a final concentration of 0.2 mM of each NTP)
5 pmol	Primer 1
5 pmol	Primer 2
50 ng	Template DNA

1 unit Phusion enzyme (high fidelity DNA polymerase; New England Biolabs)

Reactions as above but containing primers 3 and 4, instead of primers 1 and 2, were also set up.

The PCR protocol consisted of an initial 30 s denaturation phase at 98°C followed by 20 cycles of the amplification phase. This phase had a 10 s denaturation step at 98°C, a 30 s annealing step at 67°C and a 72°C elongation step that ran for 15-30 s per kb of sequence being synthesised. Finally, the temperature was held at 72°C for 5 mins to ensure that the polymerase was given adequate time to synthesise double stranded products in full. This protocol applied to all PCRs carried out. To check that the correct sized product was being made half the reaction mixture was run on an agarose gel. The process of running an agarose gel is described later (see 1.1.5). For each mutant clone produced, two PCRs were carried out, one with primers 1 and 2 and a second with primers 3 and 4 (see fig 2.2). The products of these reactions were purified using a MinElute PCR purification kit (QIAGEN) and used as a template for the next set of PCRs to amplify the sequence for subsequent cloning into the expression vector. These reactions were set up as follows and made up to 20 µl with PCR grade water:

4 µl	5x Phusion buffer
0.4 µl	10 mM dNTPs (to give a final concentration of 0.2 mM of each NTP)
5 pmol	Primer 1
5 pmol	Primer 4
1 µl	Purified product of first PCR
1 µl	Purified product of second PCR

1 unit Phusion enzyme

Again, the product of this reaction was run on an agarose gel to ensure the reaction was successful. Then the reaction was scaled-up by five times to allow production of adequate amounts of DNA to be digested for cloning into the expression vector. The scaled-up reaction was then purified using a MinElute PCR purification kit (QIAGEN).

2.1.2 Cloning Into expression vectors

The purified PCR products from the above reactions were digested to give a fragment to be inserted into an appropriate expression vector. For clones where the mutation was introduced into K_{ir}6.1 wild type sequence, the DNA was digested with *EcoRV* and *BamHI*. For clones originating from K_{ir}6.2 wild type, DNA was digested with *NdeI* and *BamHI* (except the IRD mutant where *SacII* and *NdeI* were used). All restriction digests were set up under the conditions laid out by the manufacturer of the enzymes (New England Biolabs). These digests were run on agarose gels, to purify the fragment of interest from the rest of the template, and purified using a QIAquick gel extraction kit (QIAGEN). In order to clone these fragments into a vector, the vector had to be digested with the same enzymes. The vector digest and the insert were then combined and ligated together. To prevent the digested vector re-circularising due to only being cut at one site, it was first treated with shrimp alkaline phosphatase (MBI Fermentas). The following was added to the original digest:

1 unit Shrimp alkaline phosphatase (SAP)

(variable amounts of 10x SAP buffer and PCR grade water were added to dilute the buffer to 1x)

Dephosphorylated vector digest was purified using a QIAquick reaction clean-up kit (QIAGEN). This meant that ligation should have only occurred between the vector and the mutant insert. Specific concentrations of insert fragment and vector digest were needed in the ligation reaction so their concentrations were estimated by running a known volume of each against a DNA ladder containing known amounts of DNA (Hyperladder I; Bionline) on an agarose gel. By comparing the intensity of the digested bands against those of the ladder using spot densitometry (using Alphamager 1220 v5.5 software; Alpha Innotech) the concentrations were quantified. As the ends of the DNA fragments were 'sticky' the ligation reactions were set up as follows and made up to 20 μ l with PCR grade water:

4 μ l	5x T4 DNA ligase buffer
90 fmol	Insert DNA
30 fmol	Vector digest
1 unit	T4 DNA ligase

The ligation was incubated at room temperature for a minimum of 5 mins.

2.1.3 *Transforming Escherichia coli*

Ligated DNA was used to transform sub-cloning grade chemically competent *E. coli* (DH5 α ; Invitrogen). 50 μ l of frozen cells were briefly thawed on ice then 2 μ l of the ligation reaction was added. This was incubated on ice for 20 minutes then heat

shocked at 42°C for 45 s. Following a further 2 minute incubation on ice, 950 µl of SOC medium was added and incubated at 37°C, with shaking at 200 r.p.m., for an hour. This culture was then spread on Luria Bertani (LB) agar plates, containing an appropriate selection antibiotic, and incubated overnight at 37°C. Colonies were picked from these plates and streaked out on new plates. These streaked colonies were then used to inoculate LB medium to allow extraction of the plasmid DNA using a QIAprep Spin Miniprep kit (QIAGEN). Extracted DNA was digested to check for successful transformation with vector plus mutant insert. The restriction enzyme used was dependent on what restriction site was introduced or removed by the silent mutation in the primer. As a final check, extracted DNA was sequenced by the university protein and nucleic acid chemistry laboratory (PNAACL) using the upstream primer (primer 1 in fig 2.2) from the PCRs.

2.1.4 Media

All media listed below were sterilised by autoclaving and all concentrations are final concentrations. In the case of SOC, the first four items listed were made up and autoclaved. The additional items in bold were filter sterilised with a 0.2 µm sterile filter unit and added when preparing the medium for use.

SOC:

2%	Tryptone
0.5%	Yeast Extract
10 mM	NaCl
2.5 mM	KCl

10 mM **MgSO₄**

10 mM **MgCl₂**

20 mM **Glucose**

Luria Bertani medium:

5 g/L NaCl

10 g/L Tryptone

5 g/L Yeast Extract

(1.5% agar was added to LB to make LB agar plates)

2.1.5 Agarose gel electrophoresis

At various stages of the cloning process it was necessary to check that a reaction had completed successfully, be it PCR or restriction digestion. In order to do this, samples from the reactions were run on agarose gels. These gels separate DNA by size so it was possible to identify a band of known length if an appropriate size marker was used. Samples were prepared for loading onto the gel by mixing with 2-3 µl of loading buffer regardless of the volume of the sample. Loading buffer contained the following:

10 mM Tris

50 mM EDTA (pH 8)

50% Glycerol

0.05% Bromophenol blue

Agarose gels were made by dissolving an appropriate amount of agarose in TAE buffer; the percentage of agarose in a gel determined the size of fragments that could be

resolved. A higher percentage of agarose could resolve smaller fragments and vice versa. Ethidium bromide (EtBr; 1.25 μM) was added to the gel to allow DNA to be viewed under ultra violet (UV) light. TAE buffer was made up as follows:

40 mM	Tris
100 mM	Glacial Acetic Acid
1 mM	EDTA (pH 8)

The gel was placed in a tank with a positive electrode at one end and a negative electrode at the other. In order for a current to flow through the circuit TAE buffer was added to the tank so that it covered the whole gel. To ensure that sufficient EtBr bound to the DNA to allow visualisation it was also added to the TAE buffer in the tank (0.25 μM). The samples were added to the wells and a size marker added (1 kb ladder, Invitrogen). The circuit was then set up so that the negative electrode was at the end of the gel with the samples in it (as they would move away from this electrode and pass through the gel). A potential difference of 100V was applied across the gel. When the dye in the wells reached ~ 2 cm from the end of the gel it was removed from the tank and viewed under UV light using a MultiImage Light Cabinet and Alphamager 1220 v5.5 software (Alpha Innotech).

2.2 Tissue culture

In order to more easily manipulate and record from ion channels, expression systems are used. For this study they allowed the expression of non-native K_{ATP} subunit combinations i.e. $K_{\text{ir}}6.1$ and SUR2A.

2.2.1 *Maintenance of cell lines*

Chinese hamster ovary (CHO) cells were extensively used in this study. These cells were cultured in plastic flasks bathed in media to provide the nutrients they required. This medium consisted of F-12 nutrient mixture (Ham) with Glutamax supplemented with 10% foetal calf serum and 1% penicillin and streptomycin (all from Invitrogen). Cells were cultured at 37°C and 5% CO₂. Once the cells became confluent they were detached and seeded into another flask i.e. a fraction of the cells were removed and transferred to another flask, to allow them to continue to grow. To do this the medium was aspirated and cells were washed twice with sterile, calcium free, phosphate buffered saline (PBS). A volume of trypsin-EDTA, sufficient to cover the cells e.g. 7 ml for a 75 cm² flask, was added and left on for ~1 min. Trypsin/ EDTA was carefully aspirated and the cells detached from the surface by tapping the flask. 10 ml of medium was added and washed around the flask to ensure all of the cells were detached and separated to form a suspension. 0.7 ml of this was added to a 75 cm² flask containing 15 ml medium. The medium was changed on the cells every two days. In preparation for an experimental day, 3 drops of this cell suspension were plated out in a 60 mm plastic Petri dish containing autoclaved 8 mm glass coverslips and 5 ml medium. Some whole cell experiments (specifically experiments involving 14-3-3, see chapter 5) were carried out on transfected cells following their isolation from the Petri dish. Cells were incubated with 3 ml trypsin/ EDTA for ~2 mins then tapped to dislodge the cells. This suspension of cells was spun for 3 mins at 1000 r.p.m. then resuspended in 0.5-2 ml of whole cell external solution, depending on the size of the pellet.

2.2.2 Transfections

One or two days before an experiment the mutant or wild type DNA was transfected into the cells using lipid based transfection. 500 μ l of optiMEM (Invitrogen) was added to two tubes. The DNA was added to the first and 12 μ l of lipofectamine 2000 (Invitrogen) was added to the second. These were incubated at room temperature for 1 min then mixed and incubated for a further 15 mins before being added to the cells. During this incubation the medium was removed from the cells, they were washed with optiMEM and finally left in 5 ml of optiMEM. The cells were incubated in the transfection mix at 37°C for a minimum of 2 hours after which time they were washed and returned into 5 ml of F12 medium. Due to the presence of EGFP/EGFP-F coding sequence in the plasmid, successfully transfected cells appeared green when excited at 488 nm allowing cells expressing K_{ATP} channels to be selected.

2.3 Electrophysiology

Various techniques have been developed for the measurement of the electrical activity of cells. Here I will detail those used in this study.

2.3.1 Patch clamp

The technique of patch clamping was developed in the 1980s to allow high resolution current recording with low background noise and the ability to clamp the voltage of a whole cell or patch of membrane (Hamill *et al.*, 1981). Whole cell and inside-out recordings were used extensively in this study. Figure 2.3 shows the different configurations that can be achieved using the patch clamp technique.

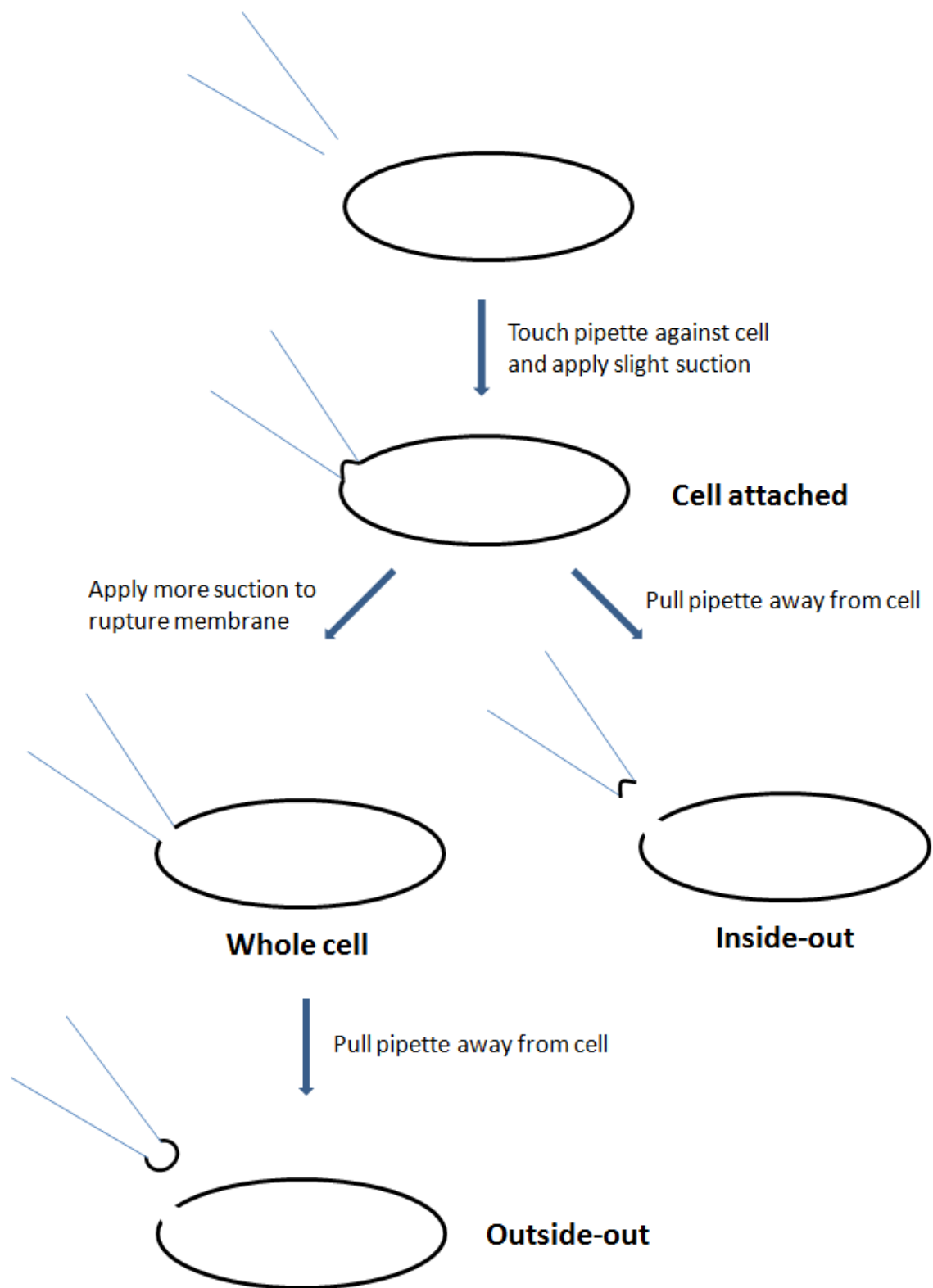


Figure 2.3 - Patch clamp configurations

2.3.2 *Pulling electrodes*

Filamented borosilicate glass capillaries (Harvard Apparatus) were heated and pulled in two stages using a Narishige PP-83 vertical electrode puller. This allowed reproducible creation of pipettes with fine tips. The non-pulled ends of the capillaries were fire polished to give smooth surfaces to reduce removal of the silver chloride from the recording electrode wire. Electrodes used in patch clamping have wider tips than those used for other intracellular recording as they are required to seal onto the surface of a cell rather than puncture its membrane. For excised patches to be used for macroscopic current recording, thin walled glass (outer diameter 1.5 mm, inner diameter 1.17 mm) was used to yield electrodes with a resistance of 3-6 M Ω when filled with solution. For whole cell (or single channel) recordings, thick walled glass (outer diameter 1.5 mm, inner diameter 0.86 mm) was pulled to give pipettes with a resistance of 4-8 M Ω (8-12 M Ω for single channel) when filled with solution. Electrodes were always pulled on the day of use.

2.3.3 *Whole cell patch clamp*

Following selection of a green cell (to denote successful transfection) a slight positive pressure was applied to the pipette before entering the external solution. This prevented the electrode from becoming blocked with debris from the external solution. A gigaohm seal was necessary to give recordings with low noise and provided the starting point for all patch clamp techniques. This was achieved by removing the positive pressure and applying suction to the pipette when it was pressed against a cell. In order to monitor the progress of the electrode sealing onto the cell the

resistance of the electrode was monitored. This was achieved by applying voltage pulses of 5mV for 10 ms at 100 Hz. As the electrode sealed onto the cell, the resistance of the electrode increased until it exceeded 1 G Ω . This is known as a gigaohm seal and this configuration is called cell attached. Whole cell recording was achieved by applying further suction, in short, sharp bursts, to the pipette until the patch of membrane within the tip of the pipette was ruptured. At this point the solution contained within the pipette diffused into the cytosol and became the “internal” solution. Whole cell capacitance and series resistance were measured using the “whole cell parameters” function of the amplifier. Series resistance was compensated for using the “series resistance compensation” circuits built into the amplifier. Outside-out patches were excised by slowly moving the pipette away from the cell once the whole cell configuration was achieved. However, this technique was not used in this study. All currents recorded in the whole cell configuration were carried out at a constant holding potential of 0 mV.

2.3.3.1 Inside-out patch clamp

A gigaohm seal was achieved as described above. An inside-out patch was excised by taking the pipette away from the cell. The patch of membrane to which the pipette sealed was pulled away from the cell and its inner surface exposed. This was essential when investigating the effect of compounds that could not cross the membrane e.g. ATP, which bound to the intracellular side of the K_{ATP} channel, as the bath solution became the internal solution and could therefore be changed. Currents were recorded at -60 mV throughout the experiment. After patch excision the amplifier controlled

external membrane potential relative to internal (opposite to whole cell) therefore this was achieved by recording at +60 mV. All experiments were carried out at 30°C.

2.3.3.2 Patch clamp solutions

For whole cell recordings the bath solution was equivalent to the extracellular solution and consisted of (in mM) 135 NaCl, 6 KCl, 0.33 NaH₂PO₄, 5 Na-pyruvate, 10 glucose, 10 HEPES, 1 MgCl₂ and 2 CaCl₂, adjusted to pH 7.4 with NaOH. The calcium and magnesium were added just prior to use and pH was readjusted. The pipette solution was the cytosolic (internal) solution and contained (in mM) 140 KCl, 2 MgCl₂, 2.5 EGTA, 10 HEPES, 1 CaCl₂, 1 ATP, 0.1 ADP and 0.1 GTP, adjusted to pH 7.2 with NaOH. For experiments involving K_{ir}6.1, or mutants originated from K_{ir}6.1, 10 mM UDP was also added to the internal solution.

Currents were recorded in the inside-out configuration with symmetrical internal and external potassium at a concentration of 140 mM. The internal solution, this time in the bath, contained (in mM) 115 KCl, 10 EGTA, 5 HEPES, 1 CaCl₂ and 25 KOH, adjusted to pH 7.2 with NaOH. During experiments to investigate relative activation, patches were excised into magnesium-free solutions in an attempt to minimise run-down, at all other times, including when nucleotides were added during the same experiment, 1.2 mM MgCl₂ was included in the solution. The pipette solution (external) consisted of (in mM) 140 KCl, 5 HEPES, 1.2 MgCl₂ and 2.6 CaCl₂, pH 7.4.

2.3.3.3 Patch clamp apparatus

Cells were visualised with an inverted Nikon diaphot microscope fitted with a UV light source for epifluorescence. Currents were acquired using an Axopatch 200B amplifier, digitized with either a Digidata 1200 or Digidata 1440A interface, filtered at 2 kHz with an 8-pole Bessel filter and sampled at 10 kHz using pClamp 8/10 software (Axon Instruments). Cells were perfused with solution using a Gilson Minipuls Evolution peristaltic pump. However, for inside-out experiments solution exchange was too slow so a system of directly perfusing solution onto the excised patch was used that allowed much quicker solution changes (figure 2.4). This fast perfusion system consisted of five solution wells connected to a common tip. This was made by taking a pulled electrode and shortening it by snapping the last 5-6 mm from the non-pulled end. A shorter pipette allowed for quicker solution exchange. The pulled tip was then broken to give a larger diameter. This was then fitted into the end of a cut-off plastic pipette tip and connected to the end of the five wells. Fast solution exchange was achieved by manoeuvring the tip of the recording electrode into the outflow of the perfusion system.

2.3.4 Analysis

Analysis was carried out using pClamp 10 software (Axon). A combination of pClamp 10, Microsoft Excel 2003/2007 and Graph Pad Prism 4/5 were used for production of figures. Statistical analysis was performed with Graph Pad Prism 4/5 using one-way ANOVA with Dunnett's or Bonferroni's post-tests. All data is presented as mean \pm

standard error of the mean (s.e.m.). Statistical significance was achieved when $p < 0.05$.

For analysis of whole cell currents, 10 μM glibenclamide was used as the zero current level and peak current was calculated relative to this. Currents were also adjusted for cell size by dividing peak current by the whole cell capacitance, as measured using the amplifier. Single channel current amplitudes were calculated by plotted all points amplitude histograms from bursts of channel activity and fitting these histograms with the following Gaussian distribution:

$$f(x) = \sum_{i=1}^n A_i \frac{e^{-(x-\mu_i)^2 / 2\sigma_i^2}}{\sigma_i \sqrt{2\pi}} + C$$

When ATP sensitivity was calculated, the current at 1mM ATP was subtracted from that at all other ATP concentrations and currents were normalised to that in the absence of ATP. Dose response curves were fitted with variable slope sigmoidal curves as shown by the following equation:

Equation 1 -

$$y = \text{Bottom} + \frac{(\text{Top} - \text{Bottom})}{1 + 10^{(\text{LogIC}_{50} - x) * \text{Hill slope}}}$$

where y is the fractional current at a given concentration of compound, Bottom is the y value at the bottom plateau, Top is the y value at the top plateau, IC_{50} is the

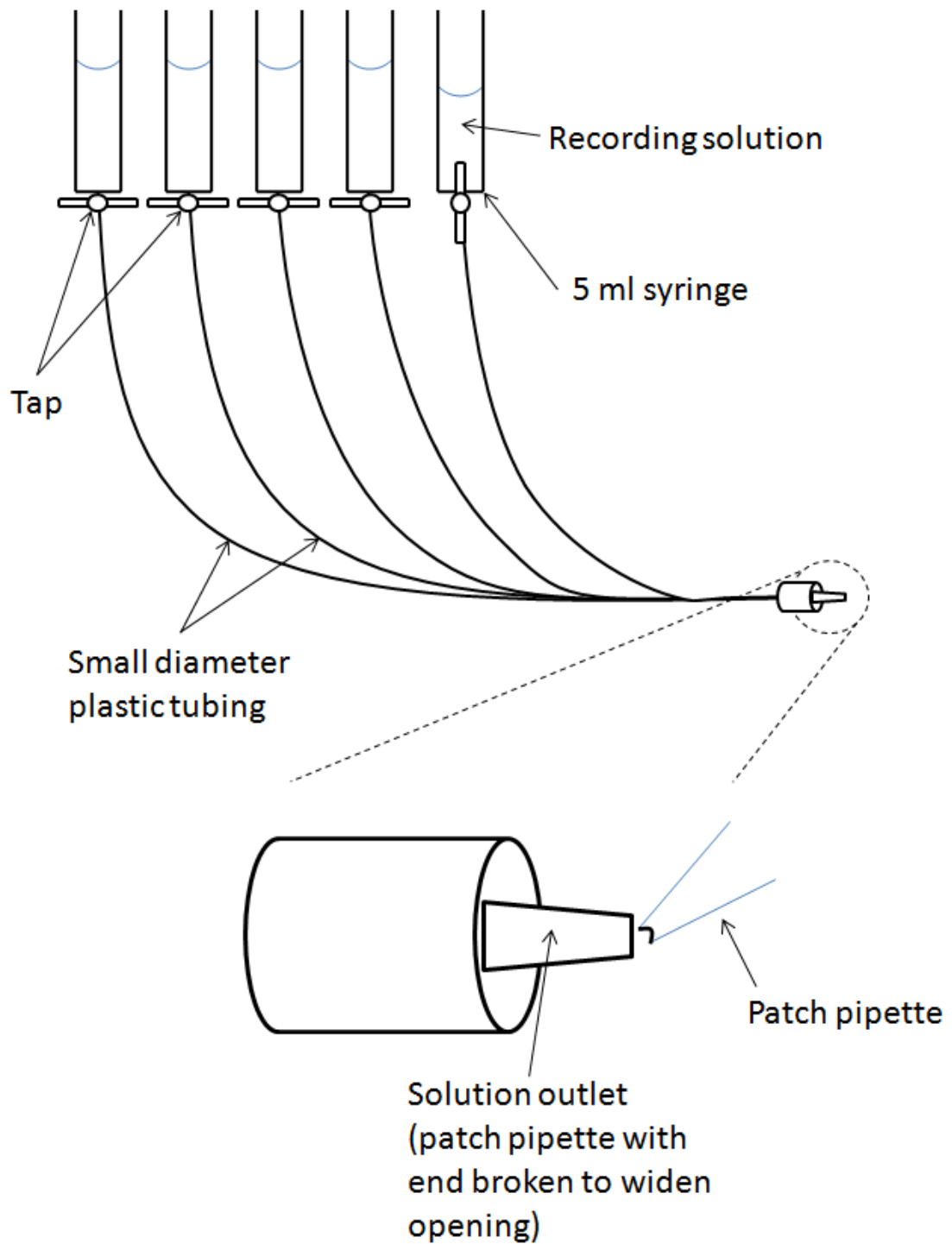


Figure 2.4 - Single channel perfusion system

Each of the 5 wells is connected to the same outlet, made by breaking the tip of a patch pipette to increase its diameter. The inside-out patch is positioned within the opening of the tip so that the patch is perfused by solution flowing from the tip.

concentration of compound that gives half-maximal inhibition and x is the concentration of compound. In the case of ATP, Top and Bottom were constrained to 1 and 0, respectively, leaving only the IC_{50} and Hill slope to be calculated. The Hill equation upon which equation 1 is based is as follows:

$$\frac{I_X}{I_A} = \frac{1}{1 + \left(\frac{[X]}{IC_{50}}\right)^{Hill\ slope}}$$

where I_X is the current in the test compound (X), I_A is the current in the absence of test compound.

Chapter Three

Characterisation of wild type K_{ATP} channels

3 Characterisation of wild type K_{ATP} channels

3.1 Introduction

Since the K_{ATP} channel subunits were identified and cloned (Aguilar-Bryan *et al.*, 1995, Chutkow *et al.*, 1996, Inagaki *et al.*, 1995a, Inagaki *et al.*, 1995b, Isomoto *et al.*, 1996, Sakura *et al.*, 1995) their recombinant expression has been an invaluable tool in testing many physical properties of the channel. Heterologous expression of K_{ATP} channel subunits has enabled researchers to investigate the subunit composition of the channel (Clement *et al.*, 1997, Inagaki *et al.*, 1997, Shyng & Nichols, 1997) as well as to identify the likely subunit combinations responsible for tissue specific channels by comparing their conductance and drug sensitivity (Inagaki *et al.*, 1995b, Inagaki *et al.*, 1996, Yamada *et al.*, 1997). Though heterologous expression is less useful in identifying signalling involving K_{ATP} , due to its atypical environment, it is ideal for studying the structure-function relationship of the channel. As such, transient expression of K_{ATP} channels in CHO cells has been used extensively in this study.

To ensure the relevance of using this system to express K_{ATP} currents, experiments have been carried out to assess a number of properties of wild type $K_{ir6.1}$ - and $K_{ir6.2}$ -containing channels for comparison with previously reported values. These experiments guarantee that the reconstituted channels resemble their proposed native counterparts, or at the very least recombinant expression systems reported elsewhere, as well as providing control values for later experiments.

While K_{ATP} is sensitive to many stimuli, including pH (Xu *et al.*, 2001) and PIP_2 (Ribalet *et al.*, 2000, Shyng & Nichols, 1998), whole cell currents in response to the K_{ATP} channel opener P1075 and inhibition by the sulphonylurea glibenclamide were used as an indication that currents being measured were through K_{ATP} channels as these compounds are highly selective for the channel. This also gives an indication of the expression level of each subtype when co-expressed with SUR2A as membrane density is reflected in whole cell current. Unitary conductance is different in $K_{ir}6.1$ -containing channels compared to those with $K_{ir}6.2$ so confirmation of unitary conductance of $K_{ir}6.1$ and $K_{ir}6.2$ here was essential before continuing with experiments. ATP sensitivity will be presented from inside-out patches for wild type $K_{ir}6.2$ only. The main reason for the absence of a value for the ATP sensitivity of channels containing $K_{ir}6.1$ was that these channels expressed too poorly to easily conduct such experiments (see chapter 4). Secondly, ATP sensitivity was not calculated for any $K_{ir}6.1$ -based mutants and therefore no control value was required.

3.2 Results and discussion

3.2.1 Whole cell recordings

To give an indication of how well both subtypes of the channel expressed when transiently transfected into CHO cells, whole cell currents elicited by 10 μ M P1075, a potent K_{ATP} channel opener with an EC_{50} ranging from 58-96 nM (Miller *et al.*, 1999, Felsch *et al.*, 2004), were recorded from $K_{ir}6.1$ or $K_{ir}6.2$ expressed with SUR2A. This concentration of P1075 ensured that maximal channel opening was achieved. Currents

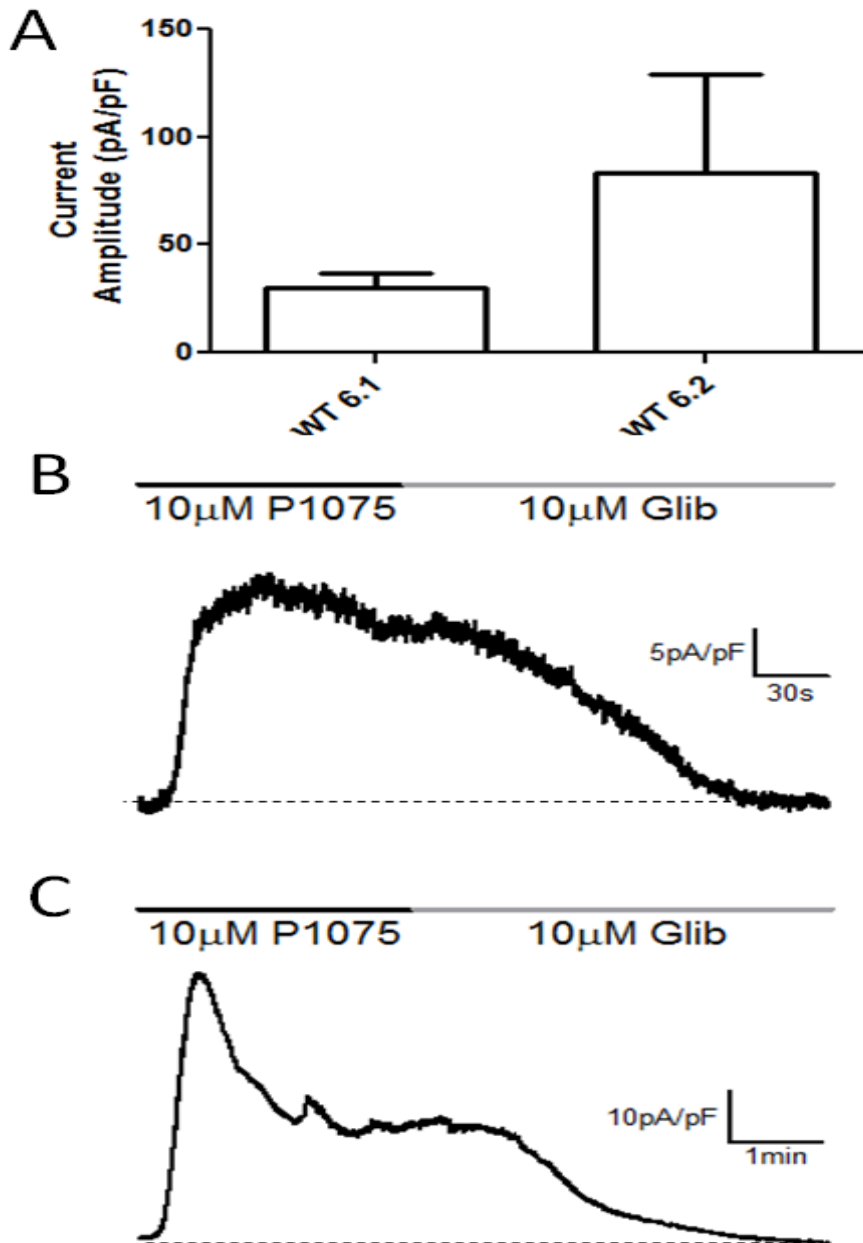


Figure 3.1 - Whole cell current amplitudes

A, whole cell current amplitudes elicited by 10 μ M P1075 for CHO cells expressing $K_{ir}6.1$ or $K_{ir}6.2$ with SUR2A. Recordings were made at 0 mV. Zero K_{ATP} current level was taken as that during perfusion of 10 μ M glibenclamide. All recordings were corrected for cell size. Each bar represents mean \pm s.e.m. for 4 or 5 cells, for $K_{ir}6.1$ and $K_{ir}6.2$ respectively.

B and C, example traces for whole cell recordings taken from cells expressing $K_{ir}6.1$ or $K_{ir}6.2$, respectively, and SUR2A. Drugs were perfused onto the cells as indicated by the bars above the traces. The dashed lines show the current when all K_{ATP} channels were closed i.e. in 10 μ M glibenclamide. Traces have been corrected for cell size. $K_{ir}6.1$ currents were recorded 46-56 hours after transfection. $K_{ir}6.2$ currents were recorded 20-30 hours after transfection.

were recorded at 0 mV N.B. $E_K = -82.25$ mV at 30°C. In order to establish a baseline of background or leak current 10 μ M glibenclamide, a potent and highly selective K_{ATP} channel blocker, was added. One day following transfection, $K_{ir}6.2/SUR2A$ channels expressed well with a mean current density of 83.2 ± 46.2 pA/pF (n=5) recorded from cells with a mean conductance of 7.6 ± 0.8 pF. However, $K_{ir}6.1$ currents took longer to achieve robust expression – two days post-transfection $K_{ir}6.1/SUR2A$ channels had a mean current density of 30.5 ± 6.7 pA/pF (n=4, mean conductance of 8.6 ± 1.3 pF). A graphical summary of these data and example traces for both subtypes of the channel can be seen in figure 3.1. The lengths of all incubations during the transfection as well as the amount of DNA transfected were altered in an attempt to address the difference in expression between $K_{ir}6.1$ and $K_{ir}6.2$. However, none of these alterations impacted expression levels so the transfection protocol in 2.2.2 was used. As expected, 10 μ M P1075 activated the channel and 10 μ M glibenclamide fully inhibited the channel. The purpose of these whole cell recordings was to give an idea of expression of the channels therefore no concentration-response curves were obtained for either drug. As such high concentrations of both drugs were used only a dramatic change in sensitivity could be detected when testing mutants. If any change in sensitivity to 10 μ M P1075 is seen for any mutants, as it would manifest as a smaller current density, it could be a reflection of altered expression, binding of the drug or translation of binding into opening. The same is true for a change in inhibition by 10 μ M glibenclamide i.e. a change in binding or translation of signal (see 4.3.1 for mutant whole cell currents); with the exception that altered expression will not affect glibenclamide sensitivity.

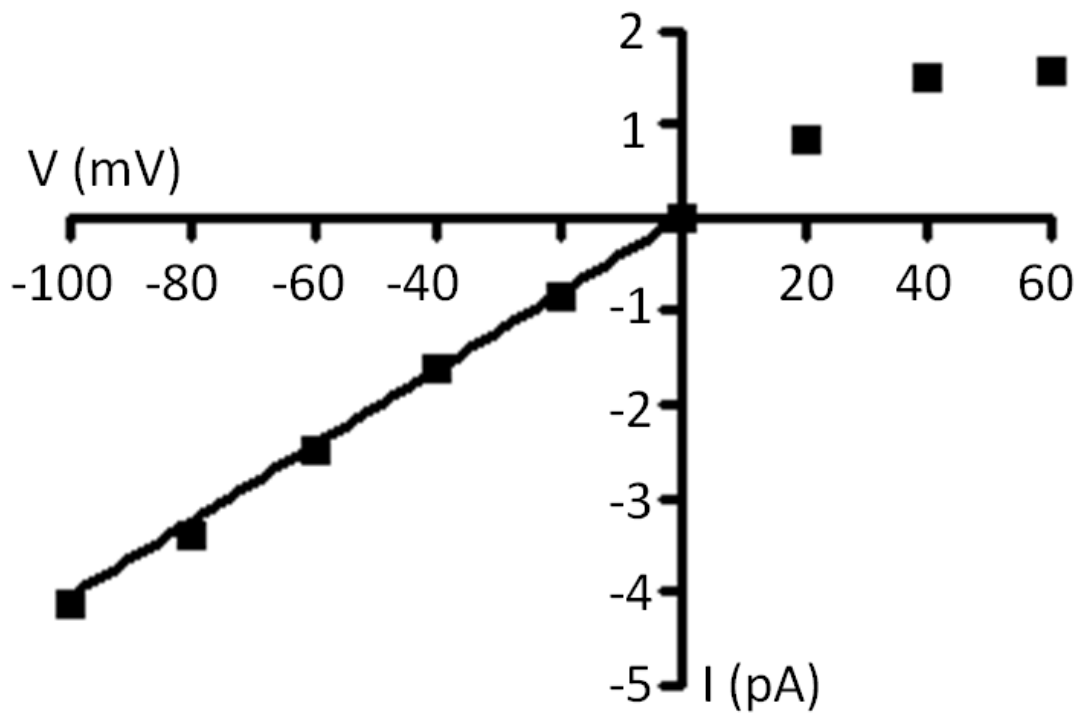


Figure 3.2 – Current-voltage relationship for $K_{ir}6.1$ and SUR2A

Single channel current-voltage relationship for $K_{ir}6.1$ and SUR2A in CHO cells. Each point represents mean \pm s.e.m. from 3 patches (1 for +60 mV) however error bars are too small to be visible. Fitted line gives conductance of 40.8 ± 3.2 pS.

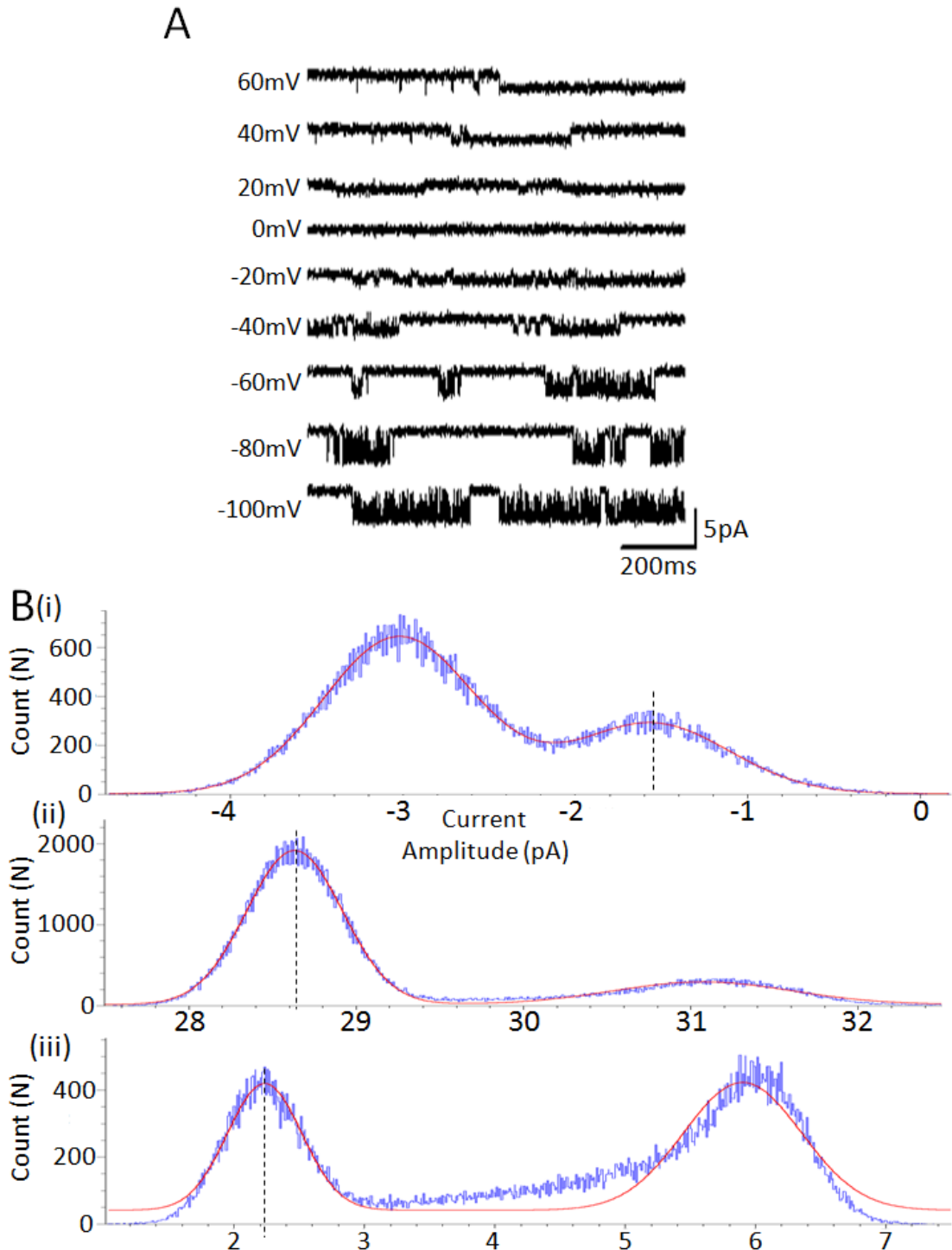


Figure 3.3 – Current-voltage relationship for $K_{ir}6.1$ and SUR2A

A, example traces of single channel recordings elicited by 10 mM UDP from an excised patch from a CHO cell expressing $K_{ir}6.1$ and SUR2A. Recordings were filtered at 1kHz. At positive potentials upward deflections are channel openings and at negative potentials downward deflections are channel openings.

B, example amplitude histograms for single channel current amplitudes of $K_{ir}6.1$ and SUR2A at (i) +60 mV, (ii) -60 mV and (iii) -100 mV. Histograms were fitted with Gaussian distributions (shown in red). The dashed lines show the peaks corresponding to the closed state.

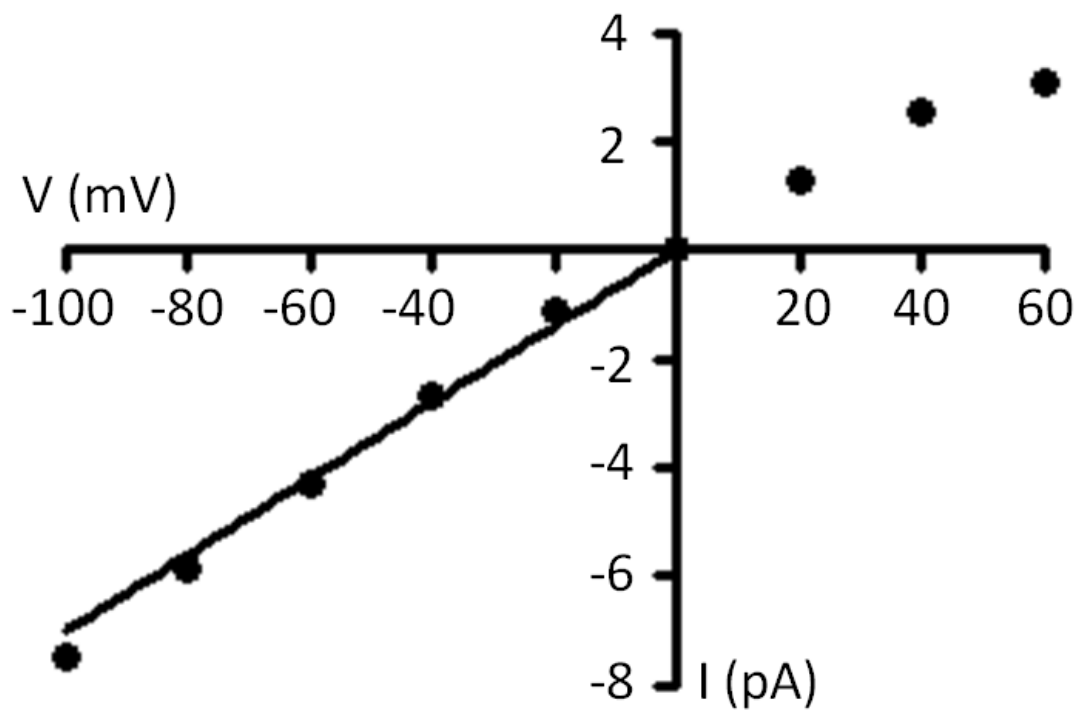


Figure 3.4 - Current voltage relationship for Kir6.2 and SUR2A

Single channel current voltage relationship for Kir6.2 and SUR2A in CHO cells. Each point represents mean \pm s.e.m. from 3 patches (2 for +60 mV) however error bars are too small to be visible. Fitted line gives conductance of 70.3 ± 1.5 pS.

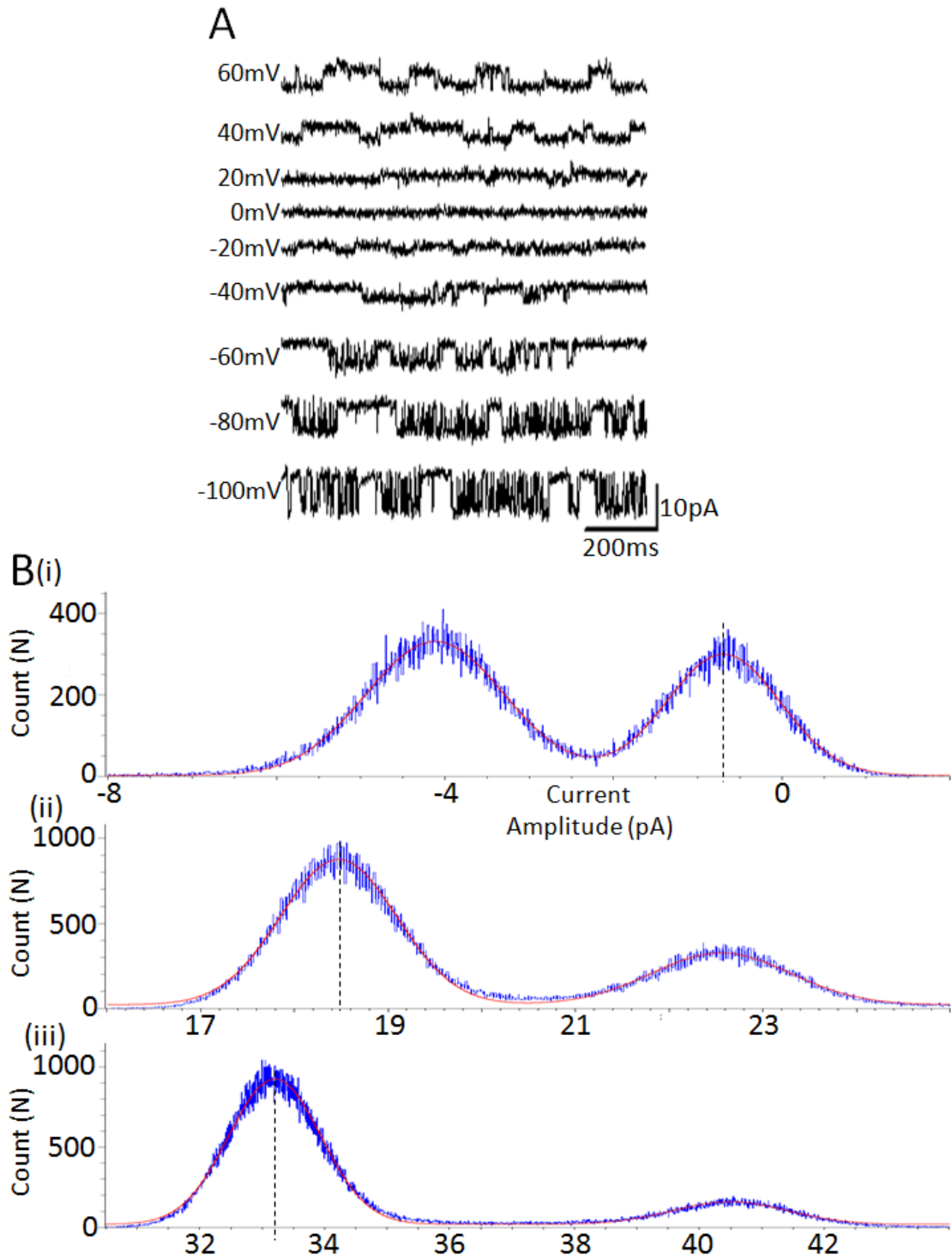


Figure 3.5 - Current voltage relationship for $K_{ir}6.2$ and SUR2A

A, example traces of single channel recordings from an excised patch from a CHO cell expressing $K_{ir}6.2$ and SUR2A. At positive potentials upward deflections are channel openings and at negative potentials downward deflections are channel openings.

B, example amplitude histograms for single channel current amplitudes of $K_{ir}6.2$ and SUR2A at (i) +60 mV, (ii) -60 mV and (iii) -100 mV. Histograms were fitted with Gaussian distributions (shown in red). The dashed lines show the peaks corresponding to the closed state.

3.2.2 *Single channel conductance of wild type channels*

The inside-out patch clamp configuration was used to obtain single channel recordings from CHO cells expressing $K_{ir}6.1$ or $K_{ir}6.2$ with SUR2A. Currents were measured at a range of membrane potentials (in 20 mV steps) and under symmetrical high (140 mM) potassium concentrations in order to construct a current-voltage relationship for both subtypes of the channel (figure 3.2 and 3.4). Each excised patch was held at membrane potentials ranging from -100 mV to +60 mV. Example traces showing single channel openings at all of the voltages for $K_{ir}6.1$ and $K_{ir}6.2$ can be seen in figures 3.3A and 3.5A respectively. All points amplitude histograms were plotted from bursts of channel activity at each voltage and fitted with Gaussian distributions, the difference in mean between the two peaks, which correspond to the open and closed states, gave the single channel current amplitude at that voltage. Examples of these histograms and the Gaussian curves fitted to them for a number of membrane potentials can be seen in figures 3.3B and 3.5B. The mean single channel current at each voltage from all patches was plotted and is shown in figures 3.2 and 3.4. As is evident from the plots, these channels display weak inward rectification at positive voltages. Consequently, measurements of the gradient to obtain values for single channel conductance were limited to the negative voltage range of the current-voltage relation. $K_{ir}6.1/SUR2A$ had a unitary conductance of 40.8 ± 3.2 pS ($n=3$). This value is a little higher than that of previously published recombinant channels of ~ 34 pS (Kondo *et al.*, 1998, Kono *et al.*, 2000) but this combination of subunits is not as frequently used as others so data is limited. The SUR subunit appears to have no impact on unitary conductance as illustrated by the conductance of $K_{ir}6.1/SUR2B$ channels of ~ 35 pS (Thorneloe *et al.*,

2002, Yamada *et al.*, 1997), confirming that the conductance obtained here for $K_{ir}6.1$ was slightly high. $K_{ir}6.2/SUR2A$ displayed a higher conductance than $K_{ir}6.1$, as expected, of 70.3 ± 1.5 pS ($n=3$). This falls within the range of values others have published, from 66-80 pS (Kondo *et al.*, 1998, Kono *et al.*, 2000, Okuyama *et al.*, 1998, Repunte *et al.*, 1999, Xie *et al.*, 1999).

3.2.3 ATP sensitivity of $K_{ir}6.2/SUR2A$

Excised inside-out patches of membrane of CHO cells expressing $K_{ir}6.2$ and SUR2A were exposed to a range of concentrations of ATP to measure the sensitivity of the channel to inhibition by ATP. This property is core to K_{ATP} channels so its measurement was essential to validate the expression system being used here. Concentrations of 1 mM, 100 μ M, 30 μ M, 10 μ M and 3 μ M ATP were tested. 1 mM ATP has previously been shown to maximally inhibit $K_{ir}6.2/SUR2A$ channels. A total of five test concentrations were selected because the number of solutions that can be tested was limited by the perfusion system being used, which only has five wells (see 2.3.3.3 and figure 2.4). The current obtained in each concentration of ATP was expressed as a fraction of that in control solution i.e. ATP-free, with the baseline taken as the current in 1 mM ATP. The dose-response curve for $K_{ir}6.2/SUR2A$ inhibition by ATP and representative current recordings are shown in figure 3.6. The concentration that inhibited current by 50% (IC_{50}) was calculated for each patch for a total of five patches but for illustration (figure 3.6A) the mean data for all five patches is plotted. The IC_{50} for inhibition of $K_{ir}6.2/SUR2A$ channels by ATP was 32.7 ± 4.3 μ M. This corresponded well to values published by others for this channel, which range from 22-43 μ M

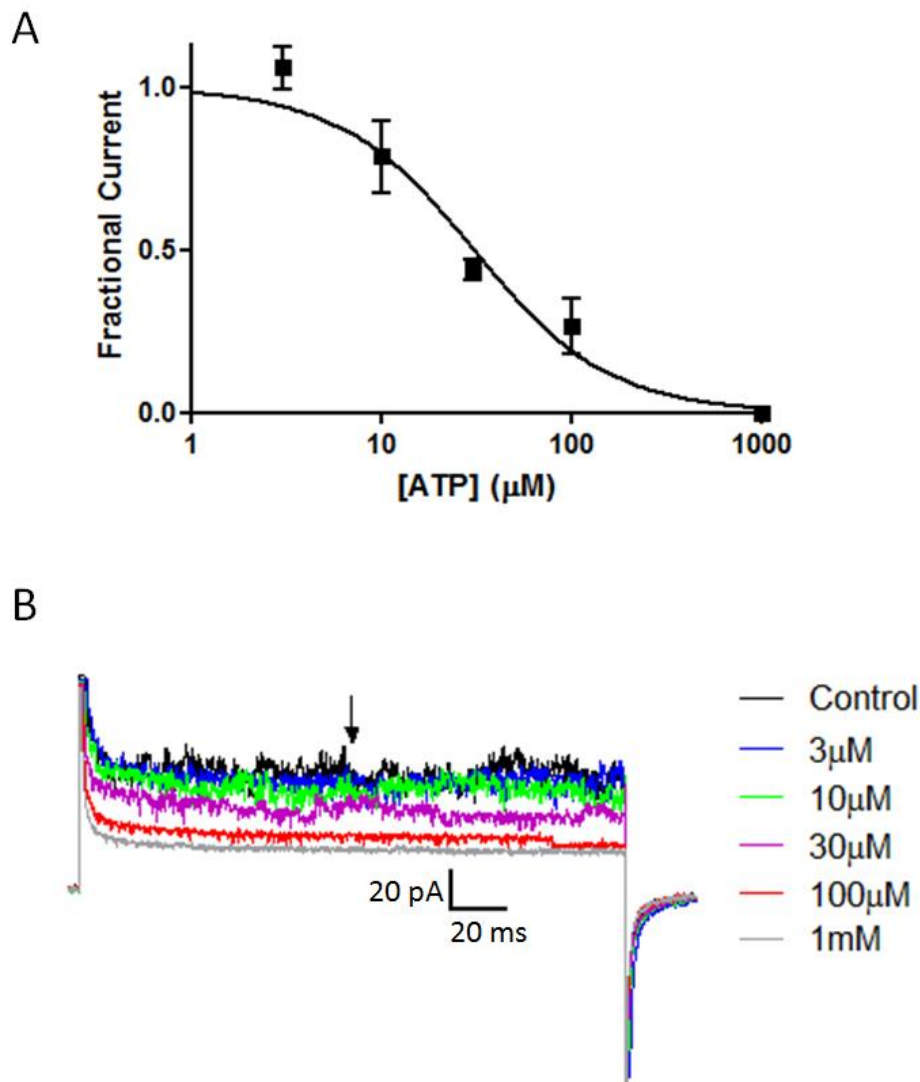


Figure 3.6 - Dose-response curve for ATP inhibiting Kir6.2 and SUR2A

A, ATP dose-response curve from excised patches from cells expressing Kir6.2 and SUR2A. Fractional current values at each concentration were calculated using the last 100 ms of a 200 ms pulse from 0 mV to -60 mV as a fraction of the value in the absence of ATP and using 1 mM ATP as the baseline. Each point represents the mean \pm s.e.m. from 5 patches. Curves were fitted using equation 1 (see 2.3.4) and the top and bottom constrained to 1 and 0, respectively. This gave an IC_{50} of $32.7 \pm 4.3 \mu\text{M}$ and a Hill slope of -1.3 ± 0.2 .

B, representative currents from Kir6.2/SUR2A in response to the concentrations of ATP shown to the right. To calculate the current in each concentration of ATP, 20 sweeps of pulses from 0 to -60 mV, for 200 ms, were recorded per concentration and the average of the last 100 ms (from the arrow to the second capacity transient) was calculated across all 20 sweeps. Traces show a single sweep, per concentration, taken from each of these 20 sweeps.

(Babenko *et al.*, 1999a, Babenko *et al.*, 1999d, Shimomura *et al.*, 2006, Tammaro & Ashcroft, 2007, Wang *et al.*, 2006).

3.2.4 Conclusion

All parameters tested for wild type Kir6.1 or Kir6.2 with SUR2A corresponded well with previously published data. Therefore, using CHO cells transiently expressing K_{ATP} channels gives a good representation of the channel and experiments to test the effect of mutating these subunits can now be carried out with confidence.

Chapter Four

Construction and characterisation of mutant $K_{ir}6.0$ subunits

4 Construction and characterisation of mutant Kir6.0 subunits

4.1 Introduction

The ability to open spontaneously when inhibitory nucleotides are removed is a defining characteristic of K_{ATP} channels containing $K_{ir}6.2$. Channels that contain $K_{ir}6.1$ do not behave in this manner and require opening either with pharmacological openers, such as pinacidil or diazoxide, or with stimulatory nucleotide diphosphates (hence channels containing $K_{ir}6.1$ are sometimes called K_{NDP}). The regions that cause spontaneous opening have been partly identified but little progress has been made determining what causes the difference in characteristics between the two subunits.

Truncation of the N-terminus of $K_{ir}6.2$ by 30 or 35 amino acids has been shown to produce channels with dramatically increased open probability (P_o ; Babenko *et al.*, 1999b, Koster *et al.*, 1999b). This was shown to be caused by an alteration in the kinetics of channel closure where the transition from the open state to the interburst closed state was all but abolished. The intraburst kinetics were unaffected by the truncation (Babenko *et al.*, 1999b, Koster *et al.*, 1999b). This suggests that the N-terminus of $K_{ir}6.2$ is either involved in stabilising the closed state or destabilising the open state of the channel and that its removal drives the channel towards the open state. Within this region of the N-terminus are several differences in amino acid sequence between $K_{ir}6.1$ and $K_{ir}6.2$. As you can see from the sequences in figure 4.1, the greatest difference occurs at residues 19-24 in $K_{ir}6.1$ (19-23 in $K_{ir}6.2$). There are numerous differences in charge as well as one more residue in $K_{ir}6.1$ than $K_{ir}6.2$. The

	1	11	21	31	41	51	61	71	75
rK _{ir} 6.1	MLARKSIIPE	EYVLARIAAE	<u>NLRKPRIRDR</u>	LPKARFIAKS	<u>GACNLAHQNI</u>	REQGRFLQDI	FTTLVDLKWR	HTLVI	
mK _{ir} 6.1	MLARKSIIPE	EYVLARIAAE	NLRKPRIRDR	LPKARFIAKS	GACNLAHKNI	REQGRFLQDI	FTTLVDLKWR	HTLVI	
hK _{ir} 6.1	MLARKSIIPE	EYVLARIAAE	NLRKPRIRDR	LPKARFIAKS	GACNLAHKNI	REQGRFLQDI	FTTLVDLKWR	HTLVI	
rK _{ir} 6.2	MLSRKGIPE	EYVLTRLAED	-PTEPRYRTR	ERRARFVSKK	<u>GNCNVAHKNI</u>	REQGRFLQDV	FTTLVDLKWP	HTLLI	
mK _{ir} 6.2	MLSRKGIPE	EYVLTRLAED	-PAEPRYRTR	ERRARFVSKK	GNCNVAHKNI	REQGRFLQDV	FTTLVDLKWP	HTLLI	
hK _{ir} 6.2	MLSRKGIPE	EYVLTRLAED	-PAKPRYRAR	QRRARFVSKK	GNCNVAHKNI	REQGRFLQDV	FTTLVDLKWP	HTLLI	
	:*:*.***	*****:*:* :	:** * *	:***:;*.	* **:*:*:**	*****:*:	*****:	***:*	

Figure 4.1 - N-termini of rat, mouse and human K_{ir}6.0

Sequence alignments were performed using ClustalW2. The residues being studied here are underlined. The symbols, which are taken from the ClustalW2 output, beneath the sequence identify whether the residues are conservative or not where "*" means that the residues in that column are identical in all sequences in the alignment; ":" means that conserved substitutions have been observed and "." means that semi-conserved substitutions are observed. The space is left blank for columns containing non-conservative residues. NCBI references/ GenBank numbers of the sequences for K_{ir}6.1 are: rat - BAA96238.1, mouse - NP_032454.1, and human - NP_004973.1; and for K_{ir}6.2 are: rat - BAA96239.1, mouse - NP_034732.1, and human - NP_000516.3.

sequence alignment using ClustalW2 shown in figure 4.1 shows that the additional residue in K_{ir}6.1 is most likely located between the aspartate and proline of K_{ir}6.2. Using this alignment to assess the extent of each substitution with respect to substituting the K_{ir}6.2 sequence with that from K_{ir}6.1 – D20E is conservative as both residues are acidic, polar and negatively charged; the P21L mutation is also conservative as both are small and hydrophobic; T22 is polar and uncharged while R23 is positively charged, making this a fairly substantial alteration; and E23K, which is the most striking of all, replaces a negative charge with a positive one. The proline at position 21 in K_{ir}6.2 also adds a structure break or possible hinge. A common single nucleotide polymorphism in KCNJ11 linked with type 2 diabetes, a guanine to adenine mutation resulting in the E23K amino acid switch (Sakura *et al.*, 1996), produces a channel with an increased P_o and concurrent decrease in ATP sensitivity (Schwanstecher & Schwanstecher, 2002). It is for these reasons that this region is a very attractive candidate for exchange between the subtypes.

A study in which all of the positive charges in the N-terminus of K_{ir}6.2 were systematically mutated to alanine identified several residues that affect the P_o of the channel (Cukras *et al.*, 2002a). Two of these mutants, R16A and R27A, caused an increase in P_o to a value close to its theoretical maximum. This would suggest that these residues are important in open state stability. These residues are conserved in K_{ir}6.1 (R16 and R28) therefore it is impossible that they are directly responsible for the difference in spontaneous opening. However, their flanking residues are not conserved. Exchanging the triplet of residues including R16 and R27/28 between K_{ir}6.1

and Kir6.2 will give an indication as to whether the immediate tertiary environment of these arginine residues affects open state stability.

Most remarkably, a method of measuring spontaneous opening similar to that used here was used to identify short regions of the N- and C-termini of Kir6.2 that, when simultaneously exchanged for the equivalent residues in Kir6.1, produced channels with spontaneous opening characteristics similar to Kir6.1 (Kondo *et al.*, 1998). This study identified a region of 9 amino acids in the N-terminus and 6 in the C-terminus that are a structural prerequisite for the spontaneous opening of Kir6.2, or the lack thereof in Kir6.1. Neither region was further dissected. The region of the N-terminus identified contains only four disparate amino acids between Kir6.1 and Kir6.2.

It was hoped that by exchanging the above regions/residues between Kir6.1 and Kir6.2 it would be possible to identify more precisely the structures within these subunits that give rise to their differing spontaneous opening characteristics.

4.2 Production of mutant cDNA

In order to investigate the functional significance of various N-terminal structural elements of the pore-forming subunit of K_{ATP} , a set of mutant Kir6.1 and Kir6.2 subunits was produced. Overlap PCR and restriction digestion were the techniques used to produce mutant cDNA in vectors allowing expression in the CHO mammalian cell line. To illustrate this, I will describe the steps employed to produce one Kir6.1-based mutant – DPTE, and one Kir6.2-based mutant – N41A.

4.2.1 Overlap PCR to produce mutant $K_{ir}6.0$ cDNA

The process of overlap PCR was described earlier (2.1.1, see also figure 2.2). PCRs for production of all mutants used two common primers that formed the 5' and 3' ends of the full length product. For $K_{ir}6.1$ mutants these primers were called 61-1 and 61-2 (62-1 and 62-2 for $K_{ir}6.2$). Similarly, PCRs to mutate each subunit shared templates. For $K_{ir}6.1$ mutants this was the *Xenopus* oocyte expression vector containing wild type rat $K_{ir}6.1$ cDNA – pBFTr6.1 (pBFTr6.2 for $K_{ir}6.2$ mutants). Plasmid maps of these templates can be seen in figure 4.2. The pBFTr6.1/2 cDNA clones were selected as a template, rather than a mammalian equivalent, as they could produce large enough cDNA fragments from restriction digests for easy manipulation in later steps but small enough fragments to minimise the risk of unwanted second site mutations. *Taq* polymerases are error prone where the larger the fragment being produced, the greater the risk of error, but despite using a proof-reading polymerase the easiest way to minimise error was to use as small a fragment as possible during cloning. As a redundancy, this cloning method also gave the option of expressing the channels in *Xenopus* oocytes. Two overlapping primers were produced for each mutant containing the mutated sequence, which did not bind in early stages of PCR, and a region of sequence complementary to the template, to bind in these early stages (see figure 2.2 for diagram of these primers' interaction; see table 4.1 for all primer sequences). These overlapping primers also had an important role in checking the success of the cloning strategy. Along with the mutation to the coding sequence, a silent mutation was introduced i.e. that changed the DNA sequence but not the coding sequence.

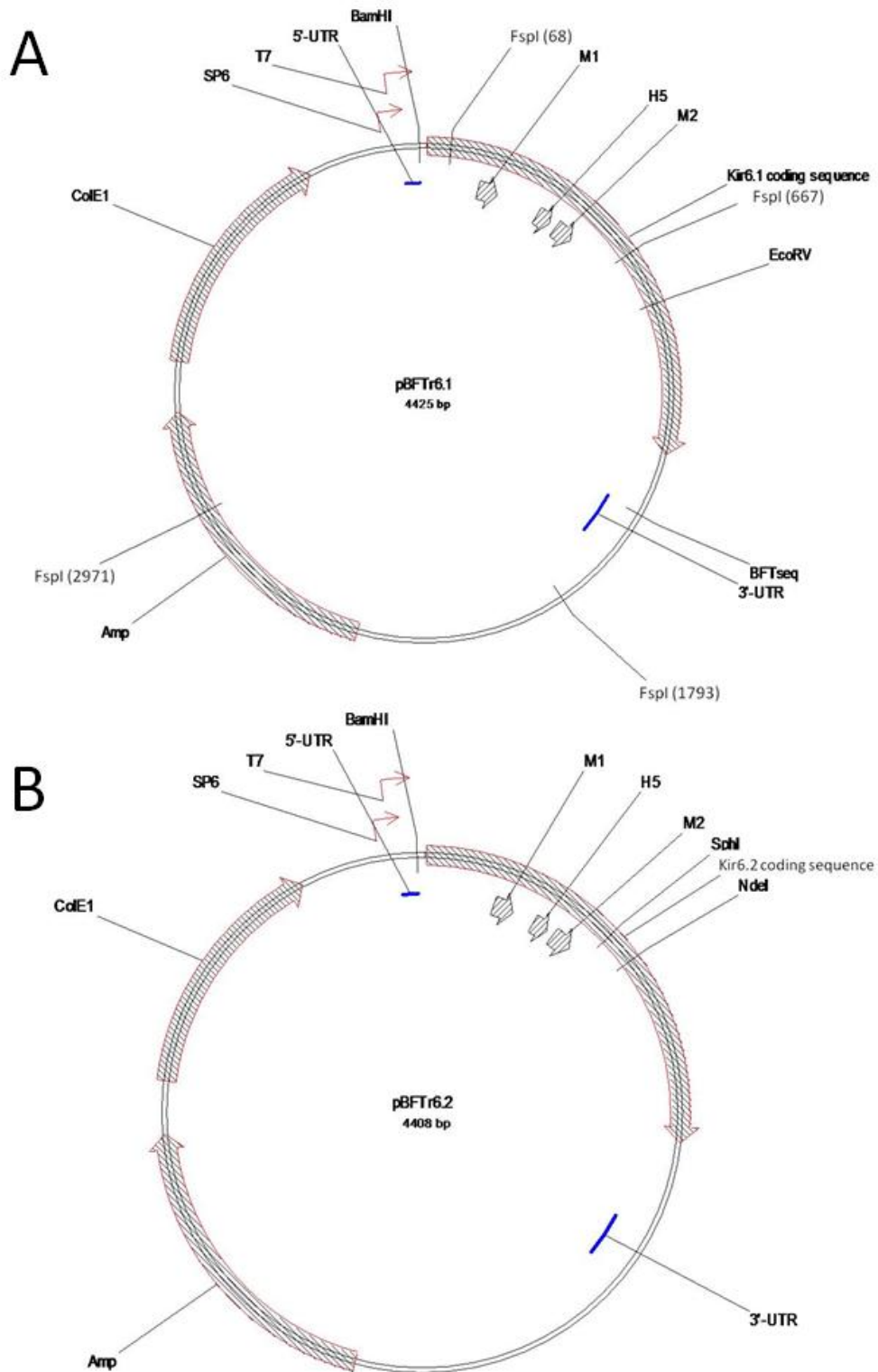


Figure 4.2 - Maps of *Xenopus* oocyte expression vector for Kir6.1/2

A, *Xenopus* oocyte expression vector for Kir6.1.

B, *Xenopus* oocyte expression vector for Kir6.2.

All restriction sites for cloning (in the examples that follow – DPTE and N41A) and checking for successful mutation have been shown. All other restriction sites have been omitted for clarity. These vectors served as a template for overlap PCR and were digested to allow insertion of mutant DNA.

	Primer 1 Sequence	Primer 2 Sequence	Check Enzyme
ARI	<u>GATTC</u> (<u>TGGCCA</u>) GC CACATATTCCTCAGGGATAATGC	AATATGTGC (<u>TGGCCA</u>) <u>GAATC</u> GCAGAGGACCCTACAGAGCC	<i>MscI</i>
ENLRK	<u>TT</u> (<u>TGCGCA</u>) <u>GGTTCTCCT</u> CTGCCAGCCGGGTCA	CAGAGGAGAA <u>ACC</u> (<u>TGCGCA</u>) <u>A</u> ACCAGGTACCGTACTCGGG	<i>FspI</i>
IRD	<u>ATCGC</u> (<u>GGATCC</u>) TGGGCTCTGTAGGGTCC	CAGAGCCCA (<u>GGATCC</u>) <u>GCGAT</u> CGGGAGAGGAGGGCCC	<i>BamHI</i>
S37A	AGTTGCCTTTC (<u>TTGGCC</u>) ACGAAGCGGGCCCTC	GCCCCGCTTCG (<u>TGGCCA</u>) AGAAAGGCAACTGCAACGT	<i>MscI</i>
K39S	(TCCGGA)CTTGGACACGAAGCGGG	GCTTCGTGTCCAAG (TCCGGA) AACTGCAACGTCGCCC	<i>BspEI</i>
N41A	(<u>GCA</u> <u>TGC</u>) GCCTTTCTTGGACACGAAGC	TGTCCAAGAAAGGC (<u>GCA</u> <u>TGC</u>) AACGTGCCCCACAAGAACA	<i>SphI</i>
V44L	GTTCTTGTGGGCC <u>CAG</u> GTTGCAGTTGCCTTTCTTGG	GGCAACTGCAAC <u>CT</u> TGGCCCCACAAGAACATCCGA	N/A
ASAL	<u>CAG</u> GTTGCAG <u>GC</u> (TCCGGA) CTTGGCCACGAAGCGGGCCCTC	<u>GCCA</u> AG (TCCGGA) <u>GCCT</u> GCAAC <u>CT</u> TGGCCCCACAAGAACATCCGA	<i>BspEI</i>
S40K	(<u>GCA</u> <u>TGC</u>) TCCTTTCTTGGCGATGAAGCGGG	TCGCCAAG <u>AAA</u> GGA (<u>GCA</u> TGC) AACCTGGCTCACAAGAACATC	<i>SphI</i>
A42N	<u>GTT</u> (TCCGGA) CTTGGCGATGAAGCGGG	TCATCGCCAAG (TCCGGA) <u>AACT</u> GCAACCTGGCTCACAAGAAC	<i>BspEI</i>
DPTE	<u>CTCTGTAGGGTCCG</u> CCGCGATGCGGGCCAGCACAT	TCGCGGCG <u>GACCCTACAGAG</u> CCGCGCATCCGCGACCGCCTCC	<i>FspI</i> (removed)
TRL	<u>CAGTCTT</u> (<u>GT</u> TAAC) ACATACTCCTCCGGGATGA	GTATGT (<u>GT</u> TAAC) <u>AAGACT</u> GCGGCGGAGAACCTGC	<i>HpaI</i>
YRT	TGGGGAGGCGT <u>GTTCTGTA</u> (CCGCGG) TTTGCGCAGG	G <u>TACAGAACACGCCT</u> CCCCAAAGCC	<i>SacII</i>
K _r 6.1	ATTACCGCCTTTGAGTGAGC (a.k.a. 61-1)	TCCCTCCTCCTCAGTCACAA (a.k.a. 61-1)	
K _r 6.2	ACCGTATTACCGCCTTTGAG (a.k.a. 62-1)	TGGTGGAGAGGCACAACCT (a.k.a. 62-2)	
(pIRES) 6.2-5	CGTGTACGGTGGGAGGTCT		

Table 4.1 - PCR primers

Primer sequences for all PCR primers. Above the horizontal bold line are overlapping primers, below are the subunit specific primers used in PCRs for the relevant subunit. Underlined sequence indicates the mutated codons. Bold, italic letters are additional silent mutations. Sequence in parenthesis shows the relevant restriction site used (see “Check Digest” column for enzyme) to check for successful mutation. V44L required sequencing as no silent mutation was possible. In the case of YRT2, the guanine at the 5’ end is a silent mutation to introduce a *SacII* site however the rest of the site already existed in the wild type cDNA and did not need to be included in the primer sequence. (pIRES) 6.2-5 was an additional subunit specific primer used in the production of S37A, V44L and ASAL as these were produced separately to the other mutants and cloned directly into pIRES2 so they required a different 5’ subunit specific primer. 62-2 was still used as the 3’ primer in these cases.

	PCR 1	PCR 2	Overlap PCR	Digest of Overlap PCR	pBFT Check Digest	Digest of pBFT Clones	pIRES2 Check Digest
ARI	359	672	1012	667 (<i>Bam</i> HI/ <i>Nde</i> I)	4018 + 390	1440	5256, 1001, 444, 109 + 13
ENLRK	380	654	1015	670 (<i>Bam</i> HI/ <i>Nde</i> I)	1525, 1178, 667, 594 + 444	1440	5256, 1001, 444, 112 + 13
IRD	392	639	1012	810 (<i>Nde</i> I/ <i>Sac</i> II)	4314 + 92	1583	3854, 2889 + 215
S37A	213	607	793	417 (<i>Nhe</i> I/ <i>Bsp</i> EI)	N/A	N/A	2627, 2244, 1608 + 324
K39S	428	603	1012	667 (<i>Bam</i> HI/ <i>Nde</i> I)	3368 + 1040	1440	5256, 1001, 444, 109 + 13
N41A	434	597	1012	667 (<i>Bam</i> HI/ <i>Nde</i> I)	3974 + 434	1440	5256, 1001, 444, 109 + 13
V44L	233	586	793	417 (<i>Nhe</i> I/ <i>Bsp</i> EI)	N/A	N/A	N/A – sequenced
ASAL	221	595	793	417 (<i>Nhe</i> I/ <i>Bsp</i> EI)	N/A	N/A	4151, 1612 + 1040
S40K	429	889	1300	854 (<i>Bam</i> HI/ <i>Eco</i> RV)	Linearised	1457	3854, 2092, 663 + 231
A42N	426	892	1300	854 (<i>Bam</i> HI/ <i>Eco</i> RV)	3350 + 1075	1457	3854, 2092, 663 + 231
DPTE	366	949	1300	851 (<i>Bam</i> HI/ <i>Eco</i> RV)	2128, 1178 + 1116	1457	3854, 2092, 663 + 228
TRL	351	966	1300	854 (<i>Bam</i> HI/ <i>Eco</i> RV)	Linearised	1457	3854, 2092, 663, 154 + 77
YRT	397	921	1300	854 (<i>Bam</i> HI/ <i>Eco</i> RV)	4189 + 236	1457	3854, 2092, 663 + 231

Table 4.2 - PCR and restriction digest fragment sizes

All fragment sizes (in base pairs) for all PCRs and restriction digests for mutant K_{ir}6.1 and Kir6.2 (below and above horizontal bold line, respectively). PCR 1 refers to reactions using the 5' subunit specific primer (61-1 or 62-1) and mutant primer 1. PCR 2 refers to reactions using the 3' subunit specific primer (61-2 or 62-2) and mutant primer 2. Enzymes used in pBFT check digest are listed in table 4.1. All pBFT clones were treated with *Bam*HI and *Bgl*II with the exception of IRD which was digested with *Sac*II and *Bgl*II. ARI, ENLRK, K39S and N41A used *Apa*I; S37A used *Msc*I; ASAL used *Bsp*EI; IRD and all K_{ir}6.1 mutants used *Hinc*II as pIRES check digests. pBFT check digests and digests of pBFT clones for S37A, V44L and ASAL are not included because these were inserted straight into pIRES2.

Codon usage charts were used to ensure that no rare codons were being introduced by these silent mutations. In DPTE this silent mutation removed an *FspI* site while for N41A an additional *SphI* site was introduced (compare restriction sites in figures 4.2 and 4.5). This meant that at the end of the cloning process, a further restriction digest reaction could be set up where the fragments obtained from mutant cDNA would be different from wild type cDNA. A similar strategy was employed for all mutants (see table 4.1 for list of added/removed restriction sites).

For both DPTE and N41A, two reactions were set up containing different sets of primers. To use the example of DPTE, the reaction containing primers 61-1 and DPTE1 produced a fragment containing the mutated sequence at its 3' end and the 5' end of the eventual full length product. This fragment was expected to be 366 base pairs (bp) in length. The reaction using 61-2 and DPTE2 produced a fragment containing the mutated sequence at its 5' end and the 3' end of the eventual full length product. This fragment was expected to be 949 bp. The same can be said for N41A – 62-1 and N41A1 gave a product of 434 bp while 62-2 and N41A2 produced a 597 bp fragment. Photographs of agarose gels of the PCRs can be seen in figure 4.3A and B.

A second PCR was then carried out containing the products of the first two PCRs and the subunit specific primers 61-1/2 or 62-1/2. The overlapping nature of the products of the first set of reactions (see figure 2.2) meant that during this second set they acted as both primers and templates. This produced relatively small amounts of the full length fragment which were amplified by binding of the 61-1/2 or 62-1/2 primers in later cycles. For DPTE the product of this reaction was expected to be 1300 bp while

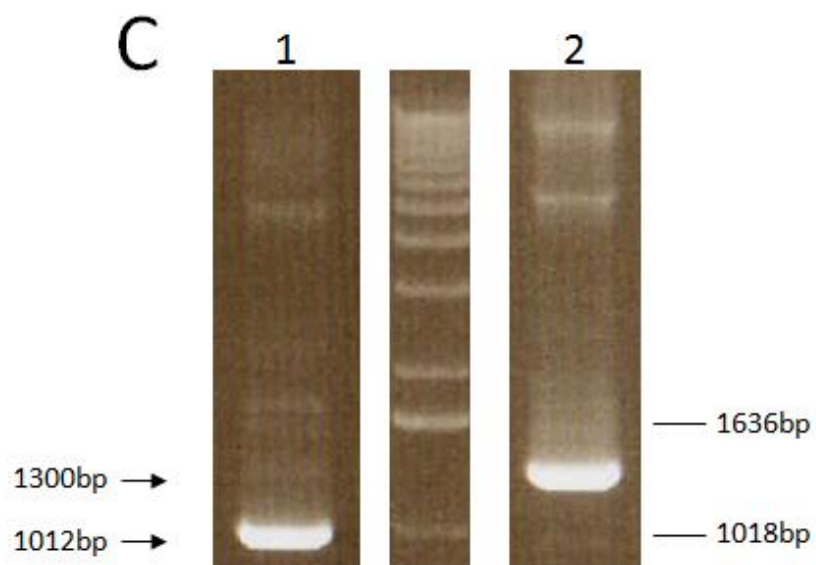
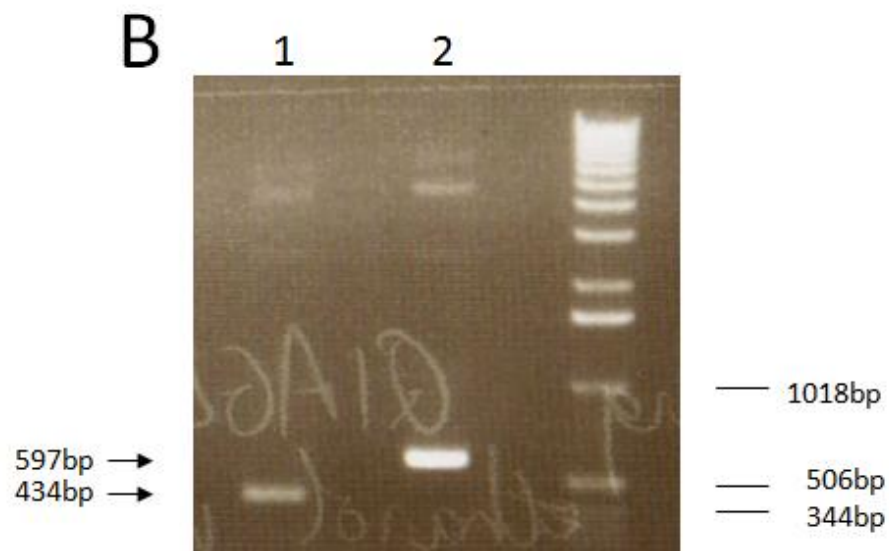
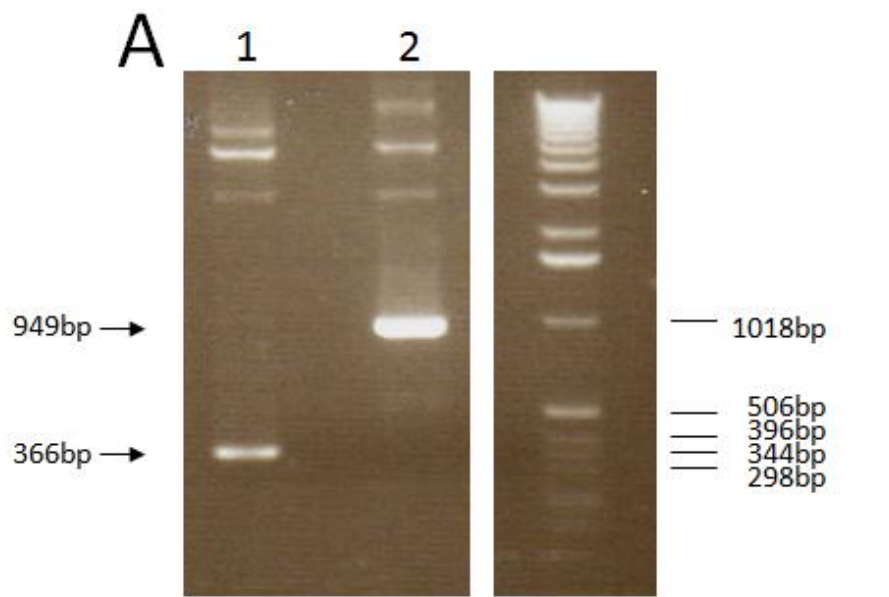


Figure 4.3 - Agarose gel electrophoresis of PCR products for DPTE and N41A mutants

Figure 4.3 – Agarose gel electrophoresis of PCR products for DPTE and N41A mutants

A, product of the PCR to create the DPTE mutant. Lane 1 shows the product of the PCR using primers DPTE1 and 61-1 expected to be 366 base pairs. Lane 2 shows the product of the PCR using primers DPTE2 and 61-2 expected to be 949 base pairs. Both PCRs used pBFTr6.1 as a template.

B, product of the PCR to create the N41A mutant. Lane 1 shows the product of the PCR using primers N41A1 and 62-1 expected to be 434 base pairs. Lane 2 shows the product of the PCR using primers N41A2 and 62-2 expected to be 597 base pairs. Both PCRs used pBFTr6.2 as a template.

C, products of the overlap PCRs for DPTE and N41A. These reactions used the products of earlier PCRs, shown in A (lane 2) and B (lane 1), as both templates and primers. A further set of primers that provided a start point and end point for the cDNA fragment was also included. For lane 1 these additional primers were 62-1 and 62-2. For lane 2 these additional primers were 61-1 and 61-2. Overlap PCR products in lanes 1 and 2 were expected to be 1012 and 1300 base pairs, respectively.

Arrows point to fragments of the indicated size in the test lanes. All sizes on the right hand side of the photographs indicate fragments in the 1kb ladder used for size reference.

the N41A product was expected to be 1012 bp (figure 4.3C). Once this second phase of PCRs was proved to be successful, by agarose gel electrophoresis, reactions were scaled up five fold and repeated. This allowed production of enough DNA to treat with restriction endonucleases to produce a fragment of mutated cDNA for insertion into the expression vector.

4.2.2 Cloning mutant cDNA into *Xenopus* oocyte expression vector

With enough full length PCR product purified, a double restriction digest was set up to excise part of the mutated $K_{ir}6.0$ cDNA for insertion into the *Xenopus* oocyte expression vector, pBFT. For DPTE this involved digesting with *EcoRV* and *BamHI* to generate a fragment of 851 bp for insertion. For N41A, *BamHI* and *NdeI* were used giving a 667 bp fragment for insertion. The location of these restriction sites on the recipient vector can be seen in figure 4.2. Also, pBFT6.1 was treated with *EcoRV* and *BamHI* and pBFT6.2 digested with *BamHI* and *NdeI* to remove the wild type sequence and create the insertion site. To minimise vector re-circularisation in ligation reactions the vector digests were also treated with shrimp alkaline phosphatase (SAP). All of the reactions were incubated overnight to ensure the DNA was fully digested. The combinations of restriction enzymes used for all mutants and expected fragment sizes are shown in table 4.2. The restriction digests of PCR products and dephosphorylated vector were run on an agarose gel to separate the fragments of interest from unwanted DNA. The gels were viewed under UV light and each fragment was cut out of the gel and purified. Ligation reactions were set up and ligated DNA was used to transform chemically competent DH5 α cells (see 2.1.2 for details). Transformed cells were grown on agar plates. Colonies were used to create a suspension culture that was

used to replicate cDNA to high quantities before isolation and purification (see 2.1.3 for details).

To check for successful insertion of mutated cDNA into the vector, *FspI* and *SphI* digests were set up for DPTE and N41A, respectively, alongside digests of pBFTr6.1 and 6.2 for comparison. This allowed identification of those clones that had had mutant cDNA correctly inserted. Agarose gels were run to visualise the results of these digests (figure 4.4). Successfully mutated DPTE and N41A clones gave fragments of 2128, 1178 and 1116 bp or 3974 and 434 bp, respectively. The gels show that all DPTE clones and N41A clones 1, 2 and 4 were successfully mutated (figure 4.4). Each of these clones was then sequenced to confirm successful mutation and to ensure that no other bases had been altered. Plasmid maps of pBFTr6.1-DPTE and pBFTr6.2-N41A can be seen in figure 4.5.

4.2.3 Cloning mutant cDNA into mammalian expression vector

In order to express the mutant subunits in CHO cells they also required sub-cloning into the pIRES2 vector (see figure 4.6). This vector possesses a CMV promoter and an internal ribosome entry site (IRES) that allows expression of a bicistronic mRNA transcript i.e. simultaneous expression of two proteins. In this case, wild type or mutant K_{ir}6.0 expressed alongside a farnesylated version of enhanced green fluorescent protein (EGFP-F).

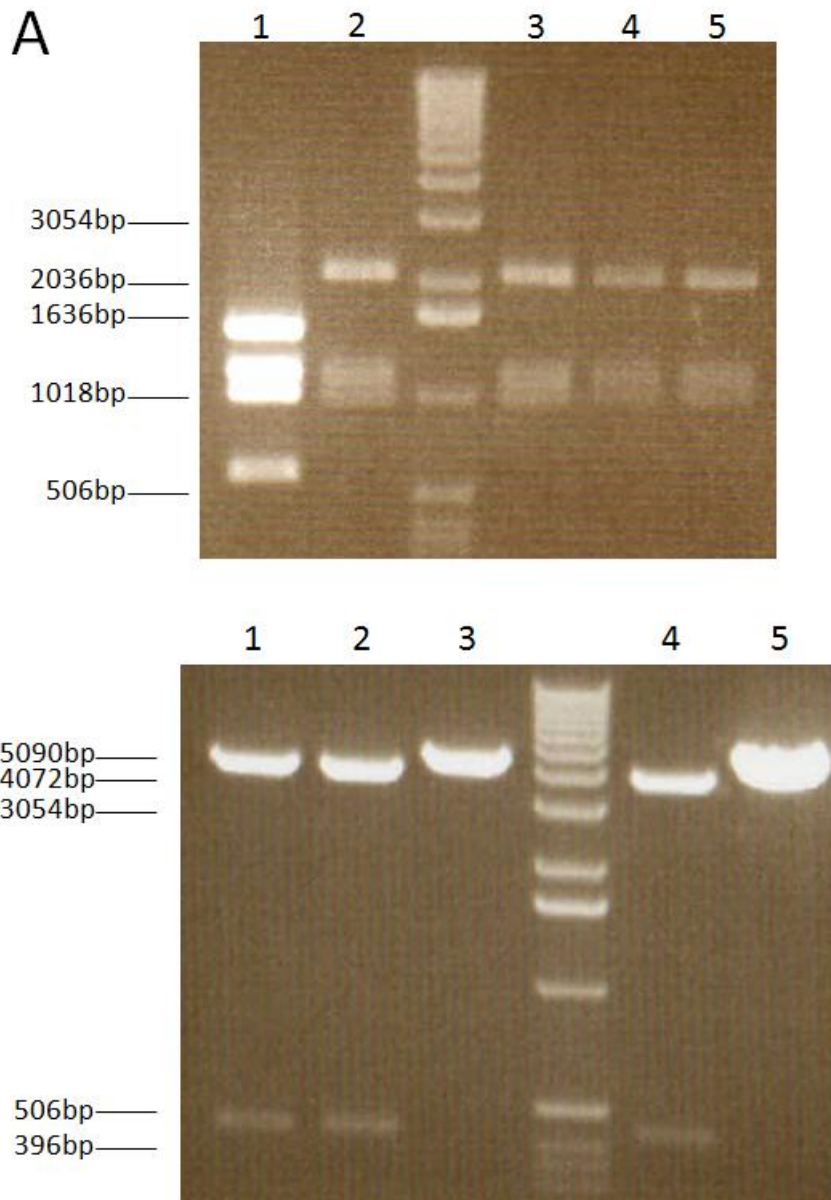


Figure 4.4 - Agarose gel electrophoresis of restriction digests to check for successful cloning of mutant cDNA into the *Xenopus* oocyte expression vector pBFT

A, photograph of *FspI* digest of pBFT6.1 (lane 1) and possible pBFT6.1-DPTE clones (lanes 2-5). Successfully mutated and inserted DPTE cDNA would give fragments of 2128, 1178 and 1116 base pairs. All four clones show successful insertion of mutated cDNA.

B, photograph of *SphI* digest of pBFT6.2 (lane 5) and possible pBFT6.2-N41A clones (lanes 1-4). Successfully mutated and inserted N41A cDNA would give fragments of 3974 and 434 base pairs. Clones 1, 2 and 4 show successful insertion of mutated cDNA. All sizes alongside the photographs indicate fragments in the 1kb ladder used for size reference.

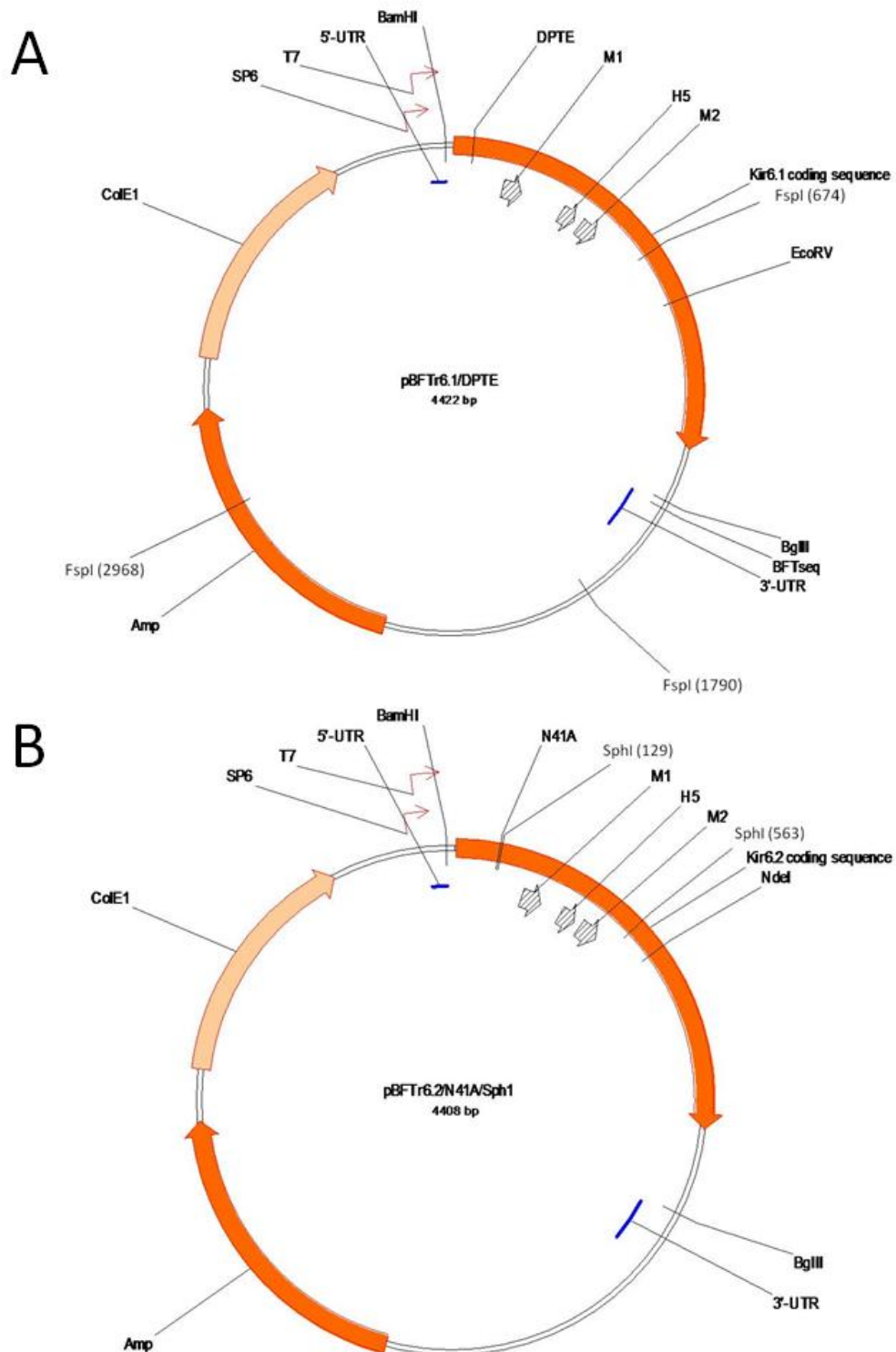


Figure 4.5 - Maps of *Xenopus* oocyte expression vectors for pBFTTr6.1/DPTE and pBFTTr6.2/N41A/Sph1

A, *Xenopus* oocyte expression vector encoding DPTE. When the DPTE mutation was made an *FspI* restriction site was removed (see pBFTTr6.1 in figure 4.2).

B, *Xenopus* oocyte expression vector encoding N41A. When the N41A mutation was made a *SphI* restriction site was inserted (see pBFTTr6.2 in figure 4.2).

All features that were important for this work are highlighted but not all features of the plasmids are shown for clarity.

In contrast to cloning of the mutant subunits into pBFT, the pIRES2 vector used only encoded EGFP-F so the whole $K_{ir}6.0$ cDNA had to be inserted. To do this a double digest was once again performed to excise the cDNA from pBFT (see table 4.2 for combinations used for all mutants). For both DPTE and N41A a *Bam*HI and *Bgl*II digest was set up. The location of these restriction sites relative to the $K_{ir}6.0$ coding sequence in pBFT can be seen in figure 4.5. These enzymes produce the same sticky ends when cleaved so only a single digest of the pIRES2-EGFP-F vector, with *Bgl*II, was necessary to accommodate the insert. As before, the digested vector was dephosphorylated with SAP and both the insert fragment and linearised vector were purified from an agarose gel and quantified prior to ligation of insert into vector and transformation of DH5 α cells. It should be noted that the antibiotic resistance conferred on *E. coli* by pIRES2 is kanamycin. To check for successful ligation and transformation, a restriction digest was set up. For $K_{ir}6.1$ -based mutants *Hinc*II was used and in the case of DPTE this would give fragments of 228, 663, 2092 and 3854 bp if DPTE cDNA was successfully inserted (figure 4.7A). For $K_{ir}6.2$ -based mutants *Apa*I was used and successful insertion of cDNA gave fragments of 13, 109, 404, 1001 and 5256 bp for N41A (figure 4.7B). Successful clones were sequenced to further confirm error-free insertion. Plasmid maps of the final DPTE and N41A expression vectors can be seen in figure 4.8. The name of each mutant created and a brief description of the alteration to the amino acid sequence can be seen in table 4.3.

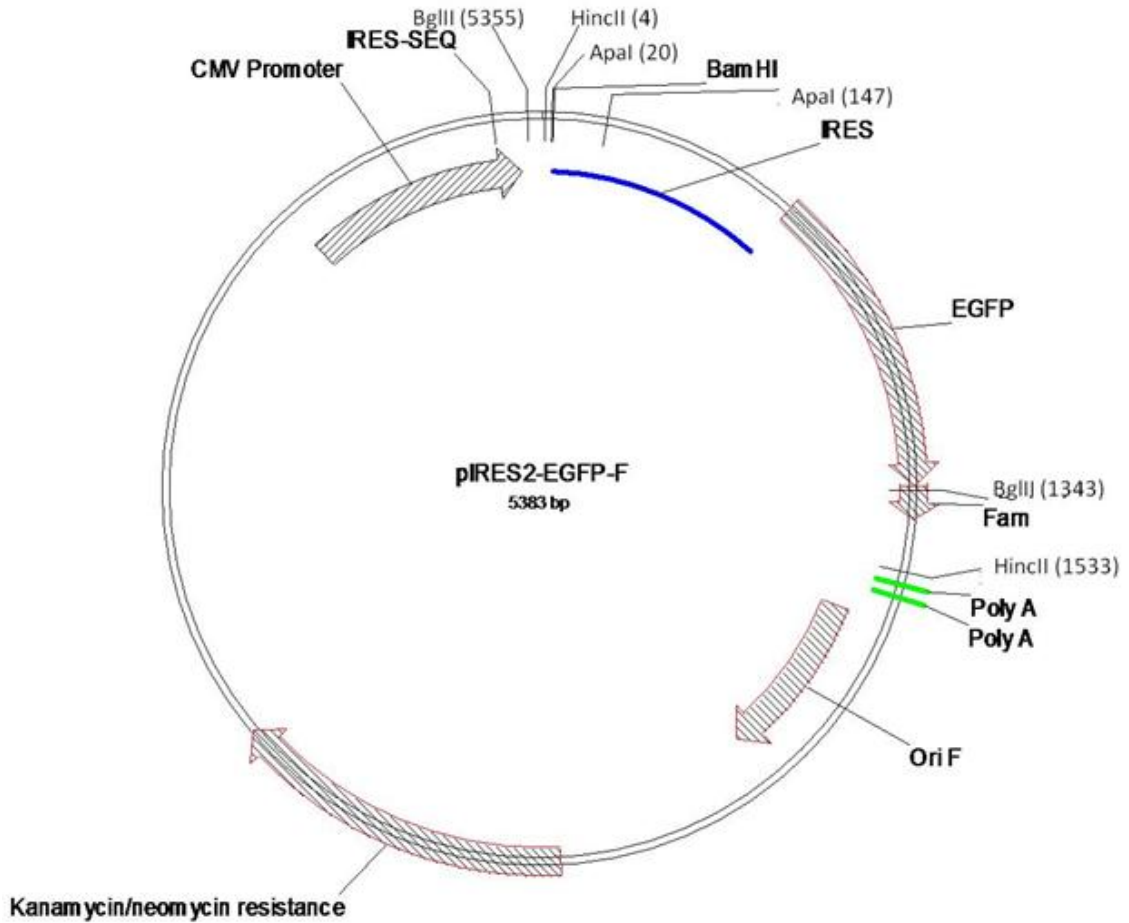


Figure 4.6 - Mammalian expression vector pIRES2-EGFP-F

Plasmid map of pIRES2-EGFP-F. All restriction sites for cloning of mutant cDNA into the vector (in the examples followed – DPTE and N41A) and for checking success of mutation have been shown. Due to the small number being used compared to the total number of sites present, all other restriction sites have been omitted for clarity.

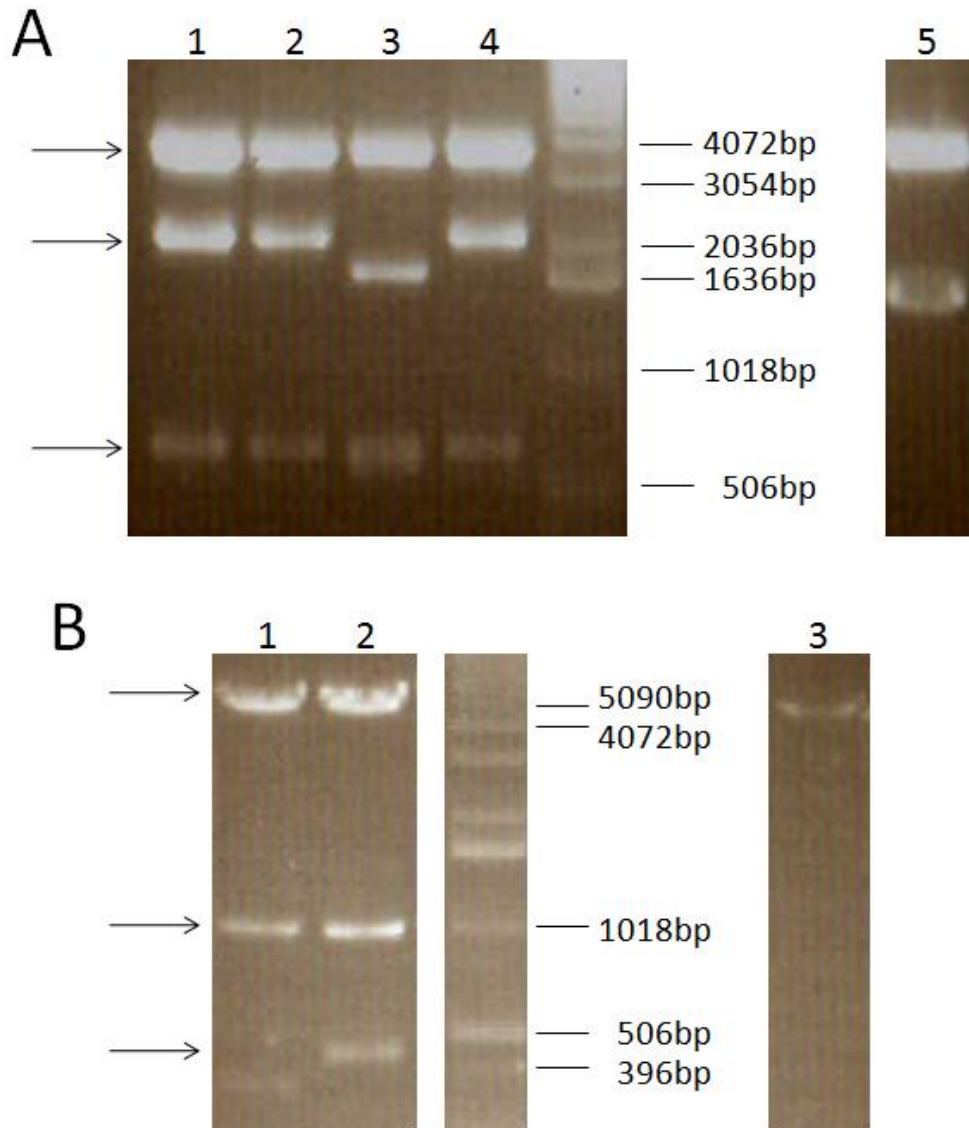


Figure 4.7 - Agarose gel electrophoresis of restriction digests to check for successful cloning of mutant cDNA into the mammalian expression vector pIRES2

A, photograph of *HincII* digest of pIRES2-EGFP-F (lane 5) and possible pIRES2-EGFP-F/Kir6.1-DPTE clones (lanes 1-4). Successfully inserted DPTE cDNA would give fragments of 228, 663, 2092 and 3854 base pairs. Clones 1, 2 and 4 show successful insertion of Kir6.1-DPTE cDNA into the vector.

B, photograph of *ApaI* digest of pIRES2-EGFP-F (lane 3) and possible pIRES2-EGFP-F/Kir6.2-N41A clones (lanes 1 and 2). Successfully inserted N41A cDNA would give fragments of 13, 109, 444, 1001 and 5256 base pairs. Clone 2 shows successful insertion of Kir6.2-N41A cDNA into the vector.

All sizes alongside the 1kb ladder indicate fragments used for size reference. Arrows indicate fragments we expected from successful cloning.

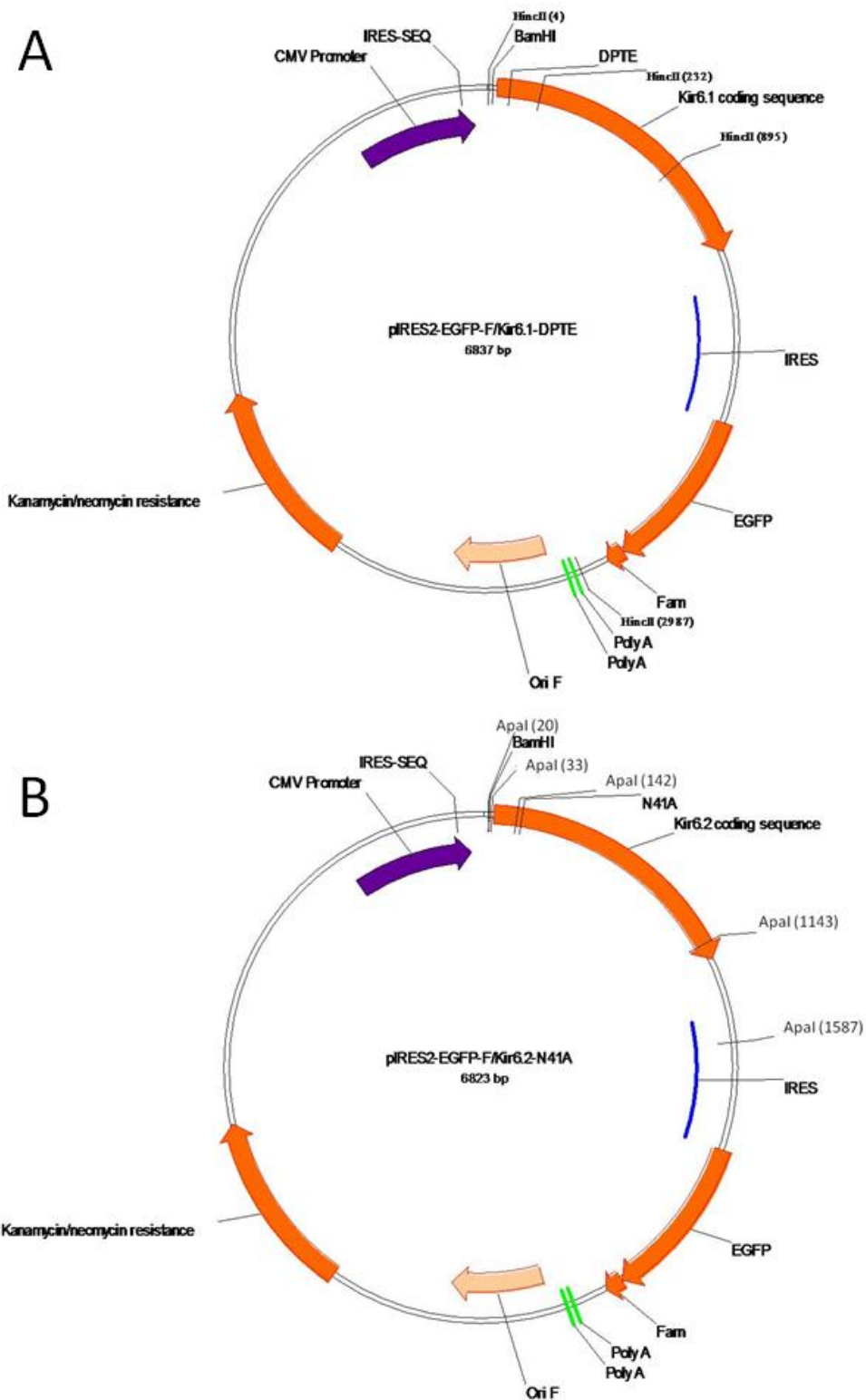


Figure 4.8 - Mammalian expression vectors for mutant $K_{ir}6.0$ subunits DPTE and N41A

A, mammalian expression vector encoding DPTE and EGFP-F.

B, mammalian expression vector encoding N41A and EGFP-F.

All restriction sites for cloning and success checking have been shown. All other restriction sites have been omitted for clarity. Note the lack of BglII site in both cases - this site was destroyed upon cloning the mutant fragments into pIRES2.

Name of mutant	Alteration made
ARI	Replaced residues 15-17 of K _{ir} 6.2 (T, R and L) with reciprocal residues from K _{ir} 6.1 (A, R and I)
ENLRK	Replaced residues 20-23 of K _{ir} 6.2 (D, P, T and E) with reciprocal residues from K _{ir} 6.1 (E, N, L, R and K)
IRD	Replaced residues 26-28 of K _{ir} 6.2 (Y, R and T) with reciprocal residues from K _{ir} 6.1 (I, R and D)
S37A	Replaced residue 37 of K _{ir} 6.2 (S) with reciprocal residue from K _{ir} 6.1 (A)
K39S	Replaced residue 39 of K _{ir} 6.2 (K) with reciprocal residue from K _{ir} 6.1 (S)
N41A	Replaced residue 41 of K _{ir} 6.2 (N) with reciprocal residue from K _{ir} 6.1 (A)
V44L	Replaced residue 44 of K _{ir} 6.2 (V) with reciprocal residue from K _{ir} 6.1 (L)
ASAL	Replaced residues 37, 39, 41 and 44 of K _{ir} 6.2 (S, K, N and V) with reciprocal residues from K _{ir} 6.1 (A, S, A and L)
S40K	Replaced residue 40 of K _{ir} 6.1 (S) with reciprocal residue from K _{ir} 6.2 (K)
A42N	Replaced residue 42 of K _{ir} 6.1 (A) with reciprocal residue from K _{ir} 6.2 (N)
DPTE	Replaced residue 20-24 of K _{ir} 6.1 (E, N, L, R and K) with reciprocal residue from K _{ir} 6.2 (D, P, T and E)
TRL	Replaced residues 15-17 of K _{ir} 6.1 (A, R and I) with reciprocal residues from K _{ir} 6.2 (T, R and L)
YRT	Replaced residues of K _{ir} 6.1 (I, R and D) with reciprocal residue from K _{ir} 6.2 (Y, R and T)

Table 4.3 - Description of mutants

Table showing the mutants created here and detailing the alteration made to the amino acid sequence by each mutation.

4.3 Characterisation of mutant channels

Following cloning, mutant subunits were transiently co-expressed with SUR2A in CHO cells and various properties of the channels were measured to assess the effect of the mutations on channel function.

4.3.1 Whole cell recordings

In order to ensure that all of the mutant channels were expressed as normal, whole cell currents were recorded following application of the potent K_{ATP} channel opener P1075 at a concentration of 10 μ M. Currents were recorded at 0 mV N.B. $E_K = -82.25$ mV at 30°C. 10 μ M glibenclamide, a potent K_{ATP} channel blocker, was used to block the current elicited by P1075. This allowed any baseline leak current to be isolated from K_{ATP} current. Using two potent, K_{ATP} specific compounds like this also served as a strong indication that any currents recorded were from K_{ATP} channels. All mutants, except S40K, produced currents in response to 10 μ M P1075 with mean peak whole cell currents that were not statistically different to their respective wild type, see figure 4.9A and 4.10A. If we assume that the larger a cell is the more channels it can produce, per unit time, then it is necessary to correct for differences in cell size in these experiments. Fortunately, the amplifier could measure whole cell capacitance – a measure of cell size. Thus, peak currents are represented as pA/pF so that cells were comparable. Mean whole-cell capacitance for each mutant can be seen in figure 4.9A and 4.10A. A second check of the sequenced DNA for S40K revealed that no current was produced because a single base was deleted at the second cloning site causing a

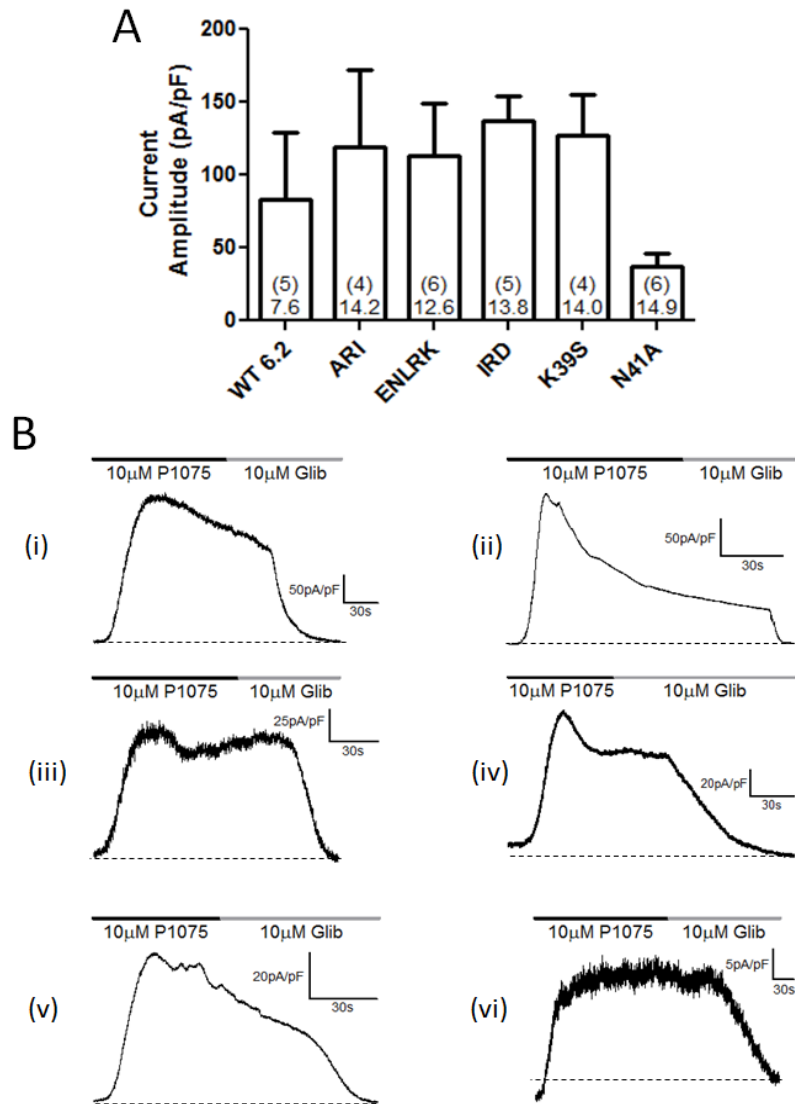


Figure 4.9 - Whole cell current amplitudes for Kir_{ir}6.2

A, whole cell current amplitudes elicited by 10 μM P1075 for CHO cells expressing wild type or mutant Kir_{ir}6.2 with SUR2A. Recordings were made at 0 mV. Zero K_{ATP} current level was taken as that during perfusion of 10 μM glibenclamide. All recordings were corrected for cell size. Each bar represents mean ± s.e.m. The numbers within the bar represent the number of cells, in parenthesis, and the mean whole cell capacitance (in pF).

B, example traces for whole cell recordings taken from cells expressing (i) Kir_{ir}6.2, (ii) ARI, (iii) ENLRK, (iv) IRD, (v) K39S or (vi) N41A, and SUR2A. Drugs were perfused onto the cells as indicated by the bars above the traces. The dashed lines show the current when all K_{ATP} channels were closed i.e. in 10 μM glibenclamide. Traces have been corrected for cell size.

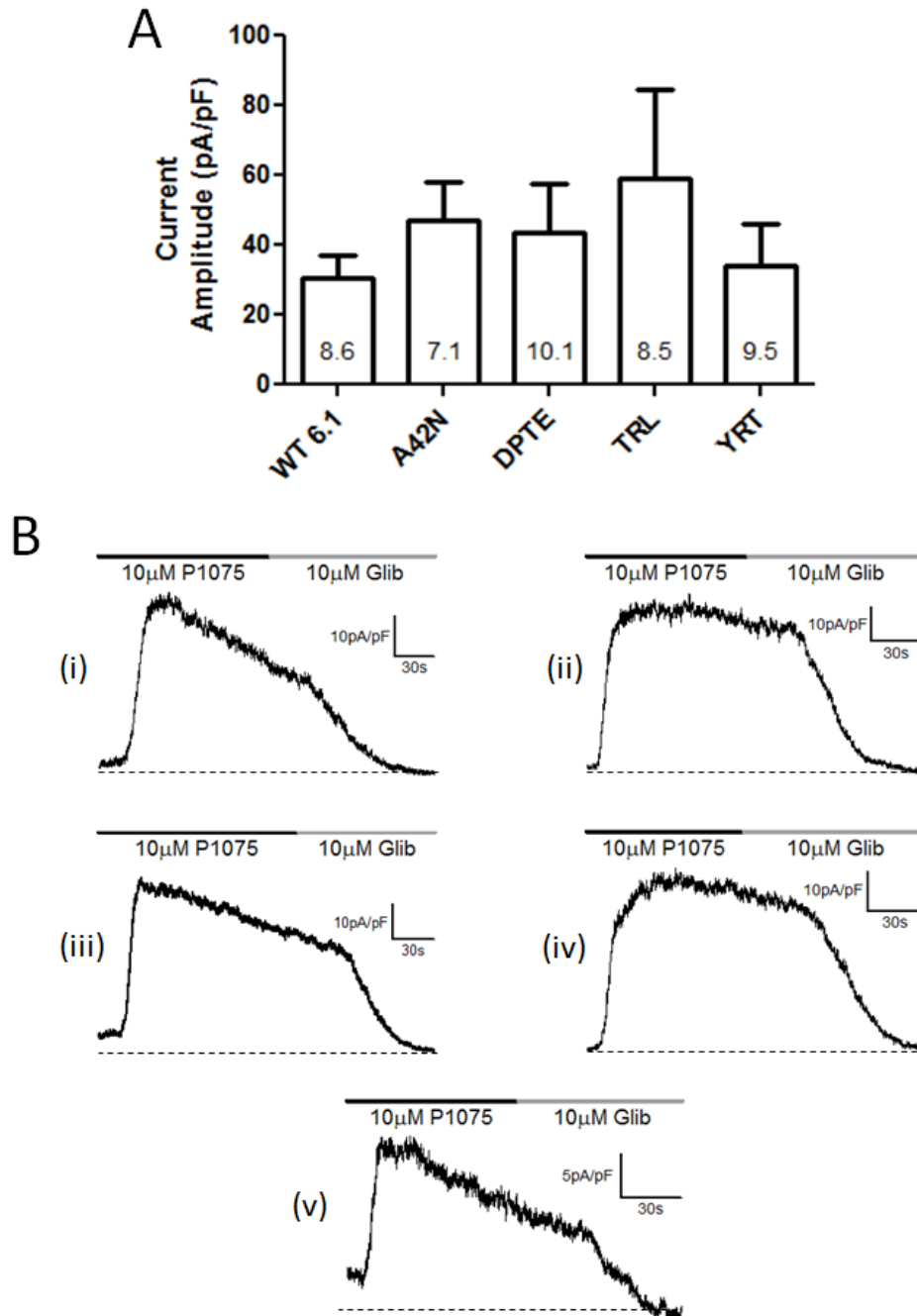


Figure 4.10 - Whole cell current amplitudes for $K_{ir}6.1$

A, whole cell current amplitudes elicited by 10 μ M P1075 for CHO cells expressing wild type or mutant $K_{ir}6.1$ with SUR2A. Recordings were made at 0 mV. Zero K_{ATP} current level was taken as that during perfusion of 10 μ M glibenclamide. All recordings were corrected for cell size. Each bar represents mean \pm s.e.m. for 4 cells. Number within the bar represents the mean whole cell capacitance of the cells used.

B, example traces for whole cell recordings taken from cells expressing (i) $K_{ir}6.1$, (ii) A42N, (iii) DPTE, (iv) TRL or (v) YRT, and SUR2A. Drugs were perfused onto the cells as indicated by the bars above the traces. The dashed lines show the current when all K_{ATP} channels were closed i.e. in 10 μ M glibenclamide. Traces have been corrected for cell size.

reading frame shift. This is believed to have prevented S40K from reaching the membrane. Most whole cell recordings showed a similar response to P1075 to that seen in a number of the examples traces (e.g. figures 4.9Bi and iv; 4.10Bi and iii). Some cells did not show a plateau following the peak (as in figure 4.9Biv) but showed a gradual decline in steady state current (as in figure 4.10Biii). This does not appear to have been a property of the channel as no consistent pattern emerged for any mutant or wild type $K_{ir}6.2$ regarding plateau versus run-down following the initial peak.

In the case of $K_{ir}6.1$ -based channels, it quickly became obvious that these currents were too small one day after cells were transfected. In these cases P1075 induced currents rarely exceeded 5pA/pF (see figure 4.11 for example – DPTE). Larger currents, but still smaller than those for any $K_{ir}6.2$ containing channels, with a mean of 43.5 ± 14.0 pA/pF ($n=4$) were obtained from DPTE 46-54 hours following transfection (figure 4.10A). Figure 4.11 shows whole cell currents recorded from two cells from the same batch of transfected cells. The first was recorded one day after transfection and the second recorded two days after transfection. Therefore, in order to obtain more robust whole cell currents all subsequent experiments involving wild type or mutant $K_{ir}6.1$ were left for 46-52 hours post-transfection before recordings were made.

It should be noted from this point on that it was decided to concentrate attention on the mutant $K_{ir}6.2$ channels. As was demonstrated with the whole cell recordings from $K_{ir}6.1$ and its mutants, expression of these channels was very low. It therefore seemed pertinent not to spend too much time attempting to make recordings, that in most cases required macroscopic currents, from cells from which it was highly unlikely to be able to measure more than one or two channels per excised patch.

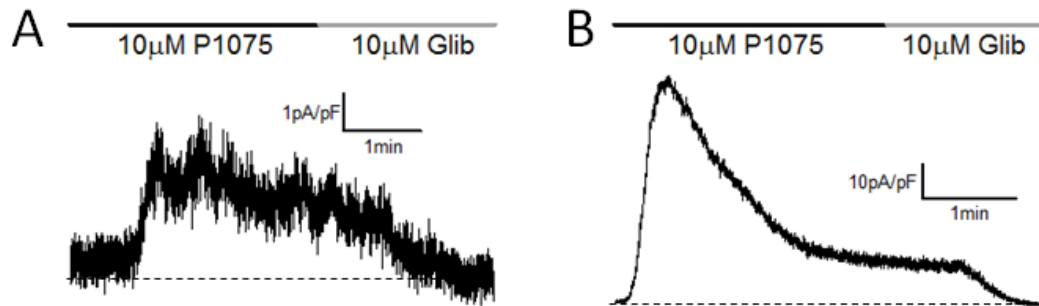


Figure 4.11 - Effect of time on current levels for a $K_{ir}6.1$ -based mutant

Example traces to show the current elicited by 10 μ M P1075 in CHO cells expressing the $K_{ir}6.1$ background mutant - DPTE. Whole cell currents recorded from the same batch of cells (A) one day and (B) two days after transfection with DPTE and SUR2A. Both traces have been corrected for cell size. Currents were recorded at a holding potential of 0 mV. Zero K_{ATP} current was calculated as that in the presence of 10 μ M glibenclamide, as shown by the dashed lines. Drugs were added as indicated by the bars above the traces.

4.3.2 *Single channel current-voltage relationships*

All mutants showed weak inward rectification as did wild type (figure 4.13). This is backed-up by calculation of relative current sizes at the positive and negative values at a single potential i.e. ± 60 mV. All channels tested showed 20-40% smaller currents at +60 mV than at -60 mV (figure 4.12B). As a result of the inward rectification displayed by all of the channels, the single channel conductance values below were calculated from the negative portion of the current-voltage relationship.

Single channel recordings were taken by excising patches from cells expressing mutant subunits (with SUR2A) to investigate any differences in properties like single channel conductance or inward rectification. To obtain a value for single channel conductance, each patch excised was held at different membrane potentials, ranging from -100 mV to +60 mV, and the single channel current was recorded under symmetrical potassium concentrations i.e. an E_K of 0 mV, and as expected the currents all reversed at 0 mV. By plotting the current amplitude seen at each membrane potential (figure 4.13), a current-voltage relationship was obtained for all $K_{ir}6.2$ -based channels and by calculating its gradient single channel conductance was calculated. For illustration purposes, current-voltage relationships are shown (figure 4.13) from the mean data for each mutant but for statistical analysis the conductance of each patch was calculated and combined to give a mean for each mutant. Wild-type $K_{ir}6.2$ had a unitary conductance of 70.3 ± 1.6 pS ($n=3$). ARI had a significantly smaller unitary conductance of 60.7 ± 1.2 pS ($n=4$) but all other mutants were not significantly

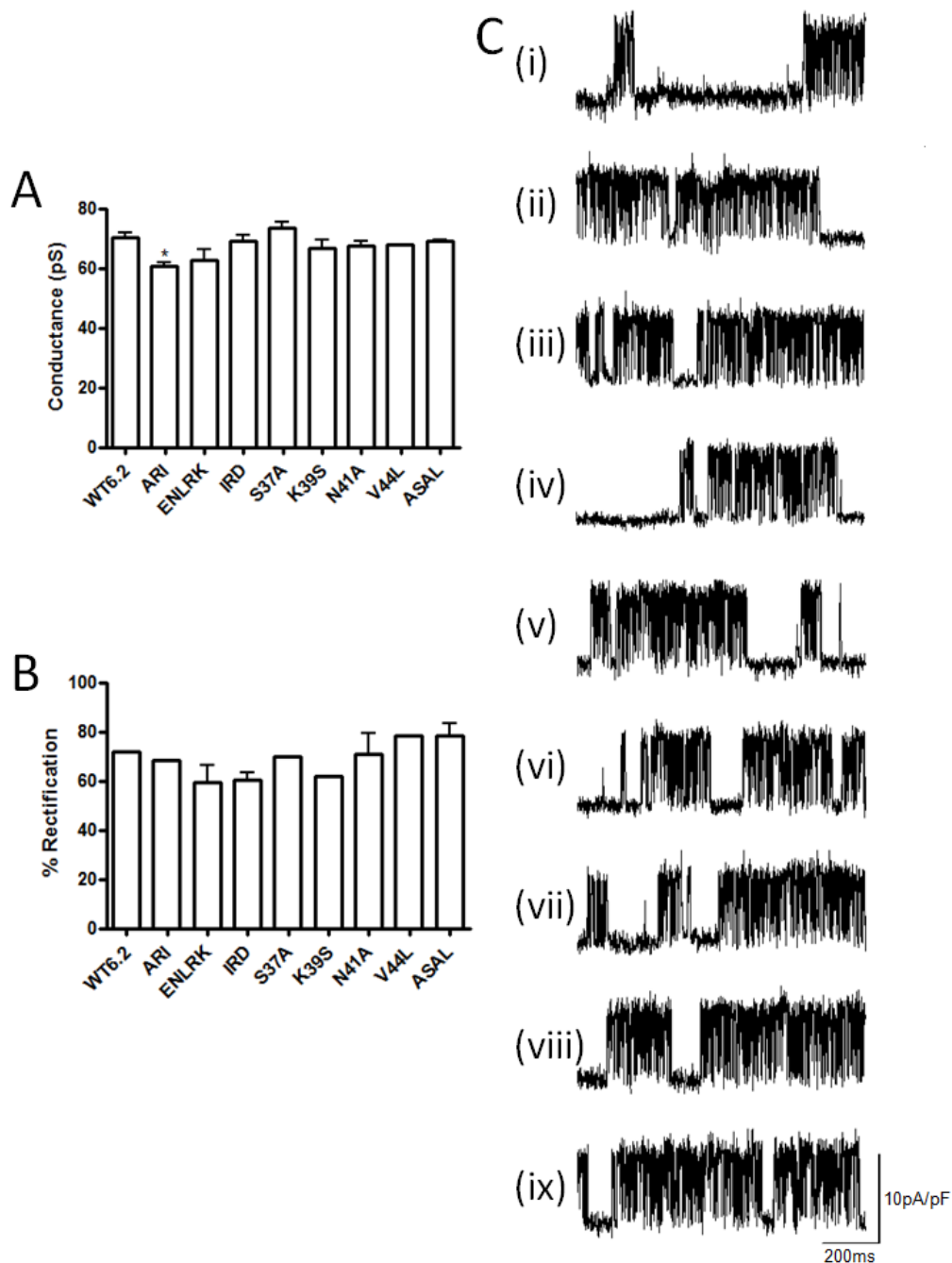


Figure 4.12 - Single channel properties of wild type and mutant Kir6.2 expressed with SUR2A

A, mean conductance values for wild type and mutant Kir6.2/ SUR2A. Current-voltage relationships from a single patch were plotted and fitted, as shown in figure 4.13. This was repeated for each patch used. Each point represents mean \pm s.e.m. current from 3 patches (2 for V44L and 4 for ARI, IRD and K39S). Bar represents mean \pm s.e.m. (excluding V44L where only mean is plotted). * - $p < 0.05$ (1-way ANOVA with Dunnett's post-test).

B, percentage rectification for wild type and mutant Kir6.2/ SUR2A. The current amplitude at +60 mV was divided by that at -60 mV from the same patch. Bars show mean from 2 patches (3 for ENLRK, N41A and ASAL, 4 for IRD with mean \pm s.e.m. for these mutants).

C, example traces for single channel currents recorded from excised patches for (i) wild type Kir6.2, (ii) ARI, (iii) ENLRK, (iv) IRD, (v) S37A, (vi) K39S, (vii) N41A, (viii) V44L and (ix) ASAL with SUR2A. Recordings were made with symmetrical potassium (140 mM) at -100 mV.

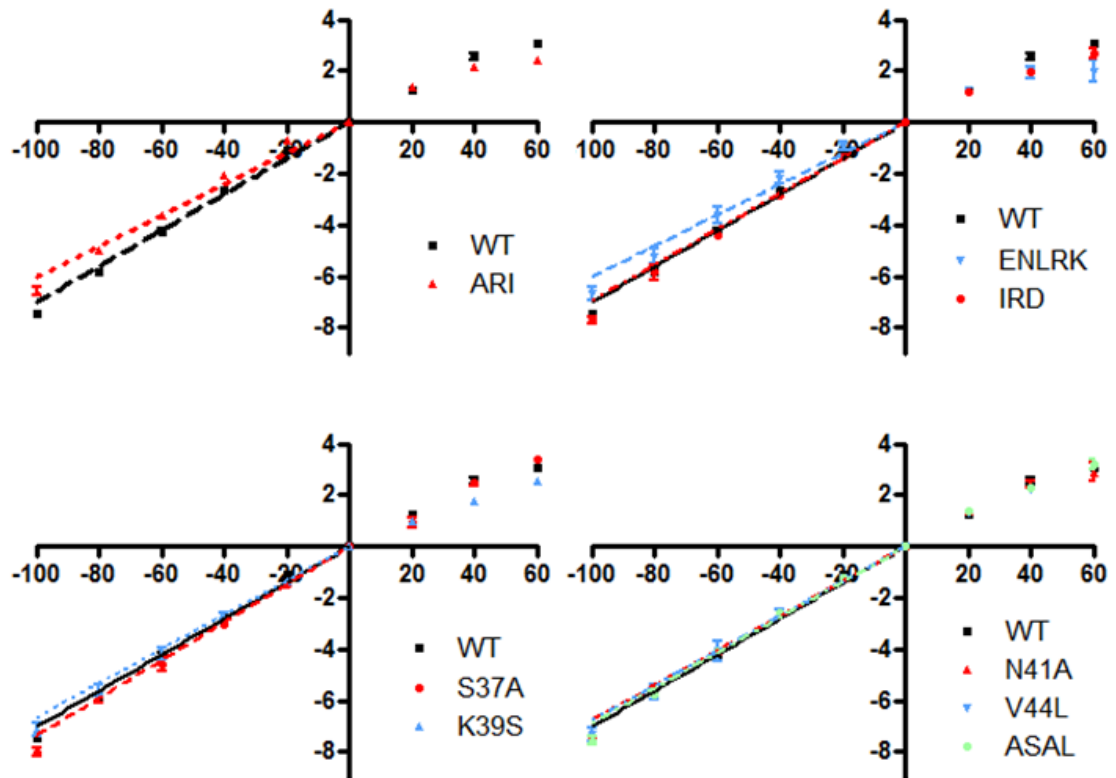


Figure 4.13 - Single channel current-voltage relationship for wild type and mutant $K_{ir}6.2$ expressed with SUR2A

Single channel current-voltage relationship for wild type and mutant $K_{ir}6.2$ / SUR2A recorded from excised patches taken from CHO cells. Some patches did not survive long enough to record a value for +60 mV but in all cases > 2 values were included. Plotted lines show conductance. Positive potentials were not included in this fit as the channels are inward rectifiers.

different from wild type, ranging from 62.7 to 73.5 pS (figure 4.12A and 4.13). Example traces of currents recorded at -100 mV for a selection of channels, including ARI, are shown in figure 4.12C.

Ideally, amongst the single channel characteristics tested for each mutant would have been P_o . However, channel run down was a major problem under the conditions used here so that wild type $K_{ir}6.2$ had a dramatically lower P_o than expected of <0.1 . This made it difficult to distinguish any differences between wild type and mutant P_o as being caused by run down or an actual change in P_o therefore this was not measured.

4.3.3 *Spontaneous opening in the absence of intracellular ATP*

As I have pointed out above, spontaneous opening of channels containing $K_{ir}6.2$ is of major interest with respect to the mutants created here. It was expected that the mutations introduced in $K_{ir}6.2$ would reduce its ability to open spontaneously. It was therefore necessary to quantify the ability of a channel to open spontaneously. To do this, patches were excised from CHO cells, expressing mutant or wild type $K_{ir}6.2$ and SUR2A, into magnesium and nucleotide free (i.e. control) internal solution. Mg-free solution was used in an effort to reduce channel run-down (Kozlowski & Ashford, 1990). The patches were also subjected to 10 mM UDP to activate the channels. The low inhibitory potency of UDP (Babenko *et al.*, 1999c) makes it ideal to stimulate the channels. The peak current when the patch was excised and perfused with control solution was then expressed as a fraction of that elicited by 10 mM UDP to give a value that I will call "relative activation". To show that 10 mM UDP produced a maximal K_{ATP} response, the effect of 40 mM UDP was also tested. 10 mM and 40 mM UDP gave

similar relative activation values for wild type $K_{ir}6.2$ but with 40 mM UDP giving a slightly smaller effect (figure 4.14Aii). Relative activation was used for comparison here rather than absolute current size as the number of channels in a patch, and therefore current size, was too variable even within the same batch of cells. But as relative activation is a normalised value for each patch, this was a valid approach. Recordings such as those in figure 4.15 were used to evaluate relative activation.

The relative activation of each mutant as well as wild type $K_{ir}6.2$ can be seen in figure 4.14Ai. The wild type channel gave a relative activation of 1.42 ± 0.12 ($n=9$). A one-way analysis of variance of this data showed that the mean relative activation values were significantly different from one another ($p = 0.0015$, $F = 3.901$). Post tests were performed to compare the groups, the results of which are shown in figure 4.14 and below. All mutants tested had similar relative activations to wild type with the exception of ENLRK and V44L which were smaller, though not significantly. Four residues (S37, K39, N41 and V44) had previously been shown to be contained within a region partly responsible for spontaneous opening in $K_{ir}6.2$ -containing channels (along with a C-terminal section; Kondo *et al.*, 1998). However, individual mutation of these residues to their $K_{ir}6.1$ counterparts did not result in any difference in relative activation (figure 4.14Ai). To confirm that these residues were important in spontaneous opening of K_{ATP} channels in the expression system being used here, the ASAL mutant was created which simultaneously mutated the four residues above to those found in $K_{ir}6.1$. This mutant should have therefore recreated the effect seen by Kondo and colleagues (Kondo *et al.*, 1998). In agreement with this, ASAL showed a

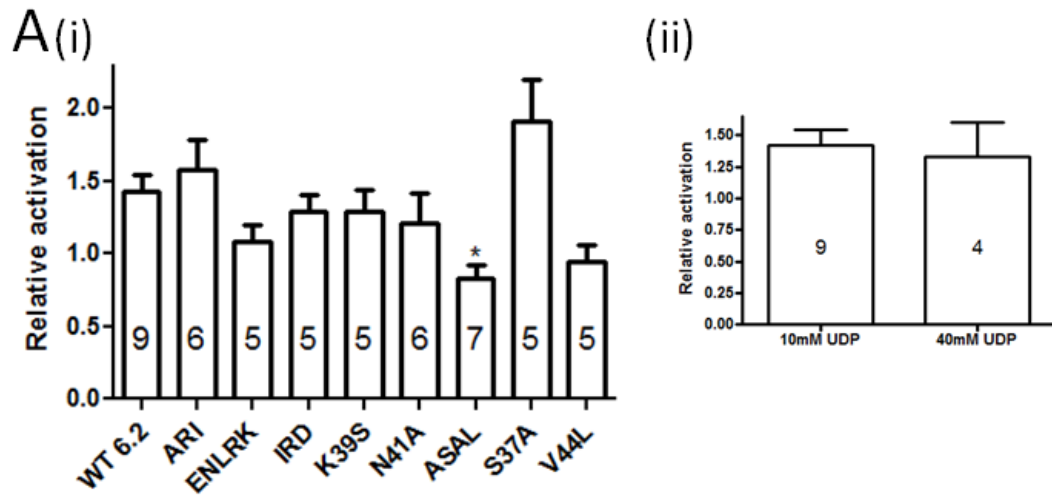


Figure 4.14 - Relative activation of K_{ATP} channels from inside-out recordings

Relative activation of K_{ATP} channels from inside-out recordings—

A (i), mean relative activation of wild type and mutant $K_{i,6.2}$ expressed with SUR2A in CHO cells. Relative activation was calculated as the peak current when patches were excised into magnesium and nucleotide-free internal solution divided by that when 10 mM UDP was applied to the patch. All K_{ATP} channels were assumed to be closed in the presence of 1 mM ATP. All recordings were made at -60 mV. Each bar represents mean \pm s.e.m. for the number of patches shown within the bar. * - $p < 0.05$ (1-way ANOVA with Dunnett's post-test).

A (ii), effect of concentration of UDP on relative activation. Data shown as mean \pm s.e.m. for the number of patches shown within each bar. Conditions as in A (i).

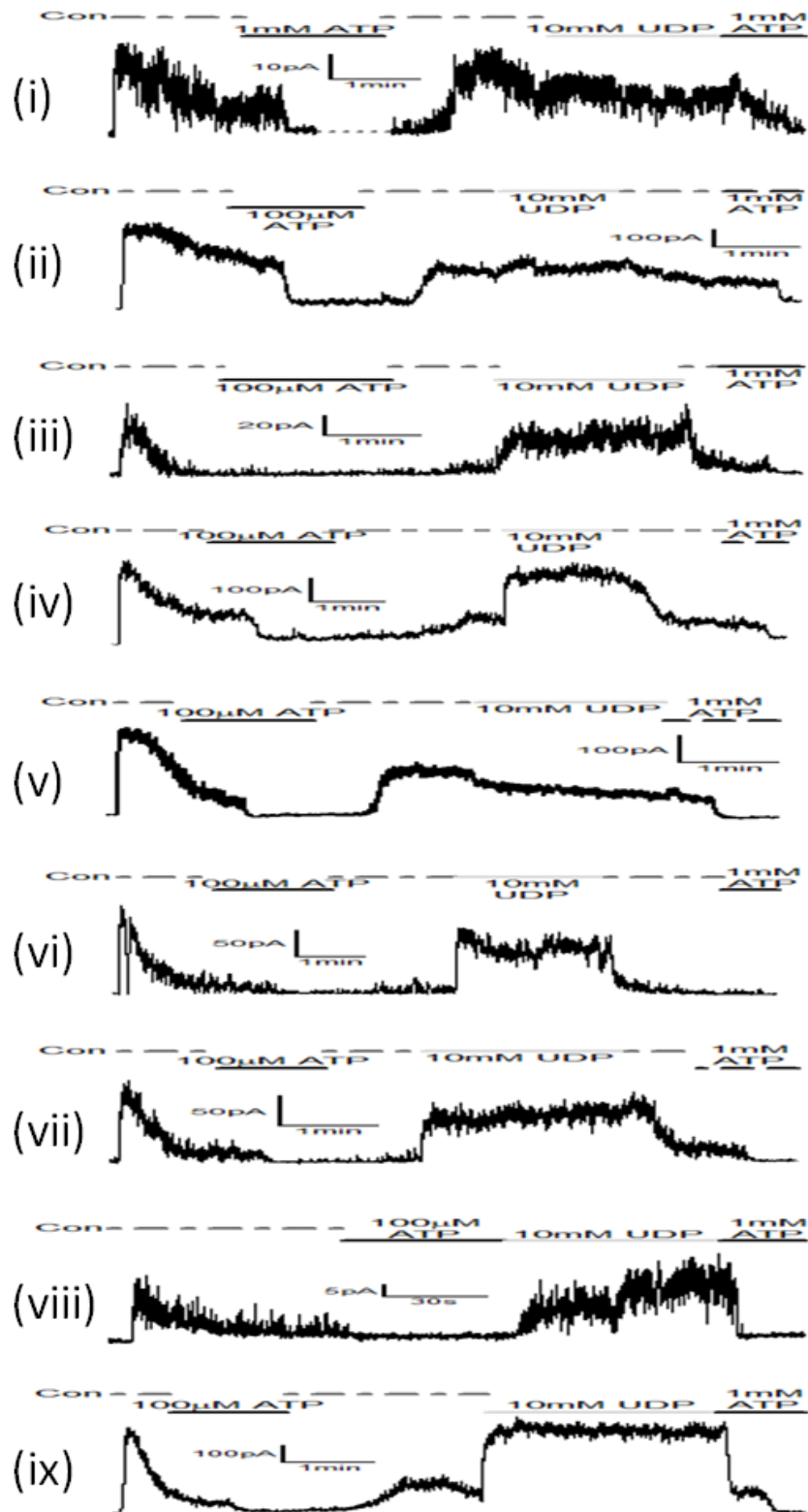


Figure 4.15 - Relative activation of wild type and mutant $K_{ir}6.2$ and SUR2A

Example traces showing relative activation recorded from excised patches from CHO cells expressing (i) wild type $K_{ir}6.2$, (ii) ARI, (iii) ENLRK, (iv) IRD, (v) S37A, (vi) K39S, (vii) N41A, (viii) V44L and (ix) ASAL with SUR2A. Recordings were made with symmetrical potassium (140 mM) at -60 mV. Drugs were added as indicated by the bars above the traces. Dashed lines within trace i indicate a long period of time spent in that solution which has been shortened for clarity.

significantly ($p < 0.05$) reduced relative activation of 0.83 ± 0.08 ($n=7$) – equivalent to ~42% lower relative activation than wild type. This is a slightly smaller reduction than that seen in the work by Kondo *et al.* (~50% lower; Kondo *et al.*, 1998) but is still comparable. This suggests that, while the residues are important, it is the interaction between at least 2 of the residues if not all four that exerts the effect on spontaneous opening rather than any individual residue.

4.3.4 ATP sensitivity

The ATP sensitivity of K_{ATP} channels may be controlled by the affinity of ATP for the channel, by the binding site, or by the open state stability of the channel, as ATP is known to preferentially bind to and stabilise the closed state of the channel (Enkvetchakul & Nichols, 2003). Thus, the ATP sensitivity of the mutants was tested to assess their influence on ATP binding or channel open/closed state stability. Only one of the residues mutated here has been suggested to be directly involved in ATP binding (K39 in $K_{ir}6.2$ lies within 4.5 Å of ATP in a binding model; Antcliff *et al.*, 2005. See also Cukras *et al.*, 2002a) so in all other cases, any changes in ATP sensitivity are likely to reflect a change in P_o rather than binding itself. Though without measuring P_o directly this could not be confirmed.

Dose-response curves for the inhibition of wild type or mutant $K_{ir}6.2$ expressed with SUR2A are shown in figure 4.16A. Traces showing examples of recordings made to measure ATP sensitivity can be seen in figure 4.17. For easier illustration, a single curve was plotted for each mutant through all of the data points from multiple patches.

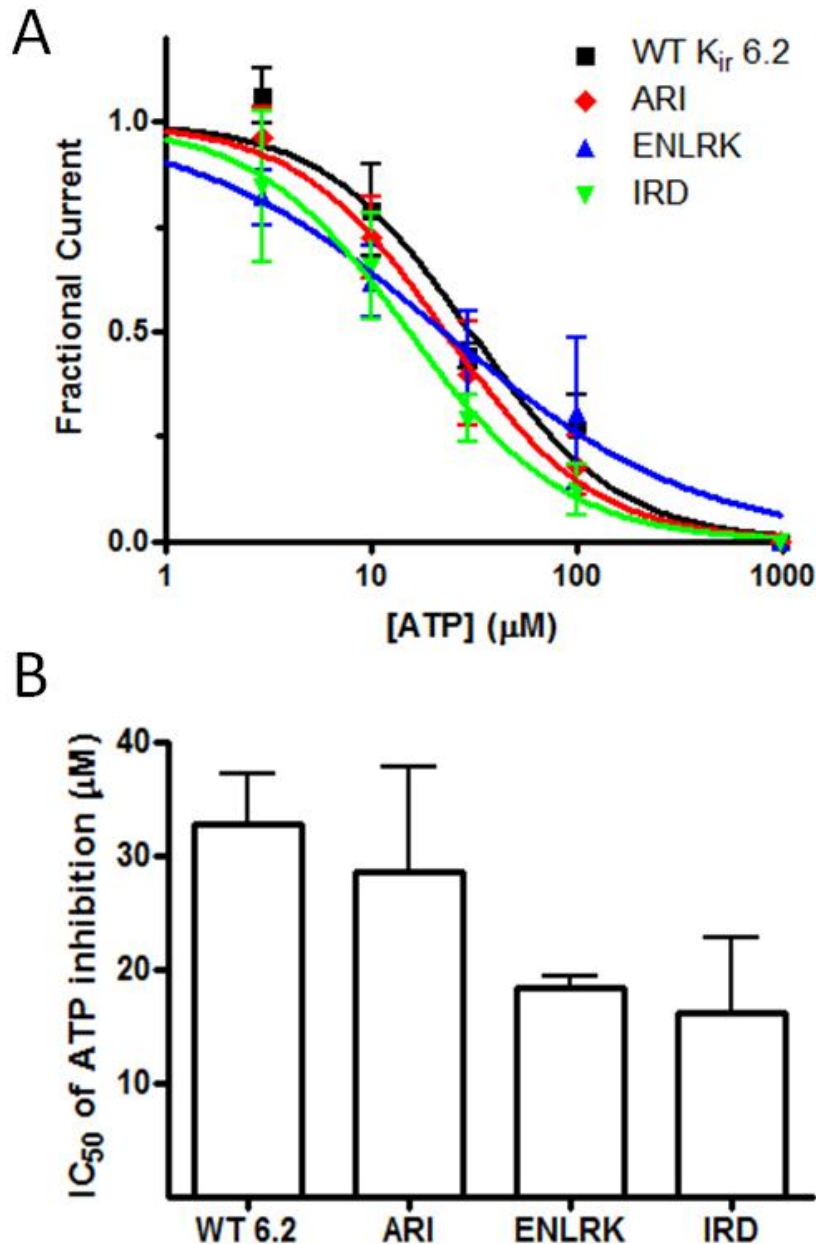


Figure 4.16 - Inhibition of mutant K_{ATP} channels by ATP

A, ATP dose response-curves from excised patches from cells expressing wild type or mutant K_{ir} 6.2 and SUR2A. Fractional current values at each concentration were calculated using the last 100 ms of a 200 ms pulse from 0 mV to -60 mV as a fraction of the value in the absence of ATP and using 1 mM ATP as the baseline. Each point represents the mean \pm s.e.m. from 4 patches (5 patches for wild type K_{ir} 6.2). Curves were fitted using equation 1 and the top and bottom constrained to 1 and 0, respectively.

B, mean IC_{50} values for inhibition of K_{ATP} by ATP for statistical comparison between wild-type and mutant K_{ir} 6.2. The dose-response curve for a single patch was plotted and fitted with equation 1 and repeated for each patch recorded from i.e. 3 for ENLRK, 4 for ARI and IRD, 5 for wild type. Mean \pm s.e.m. IC_{50} values were $32.7 \pm 4.3 \mu$ M (wild type K_{ir} 6.2), $28.4 \pm 9.3 \mu$ M (ARI), $18.3 \pm 1.0 \mu$ M (ENLRK) and $16.1 \pm 6.6 \mu$ M (IRD).

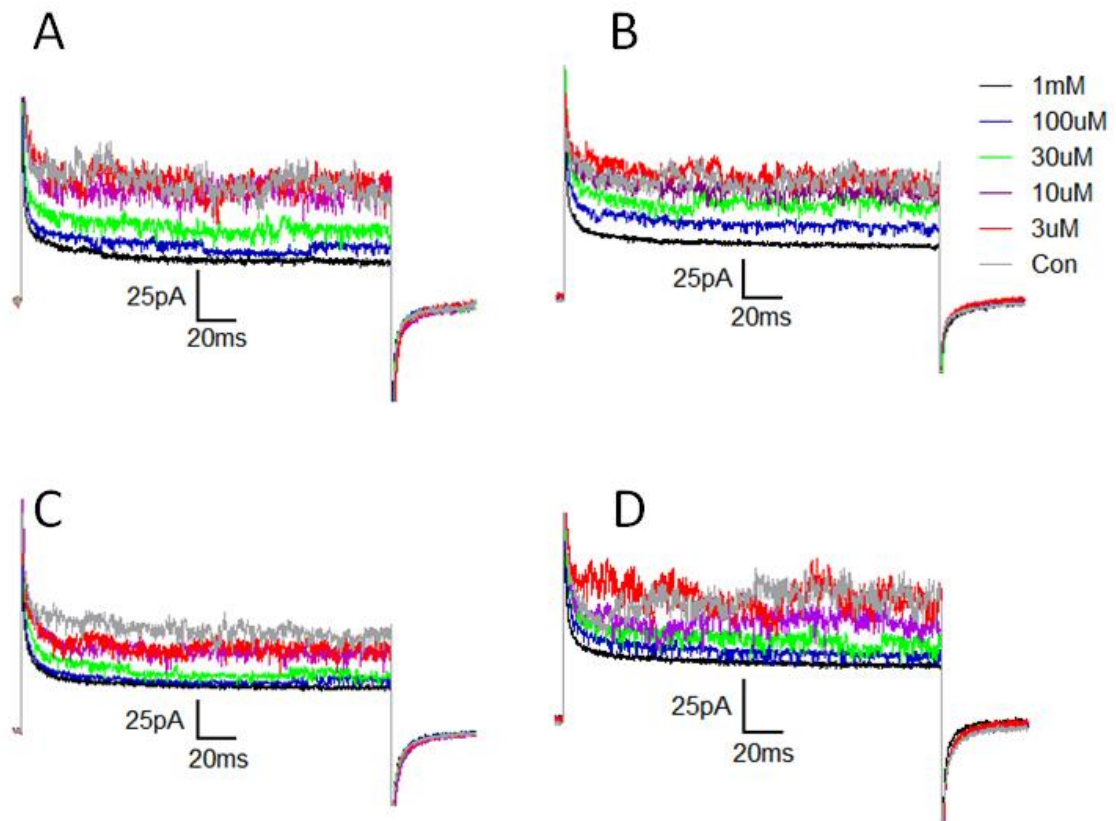


Figure 4.17 - ATP sensitivity of wild type and mutant $K_{ir6.2}$ and SUR2A

Example traces showing the ATP sensitivity of (A) wild type $K_{ir6.2}$, (B) ARI, (C) ENLRK, (D) IRD and SUR2A in response to the concentrations shown on the right of B. The same colour scheme applies to all sets of traces. To calculate the current in each concentration of ATP, 20 sweeps of pulses from 0 to -60 mV, for 200 ms, were recorded per concentration and the average of the last 100 ms was calculated across all 20 sweeps. Traces show a single sweep, per concentration, taken from each of these 20 sweeps.

However, for analytical purposes a dose-response curve was fitted to the fractional current data obtained from each patch recorded for each mutant to allow a mean IC_{50} to be obtained (figure 4.16B). This allowed statistical comparison of mutants and wild type. All mutants showed a left-ward shift in their dose-response curves compared to wild type but, though all were lower, none had a significantly lower mean IC_{50} . Though I would have liked to have measured the ATP sensitivity of ASAL, and mutants derived from it if there had been any difference to wild type, run-down was so dramatic that no patches displayed current for long enough to be able to obtain a dose-response curve. Despite extensive efforts, I eventually ran out of time to try to rectify this.

4.4 Discussion

K_{ATP} channels containing mutant pore forming subunits were expressed to assess the importance of the N-terminus of $K_{ir}6.0$ in channel function. In each case, a residue or group of residues was removed from one subunit and replaced with the equivalent residue(s) from the other thus creating a pair of mutants for each residue or region being examined – one for each subunit. In total 13 $K_{ir}6.0$ mutants were constructed – 5 mutant $K_{ir}6.1$ subunits, the reciprocal 5 mutants in $K_{ir}6.2$ and 3 additional mutants in the $K_{ir}6.2$ background (see table 4.2 or 4.3 for full list). A table summarising the effect of each mutations on all of the properties tested can be seen in table 4.4. Whole cell current recordings, from cells transiently transfected with each mutant and SUR2A, showed that all but one of the paired mutants (S40K) expressed normally. These 9 mutants exhibited similar whole cell currents, elicited by 10 μ M P1075, to their respective controls suggesting that none of the mutated residues were important in

Name of mutant	Effect on:				
	Expression	Conductance	Rectification	Relative activation	ATP sensitivity
ARI	N	Y	N	N	N
ENLRK	N	N	N	N	N
IRD	N	N	N	N	N
S37A	N	N	N	N	N/A
K39S	N	N	N	N	N/A
N41A	N	N	N	N	N/A
V44L	N	N	N	N	N/A
ASAL	N	N	N	Y	N/A

Table 4.4 - Summary of chapter 4 results

Table to show whether each mutant had a significant effect on any of the characteristics measured here. ATP sensitivity was not measured for every mutant (N/A). ARI had an effect on conductance and ASAL on relative activation.

expression of the channel as current density remained constant. The additional $K_{ir}6.2$ mutants S37A, V44L and ASAL were not tested as they were constructed towards the end of the investigation and other experiments were prioritised above recording of their whole cell currents.

Several attempts were made to open the S40K containing channel including with a different pharmacological opener – cromakalim, by lowering the intracellular pH and by metabolic inhibition with 2,4-dinitrophenol (data not shown). When none of these methods were successful in opening the channel, the sequence of the cDNA was re-checked. It was discovered that an unwanted mutation had occurred at the *EcoRV* site used during cloning. This resulted in a shift in the $K_{ir}6.1$ reading frame encoded by this cDNA downstream of the mutation introducing an early stop codon. When expressed, with the obvious exception of the S40K mutation, the protein resembled $K_{ir}6.1$ in the first 279 amino acids. Following this are only a further 13 “random” amino acids.

Using chimeras of $K_{ir}6.2$ and $K_{ir}2.1$, an inward rectifier potassium channel that does not associate with SUR, the C-terminal region absent in the S40K mutant has been shown to have little importance in the association of $K_{ir}6.2$ with SUR in biochemical assays (Giblin *et al.*, 1999, Schwappach *et al.*, 2000). Despite this, no currents were recorded from the chimera containing the C-terminus of $K_{ir}2.1$ when expressed with SUR1 suggesting that the C-terminus of $K_{ir}6.2$ is required for expression of a functional channel with or without SUR (Giblin *et al.*, 1999). Although S40K totally lacks the C-terminus where the chimera has that of $K_{ir}2.1$, both channels show that the C-terminus is important in expression of functional K_{ATP} channels as neither produced functional channels. It is also likely that were S40K to assemble and express normally it

would have severely altered properties. The C-terminus of K_{ir}6.2, absent in S40K, has also been shown to interact with the N-terminus of K_{ir}6.2 (Jones *et al.*, 2001). This interaction is important in regulation of the channel by intracellular ligands e.g. ATP.

All K_{ir}6.1-based channels exhibited lower currents than those containing K_{ir}6.2. K_{ATP} channels that contain K_{ir}6.1 have a smaller conductance than those containing K_{ir}6.2 (see 3.2.1). The difference in size of whole cell currents between the K_{ir}6.1 and K_{ir}6.2 mutants, and wild types, is too great to be simply caused by the difference in conductance of the channels. Using the example of the wild type currents - if the difference in conductance were the only factor involved then we would expect the wild type K_{ir}6.1 current to be ~58% of the wild type K_{ir}6.2 current. However, from the whole cell recordings reported here, the wild type K_{ir}6.1 is ~37% of wild type K_{ir}6.2. The discrepancy must be caused by fewer K_{ir}6.1-based channels in the membrane. Therefore there must be a limiting factor in K_{ir}6.1 expression that does not affect K_{ir}6.2. This is supported by the fact that the K_{ir}6.1 mutants began to express at a higher density after a longer period of incubation. This suggests that either each K_{ir}6.1-containing channel requires more time to be fully trafficked to the membrane than its K_{ir}6.2 counterparts or that K_{ir}6.1 causes the channels to be more frequently removed from the membrane and less frequently recycled back into it than K_{ir}6.2 thus lowering the overall channel density. It is also possible that the reverse may be true for both hypothesis in K_{ir}6.2 and that its expression is hastened rather than K_{ir}6.1 being slowed. Differences between K_{ir}6.1 and K_{ir}6.2 at the level of translation could explain the lower current density of K_{ir}6.1. Messenger RNA of K_{ir}6.1 could be degraded more quickly than K_{ir}6.2 or mRNA could be more efficiently translated in the case of K_{ir}6.2 than K_{ir}6.1.

Sadly, the experiments carried out here shed no light on what may cause this difference.

Single channel current-voltage relationships were constructed for each of the K_{ir}6.2 mutants. With a few exceptions, mutant channels displayed very similar unitary conductance to that of wild type K_{ir}6.2 at ~70 pS. ENLRK showed a slightly lower unitary conductance of 62.8 ± 3.6 pS and ARI displayed a significantly lower conductance of 60.7 ± 1.2 pS ($p < 0.05$). It is unlikely that these residues contribute directly towards the conduction pathway as the residues responsible for controlling conductance in K_{ir}6.1 and K_{ir}6.2 have been identified. In a study designed to identify the region responsible for the difference in conductance between K_{ir}6.1 and K_{ir}6.2, Kondo and colleagues constructed chimeras of the two channels. They showed that the M1-H5-M2 region was responsible for determining conductance in these channels (Kondo *et al.*, 1998). The specific residues responsible were later found to be N123-V124-R125 in the M1-H5 linker and M148 in the H5-M2 linker of K_{ir}6.1 (S113-I114-H115 and V138 in K_{ir}6.2; Repunte *et al.*, 1999). Similar to the effect of ARI and ENLRK, Kondo's chimeras showed a small decrease in conductance when the N-terminus of K_{ir}6.2 was replaced with that of K_{ir}6.1 and a small increase in conductance for the equivalent K_{ir}6.1 chimera (Kondo *et al.*, 1998). It should be noted that these effects were not specifically noted in their paper. These findings suggest a link between the N-terminus and the pore of the channel. However, N-terminal truncations of K_{ir}6.2 when expressed with SUR1 had no effect on conductance (Koster *et al.*, 1999b). This suggests that the N-terminus of K_{ir}6.2 is in a "neutral" conformation with respect to its influence on conductance and that residues in K_{ir}6.1 have a more dynamic effect. The

lack of conductance data for the reciprocal mutants to ARI and ENLRK (TRL and DPTE) make it difficult to confirm this hypothesis, as does a lack of conductance value for an N-terminally truncated $K_{ir}6.1$ here or in the literature. It is possible that mutation of regions in the N-terminus including ARI and ENLRK in $K_{ir}6.1$ (TRL and DPTE in $K_{ir}6.2$) causes a conformational change in the channel that leads to altered conduction of K^+ ions by slightly reshaping the pore. The chimeras show that replacement of the whole N-terminus of $K_{ir}6.0$ has a small effect on conductance, relative to the effect of the P-loop chimeras (Kondo *et al.*, 1998), and I have identified two regions within the N-terminus that have a similar effect. Therefore it is most likely that several regions of the N-terminus contribute to the link between the N-terminus and the pore and that disruption of any of these regions alters the influence on the permeation pathway by causing a conformational change. The R16 mutation caused an increased P_o (Cukras *et al.*, 2002a) and though no unitary conductance was quoted for this channel, the effect on gating demonstrates communication between this residue and the pore. Though the residue is conserved in ARI it is possible that disruption to its immediate environment could affect its influence on the pore. Any effects on conductance seen here are assumed to be SUR-independent as channels expressed with and without SUR have the same conductance (Tucker *et al.*, 1997).

Conductance is dependent upon ion concentration even under symmetrical concentrations. The maximum unitary conductance of a channel is saturable (Coronado *et al.*, 1980, Lopatin & Nichols, 1996). It is possible that the ARI mutation affects the extent to which the conductance is saturated (causing a rightward shift in the conductance- K^+ concentration plot). Whether or not such a shift has occurred is

not evident from the experiments carried out here. However, it would be possible to test the hypothesis by measuring the unitary conductance of ARI at varying K^+ concentrations.

Control of conductance in other inward rectifier potassium (K_{ir}) channels has been isolated to a similar region to $K_{ir}6.0$ i.e. in the H5 region (Choe *et al.*, 2000, Xu *et al.*, 2000) but in some K_{ir} channels the C-terminus also plays a role (Choe *et al.*, 2000, Zhang *et al.*, 2004). The N-terminus of the inwardly rectifying potassium channel $K_{ir}1.1$ has been shown to exert some influence on conductance. Mutations of T51 could either increase (T51H) or decrease (T51E) conductance, though no hypothesis of the cause of this effect was given except that it was not electrostatic (T51K produced conductance indistinguishable from wild type; Choe *et al.*, 1997). Though the effect seen in the $K_{ir}1.1$ T51 mutants was more dramatic than in ARI and ENLRK, it shows that the N-termini of inwardly rectifying potassium channels are capable of influencing conductance.

Given the small number of patches used in most cases to calculate the percent rectification of $K_{ir}6.2$ and its mutants it is unsurprising that there were no statistically discernable differences. The fact that all of the channels displayed similar rectification characteristics can be easily explained. Inward rectification displayed by the K_{ir} family of channels is caused by voltage dependent block of the pore of these channels with polyamines (Lopatin *et al.*, 1994) or magnesium ions (Horie *et al.*, 1987). The residues responsible for binding of polyamines and Mg^{2+} to K_{ir} channels have been localised to the M2 transmembrane helix (Fakler *et al.*, 1994, Lu & MacKinnon, 1994, Stanfield *et al.*, 1994, Wible *et al.*, 1994) and the C-terminus (Tagliatalata *et al.*, 1995, Yang *et al.*,

1995) of these channels. A similar picture has emerged for K_{ATP} where a pore lining residue in M2 (N160) of $K_{ir}6.2$ has been shown to affect rectification (Shyng *et al.*, 1997a). Residues in the C-terminus of $K_{ir}6.2$ have also been implicated in its weak rectification where S212 was shown to reduce block by spermine (Cui *et al.*, 2002) and H216 caused a pH dependent change in rectification (Baukrowitz *et al.*, 1999). Given the lack of evidence linking the N-terminus of K_{ir} channels to rectification, the lack of effect of mutations of the N-terminus of $K_{ir}6.1$ and $K_{ir}6.2$ is unsurprising.

The slightly lower response elicited by 40 mM UDP compared to 10 mM UDP is in agreement with previous findings where low concentrations of nucleotide diphosphates are known to activate K_{ATP} channels but high concentrations inhibit the channel (Hopkins *et al.*, 1992, Okuyama *et al.*, 1998). This suggests that at low concentrations nucleotide diphosphates bind to the high affinity stimulatory site on SUR while at high concentrations they will also bind to the inhibitory site on $K_{ir}6.0$ for which they have a lower affinity. These sites can be distinguished experimentally – when C-terminally truncated $K_{ir}6.2$ i.e. channels formed from $K_{ir}6.2$ alone, is exposed to ADP only an inhibitory effect is seen. However, co-expression of C-terminally truncated $K_{ir}6.2$ with SUR restores the stimulatory effect of ADP seen in wild type channels (Tucker *et al.*, 1997).

Each of the $K_{ir}6.2$ mutants tested here produced channels that opened spontaneously in the absence of nucleotides but to varying degrees. ARI and IRD displayed almost identical relative activation to wild type $K_{ir}6.2$. These mutants were created to assess whether the tertiary environment of these two arginine residues (R16 and R27) affects their ability to influence the stability of the open state of the channel. These findings

suggest that the flanking residues do not combine with these arginines to influence spontaneous bursting of K_{ir}6.2-containing channels. Given the striking effect of R16A and R27A on P_o (Cukras *et al.*, 2002a) and the fact that they are conserved between K_{ir}6.1 and K_{ir}6.2, it is still possible that the environment in which these residues exist is important. Further evidence supporting the importance of interactions within the N-terminus in the role of R16 and R27 in open state stability comes from N-terminal truncation studies. R16A and N-terminally truncated K_{ir}6.2 (removal of amino acids 2-30; ΔN2-30) have a similar phenotype with respect to P_o and ATP sensitivity (Cukras *et al.*, 2002a, Koster *et al.*, 1999b) therefore it was suggested that removal of R16 in ΔN2-30 accounts for this similarity (Cukras *et al.*, 2002a). However, in the same study that ΔN2-30 was tested, a shorter truncation was also carried out, ΔN2-20, which removed R16. Though no P_o was quoted for this channel, its ATP sensitivity was different to ΔN2-30 (Koster *et al.*, 1999b) suggesting that removal of R16 alone does not account for the characteristics of ΔN2-30 and that amino acids 20-30 also contribute to the ΔN2-30 phenotype. This could be via interaction with R16. Another study that produced N-terminally truncated K_{ir}6.2 showed that removal of the first 20 amino acids produced a lower IC₅₀ for ATP than removal of 30 residues (Babenko & Bryan, 2001). However, the ATP sensitivity of this Δ2-20 channel was still much lower than for R16A confirming that other residues are involved in producing the ΔN2-30 phenotype. Given the similar phenotypes when mutated to alanine, it is possible that R16 and R27 combine to produce the overall effect on open state stability that is lost when they are mutated individually. Despite the lack of effect when mutated separately, it would be interesting to see the effect of mutating the R16 and R27/28 triplets simultaneously i.e. to produce K_{ir}6.2-ARI-IRD and K_{ir}6.1-TRL-YRT. The lack of

structural data for Kir6.0 subunits and no reliable models of the N-terminus of Kir6.2, because present crystal structures for potassium channels do not include the N-terminus, make it difficult to predict what residues may interact with R16 and R27 if not their neighbours. Given the lack of effect on spontaneous opening for ARI and IRD it is surprising that IRD has a slightly lower IC₅₀ for ATP inhibition than wild type Kir6.2. This suggests that the effect is not as a result of a decrease in P_o leading to increased occupancy of the proposed ATP-binding interburst closed state and subsequent decrease in IC₅₀. As the ATP binding site of K_{ATP} has been well characterised and little evidence exists to suggest that any residues mutated here are involved, the most likely explanation for this change in ATP sensitivity is either that the wild type residues, YRT, represents a source of allosteric modulation of ATP inhibition or that their mutation alters the way the channel translates ATP binding into closure of the pore.

ENLRK showed a slight reduction in spontaneous opening, when compared to wild type Kir6.2, but this did not achieve statistical significance. As well as being a highly divergent region of the N-terminus between Kir6.1 and Kir6.2, these residues were selected for assessment based on the identification of residues 20-30 in truncated Kir6.2 as being involved in determining ATP sensitivity (Koster *et al.*, 1999b). Therefore this region is also likely to be involved in determining open state stability. The lack of significant alteration in relative activation of ENLRK shows that mutation of these residues to their Kir6.1 counterparts does not affect spontaneous opening. It could be argued that, given a similar increase in P_o upon truncation of Kir6.1 (which saturates after deletion of the first 33 amino acids; Babenko & Bryan, 2001) and Kir6.2 (Koster *et al.*, 1999b), both subtypes possess elements that influence the open state stability of

the channel and that supplementing one for the other, as I have done, would have little effect and only by removing these regions altogether, as with truncation, can their influence be observed. No P_o values were presented for these truncated $K_{ir6.1}$ channels and it is therefore difficult to ascertain the regions of $K_{ir6.1}$ that most effect P_o (Babenko & Bryan, 2001). As the conserved R27 residue and its divergent neighbouring residues (mentioned above) were also removed in the $\Delta N2-30$ $K_{ir6.2}$ channel, it is possible that these regions combine to produce the difference in properties between $\Delta N2-20$ and $\Delta N2-30$. Production of mutant $K_{ir6.0}$ subunits swapping ENLRK and IRD from $K_{ir6.1}$ with DPTE and YRT from $K_{ir6.2}$ and vice versa would put the difference between the $\Delta N2-20$ and $\Delta N2-30$ channels in a more relevant context as these are the non-conserved amino acids from position 20-30. If this channel possessed ATP sensitivity and P_o properties similar to $\Delta N2-30$ then, given the lack of effect of ENLRK or IRD, these regions must combine to produce the characteristics of wild type channels. As I have tested almost all of the divergent regions in the N-terminal 30 amino acids of $K_{ir6.2}$ separately and none significantly affected spontaneous opening, it is possible that multiple interactions between these divergent sequences contribute to the difference in spontaneous opening of $K_{ir6.1}$ and $K_{ir6.2}$. Mutating them individually may allow the remaining interacting parts to compensate and thus a minimal effect is seen, as with ENLRK. The small decrease in IC_{50} for ATP inhibition in ENLRK is expected given its slight decrease in spontaneous opening. Assuming that ATP preferentially binds to the closed state of the channel, a decrease in spontaneous opening is most likely a result of a greater occupancy of the interburst closed state i.e. the state that is thought to bind ATP more effectively. It is here that the lack of single channel analysis is most important as calculation of

intraburst and interburst kinetics would give a clearer picture of what might be responsible for the slight decrease in ATP sensitivity of ENLRK.

The four individual mutations of S37A, K39S, N41A and V44L did not have a significant effect on spontaneous opening of $K_{ir}6.2$, as previously described in the case of S37A (Kondo *et al.*, 1998). However, V44L displayed a slightly lower relative activation to wild type. To confirm previous findings elsewhere that lead to the creation of these mutants, a channel carrying all four mutations simultaneously, ASAL, was tested. In agreement with Kondo *et al.* who produced an almost identical channel (see chimera 122-3 in figure 4.18; Kondo *et al.*, 1998), the ASAL mutation caused a significant decrease in spontaneous opening in $K_{ir}6.2$. However, the decrease caused by ASAL was smaller than that produced by the chimera of Kondo and colleagues. Species specific differences in amino acid sequence between that study and this are unlikely to account for this as the only difference in sequence within this region is at position 44 where there is a conservative I/L variation. Once again this suggests that it is the combination of two or more of these residues that affects the change in relative activation seen in ASAL rather than the influence of any one residue alone. It is possible that only by mutating all of these residues simultaneously can any effect be resolved. This suggests that residues 37-44 of $K_{ir}6.2$ may form a stable structure that is involved in control of spontaneous bursting and that mutation of one residue within this structure is not sufficient to disrupt the overall conformation. This could be tested by performing double or triple simultaneous mutations of the four divergent residues within this region. Given that V44L had the greatest effect alone, starting with double or triple

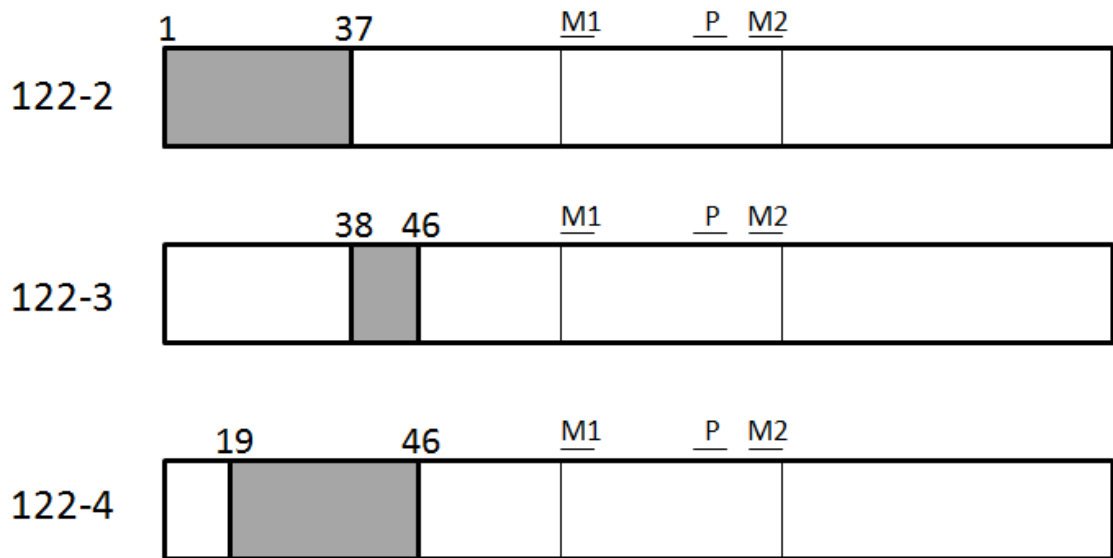


Figure 4.18 - Schematic representation of chimeras from Kondo *et al.* paper

White boxes refer to K_{ir}6.2 sequence and shaded boxes represent K_{ir}6.1 sequence. Numbers above the box refer to the amino acid position in K_{ir}6.1. M1, M2 and P are the two transmembrane helices and the pore loop, respectively. Reproduced from Kondo *et al.*, 1998.

mutations that included V44L would be sensible. N-terminal truncation studies have been carried out showing that removal of the first 32 and 44 amino acids ($\Delta N32$ and $\Delta N44$) of $K_{ir}6.2$ causes a large increase in P_o (Babenko *et al.*, 1999b). Surprisingly there is no difference in P_o between these two N-terminally truncated channels despite the fact that in this study and elsewhere (Kondo *et al.*, 1998), residues between positions 32 and 44 have been shown to influence spontaneous opening of the channel. One explanation for this discrepancy, as with other mutants I have created, is that the residues between positions 32 and 44 interact with the first 32 amino acids of the channel to affect open state stability of the channel. Therefore removing the possibility of this interaction altogether by deleting the N-terminal 32 residues has a dramatic effect on spontaneous opening, more so than when simply altering the interaction by mutating some of the elements responsible. It is unfortunate that I was not able to measure the ATP sensitivity of the ASAL mutant as I would have expected it to display a significantly lower IC_{50} to reflect the change in spontaneous opening. If this were not the case then it would suggest an interesting effect of ASAL that is likely to involve its role as a transducer of signals from SUR (see below for further discussion of this).

Kondo and colleagues produced chimeric channels with varying regions taken from the N-terminus of $K_{ir}6.1$ – one with the N-terminal 37 amino acids, a second with residues 38-46 and a third with amino acids 19-46 from $K_{ir}6.1$ and the rest from $K_{ir}6.2$ in all three (chimeras 122-2, 122-3 and 122-4 respectively, see figure 4.18; Kondo *et al.*, 1998). The difference in relative activation between these chimeras and the fact that a combined N- and C-terminal chimera has the lowest relative activation suggest that interactions both within the N-terminus and between it and the C-terminus may be

important in spontaneous activation of Kir6.2. Of particular interest here is the lower relative activation of 122-4 compared to 122-3. In combination with a C-terminal region, replacement of amino acids 37-45 of Kir6.2 produces Kir6.1-like relative activation. However, when assessed without the C-terminal mutation, extension of this region to include amino acids 19-36, including insertion of ENLRK and IRD, produces a channel with lower relative activation (Kondo *et al.*, 1998) than when residues 37-44 were mutated suggesting that residues 19-36 have an additional impact on spontaneous opening to residues 37-44. I have shown that this is not caused by the ENLRK or IRD mutations alone. Though interaction between amino acids 37-44 and the C-terminus is obviously important in generating spontaneously opening Kir6.2-containing channels, that does not eliminate the possibility of an interaction between residues 37-44 i.e. the divergent residues SKNV in wild type Kir6.2, and either DPTE, YRT or both to produce the relative activation characteristics of Kir6.2. Combining the ASAL mutation with ENLRK or IRD would clarify whether there is any interaction between these regions which produces the effect seen in the 122-3 chimera of Kondo and colleagues (Kondo *et al.*, 1998). The evidence presented here suggests that interaction of groups of amino acids rather than specific residues is more likely to be responsible for any effect.

Secondary structure prediction has suggested that the N-terminus of Kir6.2 may contain β -strands that might contribute to a conserved lipid interaction domain that reportedly controls the response of Kir channels to PIP₂ (Cukras *et al.*, 2002a, Cukras *et al.*, 2002b). These β -strands are predicted to occur at residues 34-38 and 42-46. As the only mutation I have shown to affect spontaneous opening spans these predicted

β -strands it is possible that their disruption is what underlies the effect of the ASAL mutation. It is suggested that only one of these β -strands contributes to the lipid interaction domain (Cukras *et al.*, 2002a). Given that the individual mutation that showed the greatest effect was at position 44 it is possible that the second predicted β -strand (residues 42-46) contributes to the domain. Sequence alignment with $K_{ir}3.1$, whose cytoplasmic domains have been crystallised, suggests that this is most likely the case (Nishida & MacKinnon, 2002).

It is possible that some of the effects seen here on ATP sensitivity and spontaneous opening are caused by alteration of the influence of SUR on K_{ATP} function. K_{ATP} channels containing different SUR subunits have different bursting properties and ATP sensitivity (Babenko *et al.*, 1999d). Construction of chimeras of SUR1 and SUR2A showed that the effect of SUR on bursting can be separated from its effect on ATP sensitivity, suggesting that SUR can affect gating of the channel and ATP sensitivity by different routes. The ATP sensitivity of SUR1 can be conferred onto SUR2A without affecting its P_o suggesting that SUR has an allosteric effect on ATP sensitivity either by affecting ATP binding directly or by altering the linkage between the ATP binding site and closure of the gate (Babenko *et al.*, 1999d). As SUR does not contribute directly to the ion conducting pathway of K_{ATP} its effect on gating must be communicated via an interface with the pore forming subunit. To support this, N-terminal truncation of $K_{ir}6.2$ reduced the inhibitory effect of tolbutamide, which binds to SUR, on channels co-expressed with SUR1 (Babenko *et al.*, 1999c). Also, SUR rescues wild type ATP sensitivity when co-expressed with C-terminally truncated $K_{ir}6.2$. However, N-terminal truncation of this already shortened $K_{ir}6.2$ abolishes the rescuing effect of SUR (Koster

et al., 1999b). These findings suggest that the N-terminus of K_{ir}6.2 is responsible for transducing signals from SUR to the pore. Further evidence for the role of the N-terminus in linking SUR with the pore comes from the finding that a synthetic K_{ir}6.2 N-terminal peptide (Ntp), containing residues 2-33, increases the P_o of K_{ir}6.2/SUR1 channels, similar to that that seen with N-terminally truncated K_{ir}6.2, but has no effect when applied to C-terminally truncated K_{ir}6.2 alone (Babenko & Bryan, 2002). Similarly, application of Ntp to K_{ir}6.1-containing channels induces spontaneous opening (Babenko & Bryan, 2002) though the relevance of applying a K_{ir}6.2 N-terminal peptide to K_{ir}6.1 is questionable. An explanation for this finding is that Ntp competes with native K_{ir}6.0 N-termini for a contact site on SUR and that the interaction between SUR and K_{ir}6.0 stabilises the interburst state of the channel. When Ntp binds to this site, leaving the native N-terminus of the channel unbound, the influence of SUR is not felt in the pore and this translates to an increase in P_o. As K_{ir}6.0 subunits differ in their bursting properties it is possible that their coupling with SUR is different or that the influence of SUR is interpreted differently by each subunit i.e. that a different interpretation by or “stronger” influence of SUR on K_{ir}6.1 accounts for its lack of spontaneous bursting. Though I have presented no direct evidence of this, it is possible that the small effect seen in ENLRK is caused by the mutation altering the way that the channel interprets the input of SUR, which leads to a more K_{ir}6.1-like spontaneous bursting pattern. All mutants tested showed complete inhibition by 10 μM glibenclamide. This might suggest that communication between SUR and the pore is unaffected but given that this is a supramaximal inhibitory concentration of the drug, construction of a dose-response curve would give a better indication of the sensitivity of the channels to glibenclamide. Normal sulphonylurea sensitivity could also suggest

that drug binding to SUR and SUR's influence on open state stability are transmitted to Kir6.0 differently.

Comparing the results presented here to the evidence that inspired the construction of these mutants highlights a fundamental problem with the different approaches to investigating the structure-function relationship of K_{ATP} channels. Specifically when trying to investigate the differences in properties conferred by the pore-forming subunits. The problem comes when trying to translate an effect seen in one isoform of the channel to explain why different channels have different properties and is made worse by the majority of research being carried out on Kir6.2. Truncations provide a lot of information about which parts of the channel may be involved in a certain process, however, the very reason that they are useful is because of the crude alterations that they make to the structure of the channel. Point mutations provide a more subtle approach to studying the effect of specific residues or regions, however, this depends entirely on what the sequence is mutated to. The most emphatic effects are likely to be seen with the biggest alteration. Again, this fact is the very downfall of point mutation when applied to studying the differences between isoforms as I have done because there is only one possible mutation to be made to any individual residue. As I have discussed above, the more subtle and physiologically relevant approach of exchanging residues between isoforms, especially on the scale of single residues, may simply highlight the small contribution that a residue makes to an overall effect while not producing a dramatic effect by itself.

Chapter Five

The effect of 14-3-3 on K_{ATP} channels

5 The effect of 14-3-3 on K_{ATP} channels

5.1 Introduction

As I have described previously, expression of K_{ir}6.1 and its mutants with SUR2A in CHO cells is poor. This posed the biggest problem when it came to attempt to record macroscopic currents to assess the relative activation of wild type and mutant K_{ir}6.1 channels as there were never enough channels to constitute a macroscopic current. This chapter details one of the efforts made to try to improve expression of this isoform of the channel in an attempt to make the recording of macroscopic currents possible.

14-3-3 are a family of proteins that can be broadly described as scaffold proteins or chaperones and are involved in a wide range of cellular processes from apoptosis to cell cycle control (Dougherty & Morrison, 2004). Importantly, 14-3-3 has been shown to interact with a number of ion channels, fulfilling a role as both chaperone (O'Kelly *et al.*, 2002, Rajan *et al.*, 2002, Zuzarte *et al.*, 2009) and regulatory molecule (Kagan *et al.*, 2002). Binding of the coat protein complex I (COPI) coatamer and 14-3-3 to the twin pore potassium channels TASK1 and 3 controls the surface expression of the channels (O'Kelly *et al.*, 2002, Rajan *et al.*, 2002, Zuzarte *et al.*, 2009). 14-3-3 β and ϵ bind to the extreme C-terminus of TASK 3 in a phosphorylation dependent manner (O'Kelly *et al.*, 2002, Zuzarte *et al.*, 2009). Removal of as little as one amino acid, the C-terminal valine in TASK 3, can abolish 14-3-3 binding (O'Kelly *et al.*, 2002) and similar truncations cause significantly reduced current in TASK 1 and 3 (O'Kelly *et al.*, 2002, Rajan *et al.*, 2002, Zuzarte *et al.*, 2009). Both the N- and C-termini of TASK 3 have been shown to interact

with β -COP, part of COPI, leading to localisation of TASK 3 to internal organelles rather than the cell surface (O'Kelly *et al.*, 2002, Zuzarte *et al.*, 2009). Binding of 14-3-3 to its motif in the C-terminus of TASK 3 antagonises binding of β -COP such that when 14-3-3 is bound to TASK 3 β -COP cannot bind, leading to greater surface expression of the channel (O'Kelly *et al.*, 2002, Zuzarte *et al.*, 2009) N.B. binding of β -COP to the N-terminus of TASK 3 is 14-3-3 independent (Zuzarte *et al.*, 2009).

14-3-3 has been implicated in functional regulation of many ion channels (Booij *et al.*, 1999, Chan *et al.*, 2000, Czirjak *et al.*, 2008, Li *et al.*, 2006, Zhou *et al.*, 1999) including two cardiac channels hERG and $\text{Na}_v1.5$ (Allouis *et al.*, 2006, Kagan *et al.*, 2002). To use the example of hERG regulation by 14-3-3 ϵ and η , phosphorylation of residues in the N- and C-termini of hERG by protein kinase A (PKA) allows binding of 14-3-3. This leads to an altered current-voltage relationship, a leftward shift in the voltage dependence of activation and faster activation time constants (Kagan *et al.*, 2002). 14-3-3 binding to hERG shields these phosphorylated residues from dephosphorylation suggesting that it is the stabilisation of the PKA-phosphorylated state of the channel that may produce these effects (Kagan *et al.*, 2002).

K_{ATP} channel assembly and trafficking is described in the introduction (see 1.4.2). Correct assembly of the K_{ATP} hetero-octamer is essential for expression of the channel at the cell surface. Unassembled subunits or partially assembled channels are retained in the ER via exposed retention signals present on both $\text{K}_{\text{ir}}6.0$ and SUR (Zerangue *et al.*, 1999). 14-3-3 ϵ and ζ were first identified as being involved in K_{ATP} channel expression via demonstration of their association with a C-terminal fragment of $\text{K}_{\text{ir}}6.2$, specifically involving the ER retention signal (RKR) mentioned above (Yuan *et al.*, 2003). Though

the ER retention signal in K_{ir}6.2 is located in a PKA consensus site, interaction with 14-3-3 does not require phosphorylation (Yuan *et al.*, 2003). The C-terminus of K_{ir}6.2 does not possess any canonical 14-3-3 binding motifs, however, truncation of the C-terminus by 10 amino acids drastically reduces 14-3-3 binding (Heusser *et al.*, 2006). Also, scavenging of 14-3-3 has been shown to reduce surface expression of native and heterologously expressed K_{ATP} channels (Heusser *et al.*, 2006). As expression of K_{ir}6.1-containing channels was low in this study (see 3.2.1 and 4.3.1), it was hoped that over-expressing 14-3-3 could increase their surface density, as has been demonstrated with TASK 1 in *Xenopus* oocytes (Rajan *et al.*, 2002). This strategy assumed that the number of 14-3-3 molecules present was limiting the membrane trafficking of K_{ir}6.1/SUR2A and its mutants and that supplementing endogenous 14-3-3 with recombinant 14-3-3 would improve the situation. As a positive control, the effect of 14-3-3 over-expression was also studied in K_{ir}6.2/SUR2A channels.

5.2 The effect of 14-3-3 on whole cell K_{ATP} currents

Whole cell currents were recorded from CHO cells expressing K_{ir}6.1 or K_{ir}6.2 with SUR2A and either 14-3-3 ϵ , ζ or both of these isoforms simultaneously to assess the effect of 14-3-3 co-expression on K_{ATP} currents. These 14-3-3 subtypes were selected for testing given the evidence of their interaction with the K_{ir}6.2 C-terminus (Yuan *et al.*, 2003). Co-expression of K_{ir}6.0/SUR2A with the fluorescent protein mCherry substituted for 14-3-3 served as a control for these experiments rather than simply by leaving out 14-3-3. This was to exert the same expression “load” on the cell as 14-3-3. mCherry was encoded by a pcDNA3.1 vector and its transcription, as were all the heterologously expressed proteins in this study, was under the control of the

cytomegalovirus (CMV) promoter. This strategy assumes that a component of the transcription machinery e.g. a transcription factor, is the limiting factor in expression and therefore adding the third vector, encoding 14-3-3, will reduce the expression of the other two proteins i.e. $K_{ir}6.0$ and SUR2A. Expression of a fluorescent protein was selected for the control experiment as there is no evidence to suggest any effect of mCherry on K_{ATP} currents therefore its only effect is on overall expression. For the remainder of this chapter I will refer to $K_{ir}6.0/SUR2A$ and mCherry as wild type. When setting up the transfections for these experiments, 1 μg of cDNA encoding each of the three proteins was added to the reaction. In the case of the combined expression of 14-3-3 ϵ and ζ , a total of 1 μg of their cDNA was added i.e. 0.5 μg of each.

10 μM P1075, a potent opener of K_{ATP} channels, was perfused onto the cells to open the channels while being held at a membrane potential of 0 mV at 30°C. All K_{ATP} channels were assumed to be closed i.e. only background currents remain, when a high concentration (10 μM) of the K_{ATP} channel blocker glibenclamide was added. All currents were corrected for cell size by dividing peak whole cell currents by the whole cell capacitance, which gives an indication of membrane area. In all cases, currents were measured from cells within 30 hours of transfection. Peak whole cell current for $K_{ir}6.1$ or $K_{ir}6.2$ with SUR2A and various 14-3-3 isoforms can be seen in figures 5.1A and 5.2A. As expected, $K_{ir}6.1/SUR2A$ wild type currents were considerably smaller than their $K_{ir}6.2$ counterparts (14.2 ± 3.4 pA/pF, $n=8$; and 116.4 ± 17.0 pA/pF, $n=12$; respectively). Co-expression of neither 14-3-3 ϵ , ζ , nor a combination of the two, had a significant effect on whole cell $K_{ir}6.1/SUR2A$ currents. 14-3-3 ζ and the combined

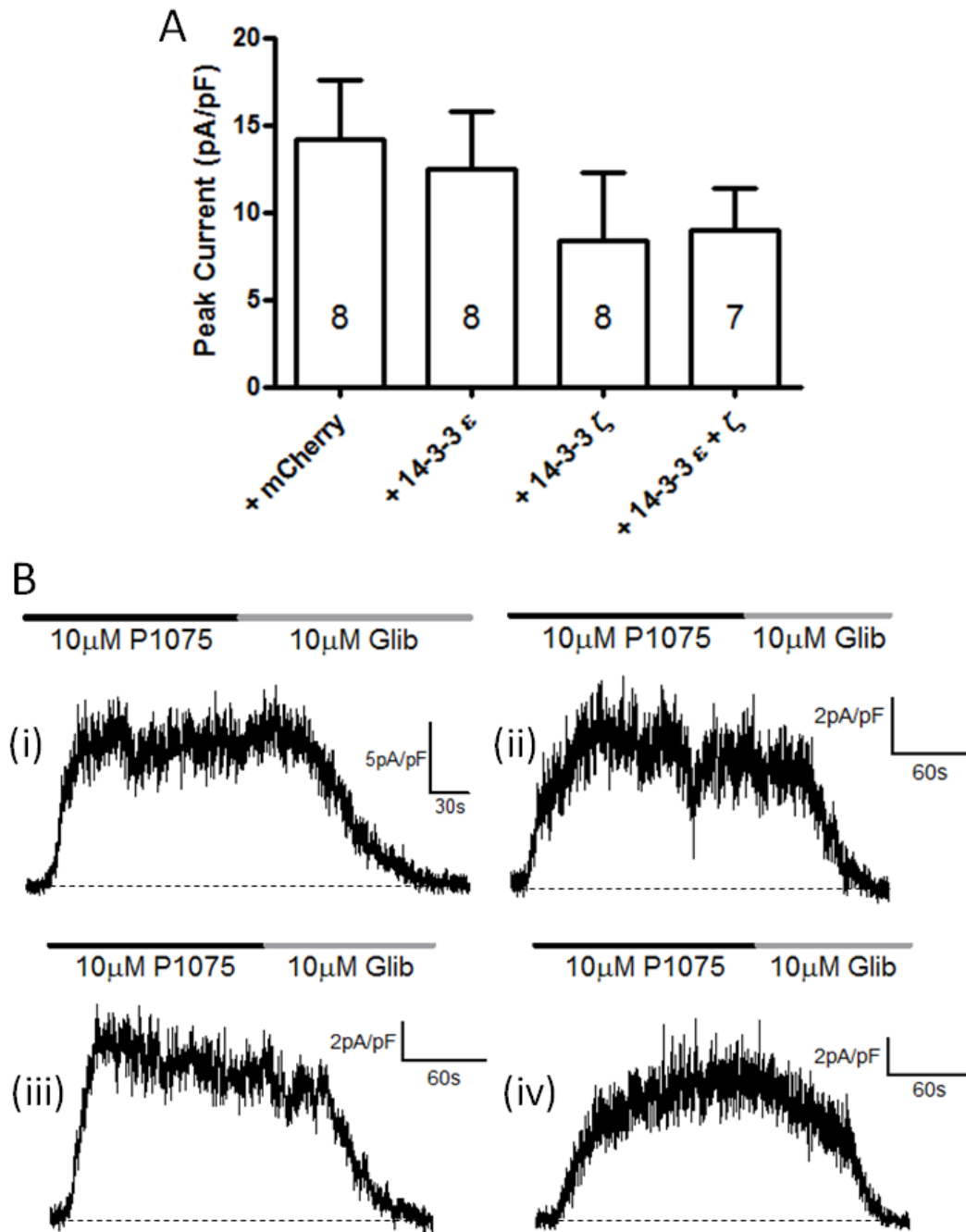


Figure 5.1 - Effect of co-expression of 14-3-3 on whole cell recombinant K_{ATP} currents in cells expressing $K_{ir}6.1$ and SUR2A

A, peak whole cell current elicited by 10 μ M P1075 from CHO cells expressing $K_{ir}6.1$, SUR2A and mCherry (control) or 14-3-3. Recordings were made at 0 mV. Zero K_{ATP} current level was taken as that during perfusion of 10 μ M glibenclamide. All currents were corrected for cell size. Each bar represents mean \pm s.e.m for the number of cells shown within the bar.

B, example trace for a whole cell recording taken from a cell expressing $K_{ir}6.1$, SUR2A and (i) mCherry, (ii) 14-3-3 ζ , (iii) 14-3-3 ϵ , or (iv) 14-3-3 ϵ and ζ . Drugs were perfused onto the cell as indicated by the bars above the trace. The dashed line shows the current when all K_{ATP} channels were closed i.e. in 10 μ M glibenclamide. Trace has been corrected for cell size.

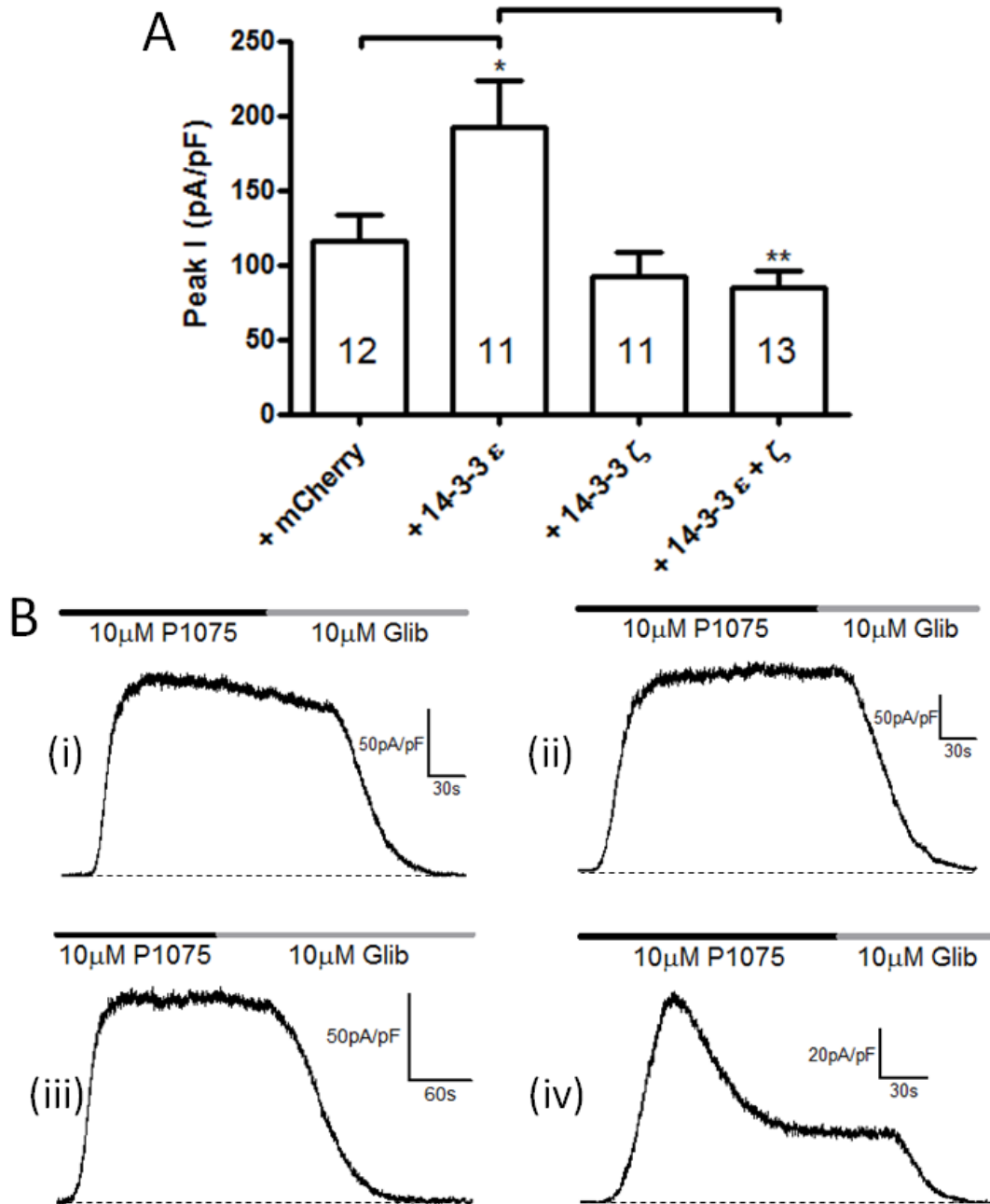


Figure 5.2 - Effect of co-expression of 14-3-3 on whole cell recombinant K_{ATP} currents in cells expressing $K_{ir}6.2$ and SUR2A

A, peak whole cell current elicited by 10 μ M P1075 from CHO cells expressing $K_{ir}6.2$, SUR2A and mCherry (control) or 14-3-3. Recordings were made at 0 mV. Zero K_{ATP} current level was taken as that during perfusion of 10 μ M glibenclamide. All currents were corrected for cell size. Each bar represents mean \pm s.e.m for the number of cells shown within the bar. * - $p < 0.05$, ** - $p < 0.01$ (1-way ANOVA with Bonferroni post-test).

B, example traces for whole cell recordings taken from cells expressing $K_{ir}6.2$, SUR2A and (i) mCherry, (ii) 14-3-3 ϵ , (iii) 14-3-3 ζ , or (iv) 14-3-3 ϵ and ζ . Drugs were perfused onto the cells as indicated by the bars above the traces. The dashed lines show the current when all K_{ATP} channels were closed i.e. in 10 μ M glibenclamide. Traces have been corrected for cell size.

co-expression of ϵ and ζ caused a small decrease in $K_{ir6.1}/SUR2A$ currents. However, given the small size of the currents and the large standard error of all the groups, it is hard to view this difference as anything other than a sampling anomaly, especially as no 14-3-3s had a significant effect on $K_{ir6.1}/SUR2A$ currents.

In the case of $K_{ir6.2}/SUR2A$, co-expression with 14-3-3 had a dramatic effect on whole cell currents. When 14-3-3 ϵ was expressed alongside the $K_{ir6.2}/SUR2A$, currents were significantly ($p < 0.05$) higher than wild type (191.9 ± 32.0 pA/pF, $n=11$; figure 5.2A). No such effect was seen with 14-3-3 ζ . However, combined co-expression of 14-3-3 ϵ and ζ produced currents significantly ($p < 0.01$) smaller than 14-3-3 ϵ alone but no different to wild type (84.5 ± 11.8 pA/pF, $n=13$) i.e. restored wild type current levels. Example traces for $K_{ir6.1}$ and 6.2 with all 14-3-3 isoforms can be seen in figure 5.1B and 5.2B. While the example trace for 14-3-3 ϵ and ζ (figure 5.2Biv) shows that there is a sharp decrease in current following the peak before the plateau and the others (figure 5.2Bi and ii) show a plateau immediately following the peak, no consistent pattern emerged in this respect. Every group exhibited both plateau phenotypes.

5.3 Discussion

The primary goal of co-expressing 14-3-3 with K_{ATP} was to improve expression of $K_{ir6.1}$ -containing channels as their low membrane density in CHO cells made it difficult to record macroscopic currents necessary to measure relative activation and ATP sensitivity of these channels. No effect was seen when either 14-3-3 ϵ , ζ , or a combination of these subtypes, were co-expressed with $K_{ir6.1}/SUR2A$. As the evidence supporting a role of 14-3-3 in K_{ATP} expression involves full length or fragments of $K_{ir6.2}$,

the lack of effect on $K_{ir6.1}/SUR2A$ current density seen here suggests that the interaction is specific to $K_{ir6.2}$. It is possible that other 14-3-3 isoforms interact with $K_{ir6.1}$ than those that bind to $K_{ir6.2}$. Testing $K_{ir6.1}$ for interaction with 14-3-3 e.g. by co-immunoprecipitation, would clarify the matter.

Whole cell current amplitude such as that recorded here can be described as $i \cdot N \cdot P_o$ where N is the number of channels in the membrane, i is the unitary conductance of the channel and P_o is open probability. An increase in whole cell current like that observed with 14-3-3 ϵ could be as a result of increasing any of these three properties. Peak current amplitude can be assumed to have been reached when application of 10 μ M P1075 caused opening of all the channels in the membrane to their maximum P_o , or at least very close to this situation. As these whole cell currents were elicited by pharmacological opening of the channels in such a manner, a change in P_o is unlikely to underlie the increase in current with 14-3-3 ϵ . Impaired recruitment of 14-3-3, by removing the last 10 amino acids from $K_{ir6.2}$, had no effect on the ATP sensitivity of K_{ATP} channels formed from SUR1- $K_{ir6.2}\Delta C10$ fusions (Heusser *et al.*, 2006) suggesting that 14-3-3 binding has no effect on K_{ATP} channel function. This argues that changing i or P_o may not be the cause. Conversely, 14-3-3 has been associated with functional changes in other ion channels (see 5.1). The interaction between hERG and 14-3-3 causes a leftward shift in the current-voltage relationship of the channel (Kagan *et al.*, 2002) suggesting it is possible for 14-3-3 to influence biophysical characteristics of ion channels. The increase in whole cell current with 14-3-3 ϵ was most likely caused by an increase in N i.e. 14-3-3 ϵ promotes trafficking of $K_{ir6.2}/SUR2A$ channels to the membrane. However, to fully eliminate the possibility that 14-3-3 binding affects

channel function, single channel recordings to confirm P_o in response to 10 μ M P1075 and single channel conductance would be necessary. It is unlikely that the effect of 14-3-3 ϵ on current density is brought about by shielding of phosphate groups, as in hERG (Kagan *et al.*, 2002), because 14-3-3 binding to $K_{ir}6.2$ has been shown to be independent of phosphorylation (Yuan *et al.*, 2003).

We know that dimerisation is important for the action of 14-3-3. In its association with ion channels there is only one example of a 14-3-3 monomer interacting with its target, the *Drosophila* calcium-dependent potassium channel slowpoke binding protein (Slob), and while this monomeric interaction is functional it was forced by preventing dimerisation of 14-3-3 (Zhou *et al.*, 2003) and therefore may not be the case in a normal physiological setting. Dimerisation is particularly important when discussing 14-3-3 ϵ as this isoform is known to preferentially form heterodimers and rarely form homodimers (Chaudhri *et al.*, 2003, Yang *et al.*, 2006) though we know that recombinant expression of single subtypes will yield homodimers as monomers are thermodynamically unstable (Aitken, 2006). This would suggest that 14-3-3 ϵ will form heterodimers with any native 14-3-3 subunits before forming homodimers. Therefore, as I have not demonstrated the presence or absence of 14-3-3 native to CHO cells, it could be heterodimerisation of 14-3-3 ϵ with a native subtype that produces the effect seen here. Similarly, the reduction in whole cell $K_{ir}6.2$ /SUR2A current back to wild type levels with 14-3-3 ϵ and ζ could be a result of heterodimerisation of 14-3-3 ϵ and ζ leading to a lack of 14-3-3 ϵ homodimers and therefore no effect. Identifying whether CHO cells possess any native 14-3-3 isoforms would address the question of whether 14-3-3 ϵ homodimers form at all or whether an unknown heterodimer of 14-3-3 ϵ and

whatever subtypes are present in CHO cells is responsible for the increase in current with 14-3-3 ϵ . It would be interesting to see what effect co-expression of other 14-3-3 isoforms with 14-3-3 ϵ would have on whole cell current. It is possible that the attenuation of the effect of co-expressing with 14-3-3 ϵ by adding 14-3-3 ζ is not specific to this combination and that other heterodimers may mimic the effect of the 14-3-3 ϵ and ζ heterodimer while other combinations might not alter the effect of 14-3-3 ϵ alone.

The predominant isoform of 14-3-3 in the heart is 14-3-3 ϵ (Liew *et al.*, 1994, Luk *et al.*, 1998, Tanaka *et al.*, 1996) though evidence from screens of heart cDNA libraries for interaction with various proteins has shown that other isoforms are expressed in the heart e.g. β , ζ , η , σ and τ (Diviani *et al.*, 2004, McKinsey *et al.*, 2000, O'Kelly *et al.*, 2002, Ogihara *et al.*, 1997). The presence of other isoforms in a tissue where 14-3-3 ϵ dominates is hardly surprising given what is known about its need for heterodimerisation. This is very interesting in the context of what I have shown about the effect of 14-3-3 ϵ on $K_{ir6.2}/SUR2A$ currents as this is the combination of subunits that comprises the cardiac K_{ATP} channel (Inagaki *et al.*, 1996) especially when taken with the fact that 14-3-3 ϵ and ζ have been shown to interact with a $K_{ir6.2}$ C-terminal construct (Yuan *et al.*, 2003). This suggests that the effect seen here may have some relevance in K_{ATP} expression in the heart but stresses the need to identify any native CHO cell 14-3-3 subtypes that may have interacted with 14-3-3 ϵ when it was expressed alone.

Chapter Six

Summary and Overall Discussion

6 Summary and Overall Discussion

In this study I have used a combination of molecular biology and electrophysiological recording to investigate two main areas of interest: the structure-function relationship of K_{ATP} channels, particularly pertaining to spontaneous opening, and ways to improve expression of K_{ATP} channels in transiently transfected CHO cells. Initial experiments were also carried out to ensure that the expression system being used here reconstituted the channels well compared to other expression systems.

6.1 Characterisation of Wild Type K_{ATP} Channels

Wild type $K_{ir}6.1$ and $K_{ir}6.2$ were heterologously expressed with SUR2A in CHO cells by transient transfection. The $K_{ir}6.2$ /SUR2A subunit combination constitutes the cardiac isoform of K_{ATP} (Inagaki *et al.*, 1996), however, there is no evidence supporting $K_{ir}6.1$ /SUR2A as a physiological subunit complex. This combination was used in favour of the physiologically relevant, proposed vascular smooth muscle K_{ATP} isoform $K_{ir}6.1$ /SUR2B (Yamada *et al.*, 1997) because keeping the SUR subunit consistent between experimental groups makes for better comparison between the two groups i.e. $K_{ir}6.1$ - and $K_{ir}6.2$ -based channels. Also, the $K_{ir}6.1$ /SUR2B combination was avoided because its expression is very poor when transiently transfected (personal communication – Dr. R. Rainbow), or even expressed in *Xenopus* oocytes, so choosing SUR2A for co-expression instead was hoped to give better recordings while also providing the consistency with $K_{ir}6.2$ -based channels.

Whole cell recordings of $K_{ir}6.1/SUR2A$ and $K_{ir}6.2/SUR2A$ from CHO cells show that I was able to reconstitute channels with opener and blocker sensitivity, P1075 and glibenclamide respectively, expected for these channels. The experiments also demonstrated that $K_{ir}6.1$ produced smaller currents than $K_{ir}6.2$ when co-expressed with SUR2A, exemplified by the need to wait two days after transfection before recording from $K_{ir}6.1/SUR2A$ but only one day for the $K_{ir}6.2/SUR2A$. Even with the extra day to express the channels, currents from $K_{ir}6.1$ channels were less than half the size of channels containing $K_{ir}6.2$. This suggests that expression of $K_{ir}6.1/SUR2A$ channels is under tighter constraint as the difference in conductance between the two channels would only be able to explain the difference in whole cell currents if they both took the same amount of time to reach their respective current densities. It is possible that the non-physiological nature of the $K_{ir}6.1/SUR2A$ complex is responsible for the apparent difference in expression as the machinery involved in recognising fully assembled channels may not be able to recognise this complex as easily as channels that form naturally.

Single channel recordings made using the inside-out patch configuration were used to obtain unitary conductance values for $K_{ir}6.1/SUR2A$ and $K_{ir}6.2/SUR2A$. Over the negative range of membrane potentials to which the patches were subjected, both channels exhibited similar unitary conductance to values previously published for the same channels. Unitary conductance of $K_{ir}6.2/SUR2A$ channels were well within the range of values seen elsewhere but $K_{ir}6.1/SUR2A$ channels were slightly higher, though still in reasonable agreement, with those obtained elsewhere. Both channels showed

the inward rectification characteristics expected when recording $K_{ir}6.0$ -containing channels.

The ATP sensitivity of $K_{ir}6.2/SUR2A$ channels was measured by exposing excised patches to varying concentrations of the nucleotide and measuring their effect on macroscopic currents. The IC_{50} for the inhibition of $K_{ir}6.2/SUR2A$ by ATP agreed well with values obtained from the literature. All of these findings meant that I was happy to use this expression system to measure similar characteristics in mutant channels to assess their effect on properties of the channels.

6.2 Construction and Characterisation of Mutant $K_{ir}6.0$ Subunits

Overlap PCR was used to mutate the sequence of $K_{ir}6.1$ and $K_{ir}6.2$ to produce 13 mutant $K_{ir}6.0$ subunits for testing (see table 4.2 or 4.3 for a list of mutants). One of these mutants (S40K) underwent an unwanted additional mutation at a restriction site that was used during the cloning process leading to a truncated, non-functional channel. The other 12 mutants produced whole cell currents similar to their respective parent subtype when expressed with SUR2A with smaller currents from $K_{ir}6.1$ -based channels maintained throughout. Given the difference in current density across the spectrum of mutants I have proposed that $K_{ir}6.1$ -containing channels must have an additional limiting factor in their expression compared to $K_{ir}6.2$ -containing channels. It is easy to exclude the possibility that $K_{ir}6.1$ mRNA is degraded more quickly as this would not result in such a dramatic increase in channel density following a longer incubation after transfection. This leaves the possibility that $K_{ir}6.1$ mRNA is translated less efficiently than that of $K_{ir}6.2$, $K_{ir}6.1/SUR2A$ requires more time to be fully

assembled and trafficked to the membrane or $K_{ir}6.1/SUR2A$ is more frequently removed from the membrane but less frequently recycled back than $K_{ir}6.2/SUR2A$ leading to its lower density. Further experiments would be required to discover what is responsible for this phenomenon. As 14-3-3 have been implicated in K_{ATP} channel assembly and trafficking (Heusser *et al.*, 2006, Yuan *et al.*, 2003) I would start by reducing overall levels or over-expressing relevant isoforms within the cell (see chapter 5 for the effect of 14-3-3 overexpression). Due to the low expression of $K_{ir}6.1$ -based channels, they were excluded from further experiments investigating the behaviour of the mutant channels. This was to save time to be used to investigate $K_{ir}6.2$ -based channels instead, especially as measurement of macroscopic currents was required in some of the latter experiments.

I also investigated some single channel properties of the mutant $K_{ir}6.2$ channels. All of the mutants tested showed the same inward rectification characteristics as wild type. However, two of the mutants showed altered unitary conductance compared to wild type. ENLRK had a slightly lower and ARI a significantly lower conductance. The effect is not likely to be caused by a direct effect on ion conduction as the residues involved in this, particularly those responsible for the difference in conductance between $K_{ir}6.1$ and $K_{ir}6.2$, have already been identified (Repunte *et al.*, 1999). In a study where chimeras of $K_{ir}6.1$ and $K_{ir}6.2$ were created, replacing the N-terminus of $K_{ir}6.2$ with that of $K_{ir}6.1$ caused a similar, but un-noted, effect on conductance to that seen in ENLRK and ARI (Kondo *et al.*, 1998). These mutants demonstrate a link between the N-terminus of $K_{ir}6.2$ and the pore whereby its disruption can lead to a decrease in conductance. This is likely to occur via conformational changes in the pore being

initiated by the N-terminus. The physiological significance of the ability of the N-terminus to influence conductance is limited, however, the demonstration of a functional link between the N-terminus and the pore is important as it is likely to affect other events e.g. drug sensitivity (Babenko *et al.*, 1999c). Such a link has been suggested before, though in a different context, by the finding that mutation of an N-terminal arginine residue of $K_{ir}6.2$ to alanine dramatically increased P_o (Cukras *et al.*, 2002a) as well as in other inward rectifier channels (Choe *et al.*, 1997).

The primary goal of all of the mutations I carried out was to assess their effect on spontaneous opening in $K_{ir}6.1$ - and $K_{ir}6.2$ -containing channels. To that end, relative activation, a gauge of spontaneous opening, was measured for each $K_{ir}6.2$ -based mutant. ASAL was the only mutant to show a significant reduction in relative activation. ENLRK showed a small decrease in relative activation but not a significantly different change. R16 and R27 in $K_{ir}6.2$ have been shown to be involved in open state stability of the channel – their mutation to alanine causes an increase in P_o to around the theoretical maximum for these channels (Cukras *et al.*, 2002a). These residues are conserved between $K_{ir}6.0$ subunits therefore I tested whether their tertiary environment can affect their influence on open state stability by mutating their neighbouring residues to those in $K_{ir}6.1$, creating ARI and IRD. This pair of mutants had the same relative activation as wild type but IRD had a slightly higher ATP sensitivity than wild type $K_{ir}6.2$, which did not reach statistical significance. The fact that ARI could affect conductance but not spontaneous opening or ATP sensitivity suggests that the influence of the N-terminus of the channel on conductance may occur via a different path from its influence on spontaneous opening. Given the dramatic effect of

the arginine to alanine mutations at both positions and the minimal effect of spontaneous opening and ATP sensitivity here, the logical conclusion is that the tertiary environment of R16 and R27 does not affect their influence on open state stability. However, given the similar effect of mutation of both residues to alanine, I propose that the residues may interact. As there is very limited structural data for the N-terminus of K_{ir}6.2 it is difficult to guess which residues interact with these arginines. Therefore, it would be interesting to assess whether the tertiary environment of the pair of residues interact to affect their influence on the stability of the open state.

The relative activation of ASAL was examined due to the lack of effect of the individual mutations that comprise it – S37A, K39S, N41A and V44L all had no effect on relative activation. These residues were selected for mutation based on the findings of Kondo and colleagues (Kondo *et al.*, 1998) who identified a nine amino acid section of K_{ir}6.1 that caused the channel to open spontaneously when replacing the equivalent residues in K_{ir}6.2. The four residues above are the only differences in sequence between the two isoforms. Simultaneous mutation of all four residues was carried out to show that the same effect could be seen here. The fact that ASAL, but none of the individual mutations, caused a decrease in relative activation suggests cooperation between the residues in this region to produce the overall effect. There are sixteen possible combinations of mutations of this quartet, I have assessed the effect of five (ASAL, S37A, K39S, N41A and V44L). To fully assess the possibility of interaction between these residues to produce the effect of the ASAL mutant, a further eleven mutants would need to be constructed and their relative activation tested.

The ENLRK mutation was carried out based on the evidence that truncating the N-terminus of K_{ir}6.2 by 20 amino acids produced a difference in ATP sensitivity compared to a truncation by 30 residues (Koster *et al.*, 1999b). As well as producing a small change in relative activation, ENLRK caused a small increase in ATP sensitivity that did not reach significance. It is possible that this change in ATP sensitivity is a reflection of the slight reduction in relative activation i.e. if the channel spends less time in the open state then ATP is able to bind more easily and decreases its IC₅₀ for the inhibition of the channel. I suggest that it is the concerted influence of ENLRK and another region of the N-terminus that produces the different ATP sensitivities of ΔN2-20 and ΔN2-30 K_{ir}6.2 observed by Koster and colleagues (Koster *et al.*, 1999b). As this region is also contained between positions 20 and 30 of K_{ir}6.2, I would first test an ENLRK-IRD mutant to see if it had any additional effect on ATP sensitivity and relative activation to ENLRK alone. The E23K mutation, present in ENLRK_K, has been shown to increase P_o and decrease ATP sensitivity of K_{ir}6.2 (Schwanstecher *et al.*, 2002a, Schwanstecher *et al.*, 2002b). However, the ENLRK mutant had the opposite effect overall – increasing sensitivity to ATP and reducing spontaneous activity. With such an extensive change in amino acid sequence caused by ENLRK i.e. multiple charge alterations, addition of a residue and removal of a potentially structurally important proline residue; it is possible that mutation of other residues within this sequence overrides the effect of E23K on the channel activity. Dissecting the sequence further may provide insight into what is happening. I would begin by removing the E23K mutation i.e. producing ENLR; to see if mutating the remaining residues had the opposite effect to E23K and by testing mutation of each of the four residues independently if their effect is more pronounced than ENLRK. The fact that the ENLRK mutation caused changes, however

minor, in so many properties suggests that it is important in linking the N-terminus of the channel to the pore. Also, the fact that the reduction in conductance, relative activation and ATP sensitivity were all small supports the hypothesis that ENLRK interacts with another region of the N-terminus to produce the effects seen in the truncation study (Koster *et al.*, 1999b).

6.3 The Effect of 14-3-3 on K_{ATP} Channels

In an attempt to improve the expression of $K_{ir}6.1$ and its mutants, as well as to gain insight into the effect on $K_{ir}6.0$ trafficking, I assessed the effect of co-expressing 14-3-3 isoforms on $K_{ir}6.1/SUR2A$ and $K_{ir}6.2/SUR2A$ channel density. Neither 14-3-3 ϵ , ζ nor a combination of the two had an effect on expression of channels containing $K_{ir}6.1$. However, 14-3-3 ϵ caused a significant increase in current density when co-expressed with $K_{ir}6.2$ and SUR2A. This effect was reversed when 14-3-3 ϵ and ζ were used. As previous evidence linking 14-3-3 ϵ and ζ with K_{ATP} channels involved a C-terminal fragment of $K_{ir}6.2$ (Yuan *et al.*, 2003) it is plausible that any interaction is specific to this isoform. In fact, the experiments here suggest that it may well be the case. It is also possible that no effect was seen with $K_{ir}6.1$ because the abundance of 14-3-3 is not a limiting factor in expression of that isoform but that it is limiting in expression of $K_{ir}6.2$. The next step to clarify this matter is to investigate whether any 14-3-3 isoforms can be shown to co-immunoprecipitate with $K_{ir}6.1$ or, assuming the interaction is localised to the same region as $K_{ir}6.2$, a C-terminal fragment of $K_{ir}6.1$.

Though there is evidence that 14-3-3 can affect ion channel function (Kagan *et al.*, 2002), as well as expression, the evidence for K_{ATP} suggests that a functional

interaction is unlikely (Heusser *et al.*, 2006). Despite this, the possibility remains that in order to increase current density, 14-3-3 ϵ overexpression either increases trafficking of channels to the membrane, increases P_o or increases unitary conductance of the channel. The latter two can be eliminated by performing single channel recordings on $K_{ir}6.2/SUR2A$ in the presence of 14-3-3 ϵ to see if there is any change. Given that the channels were pharmacologically opened, it is unlikely that an increase in P_o is responsible for the larger current density but it still needs to be eliminated as a possibility. The next question to be addressed is how 14-3-3 ϵ and ζ co-expression reverses the effect of 14-3-3 ϵ alone? As they are present in equal concentrations, it is possible that co-expression causes ϵ/ζ dimer formation, leaving few homodimers of either isoform where ϵ expression alone causes homodimer formation and that these homodimers are responsible for the effect on current density. As 14-3-3 ϵ preferentially forms heterodimers (Chaudhri *et al.*, 2003, Yang *et al.*, 2006), and only forms homodimers when recombinantly expressed by itself (Aitken, 2006), if there are any native 14-3-3 isoforms in CHO cells ϵ will form heterodimers with these isoforms before forming homodimers. Any unknown heterodimers may be responsible for the effect seen rather than 14-3-3 ϵ homodimers. To address this question it would be necessary to investigate what isoforms are present in CHO cells. This could be either by Western blotting for 14-3-3 isoforms or by immobilising R18, a peptide that binds 14-3-3 with high affinity (Wang *et al.*, 1999), incubating it with CHO cell cytosol and performing mass spectrometry to identify any proteins of ~ 30 kDa i.e. 14-3-3 isoforms; (as in Yuan *et al.*, 2003). While the matter of improving $K_{ir}6.1$ -based channel expression was not successfully addressed, finding an effect of 14-3-3 on $K_{ir}6.2$ provides an interesting future direction for this work.

Bibliography

Aguilar-Bryan L, Nichols CG, Wechsler SW, Clement JP, 4th, Boyd AE, 3rd, Gonzalez G, Herrera-Sosa H, Nguy K, Bryan J, & Nelson DA (1995) Cloning of the beta cell high-affinity sulfonylurea receptor: a regulator of insulin secretion. *Science* **268**: 423-426

Aitken A (2006) 14-3-3 Proteins: a Historic Overview. *Semin Cancer Biol* **16**: 162-172

Alekseev AE, Brady PA, & Terzic A (1998) Ligand-insensitive state of cardiac ATP-sensitive K⁺ channels. Basis for channel opening. *J Gen Physiol* **111**: 381-394

Allouis M, Le Bouffant F, Wilders R, Peroz D, Schott JJ, Noireaud J, Le Marec H, Merot J, Escande D, & Baro I (2006) 14-3-3 is a regulator of the cardiac voltage-gated sodium channel Nav1.5. *Circ Res* **98**: 1538-1546

Ammala C, Moorhouse A, & Ashcroft FM (1996) The sulphonylurea receptor confers diazoxide sensitivity on the inwardly rectifying K⁺ channel Kir6.1 expressed in human embryonic kidney cells. *J Physiol* **494 (Pt 3)**: 709-714

Amoroso S, Schmid-Antomarchi H, Fosset M, & Lazdunski M (1990) Glucose, sulfonylureas, and neurotransmitter release: role of ATP-sensitive K⁺ channels. *Science* **247**: 852-854

Antcliff JF, Haider S, Proks P, Sansom MS, & Ashcroft FM (2005) Functional analysis of a structural model of the ATP-binding site of the KATP channel Kir6.2 subunit. *EMBO J* **24**: 229-239

Ashcroft FM, Harrison DE, & Ashcroft SJ (1984) Glucose induces closure of single potassium channels in isolated rat pancreatic beta-cells. *Nature* **312**: 446-448

Ashcroft SJ, Weerasinghe LC, & Randle PJ (1973) Interrelationship of islet metabolism, adenosine triphosphate content and insulin release. *Biochem J* **132**: 223-231

Ashfield R, Gribble FM, Ashcroft SJ, & Ashcroft FM (1999) Identification of the high-affinity tolbutamide site on the SUR1 subunit of the K(ATP) channel. *Diabetes* **48**: 1341-1347

Ashford ML, Sturgess NC, Trout NJ, Gardner NJ, & Hales CN (1988) Adenosine-5'-triphosphate-sensitive ion channels in neonatal rat cultured central neurones. *Pflugers Arch* **412**: 297-304

Ashford ML, Boden PR, & Treherne JM (1990) Glucose-induced excitation of hypothalamic neurones is mediated by ATP-sensitive K⁺ channels. *Pflugers Arch* **415**: 479-483

Babenko AP & Bryan J (2003) Sur domains that associate with and gate KATP pores define a novel gatekeeper. *J Biol Chem* **278**: 41577-41580

Babenko AP & Bryan J (2002) SUR-dependent modulation of KATP channels by an N-terminal KIR6.2 peptide. Defining intersubunit gating interactions. *J Biol Chem* **277**: 43997-44004

Babenko AP & Bryan J (2001) A conserved inhibitory and differential stimulatory action of nucleotides on K(IR)6.0/SUR complexes is essential for excitation-metabolism coupling by K(ATP) channels. *J Biol Chem* **276**: 49083-49092

Babenko AP, Gonzalez G, Aguilar-Bryan L, & Bryan J (1999a) Sulfonylurea receptors set the maximal open probability, ATP sensitivity and plasma membrane density of KATP channels. *FEBS Lett* **445**: 131-136

Babenko AP, Gonzalez G, & Bryan J (1999b) The N-terminus of KIR6.2 limits spontaneous bursting and modulates the ATP-inhibition of KATP channels. *Biochem Biophys Res Commun* **255**: 231-238

Babenko AP, Gonzalez G, & Bryan J (1999c) The tolbutamide site of SUR1 and a mechanism for its functional coupling to K(ATP) channel closure. *FEBS Lett* **459**: 367-376

Babenko AP, Gonzalez G, & Bryan J (1999d) Two regions of sulfonyleurea receptor specify the spontaneous bursting and ATP inhibition of KATP channel isoforms. *J Biol Chem* **274**: 11587-11592

Baukrowitz T, Schulte U, Oliver D, Herlitze S, Krauter T, Tucker SJ, Ruppersberg JP, & Fakler B (1998) PIP₂ and PIP as determinants for ATP inhibition of KATP channels. *Science* **282**: 1141-1144

Baukrowitz T, Tucker SJ, Schulte U, Benndorf K, Ruppersberg JP, & Fakler B (1999) Inward rectification in KATP channels: a pH switch in the pore. *EMBO J* **18**: 847-853

Beech DJ, Zhang H, Nakao K, & Bolton TB (1993) K channel activation by nucleotide diphosphates and its inhibition by glibenclamide in vascular smooth muscle cells. *Br J Pharmacol* **110**: 573-582

Beguín P, Nagashima K, Nishimura M, Gonoï T, & Seino S (1999) PKA-mediated phosphorylation of the human K(ATP) channel: separate roles of Kir6.2 and SUR1 subunit phosphorylation. *EMBO J* **18**: 4722-4732

Bonev AD & Nelson MT (1993) Muscarinic inhibition of ATP-sensitive K⁺ channels by protein kinase C in urinary bladder smooth muscle. *Am J Physiol* **265**: C1723-8

Booij PP, Roberts MR, Vogelzang SA, Kraayenhof R, & De Boer AH (1999) 14-3-3 proteins double the number of outward-rectifying K⁺ channels available for activation in tomato cells. *Plant J* **20**: 673-683

Bryan J, Vila-Carriles WH, Zhao G, Babenko AP, & Aguilar-Bryan L (2004) Toward linking structure with function in ATP-sensitive K⁺ channels. *Diabetes* **53**: S104-S112

Catterall WA, Goldin AL, & Waxman SG (2005a) International Union of Pharmacology. XLVII. Nomenclature and structure-function relationships of voltage-gated sodium channels. *Pharmacol Rev* **57**: 397-409

Catterall WA, Perez-Reyes E, Snutch TP, & Striessnig J (2005b) International Union of Pharmacology. XLVIII. Nomenclature and structure-function relationships of voltage-gated calcium channels. *Pharmacol Rev* **57**: 411-425

Chan HC, Wu WL, So SC, Chung YW, Tsang LL, Wang XF, Yan YC, Luk SC, Siu SS, Tsui SK, Fung KP, Lee CY, & Waye MM (2000) Modulation of the Ca²⁺-activated Cl⁻ channel by 14-3-3epsilon. *Biochem Biophys Res Commun* **270**: 581-587

Chan KW, Zhang H, & Logothetis DE (2003) N-terminal transmembrane domain of the SUR controls trafficking and gating of Kir6 channel subunits. *EMBO J* **22**: 3833-3843

Chaudhri M, Scarabel M, & Aitken A (2003) Mammalian and yeast 14-3-3 isoforms form distinct patterns of dimers in vivo. *Biochem Biophys Res Commun* **300**: 679-685

Choe H, Sackin H, & Palmer LG (2000) Permeation properties of inward-rectifier potassium channels and their molecular determinants. *J Gen Physiol* **115**: 391-404

Choe H, Zhou H, Palmer LG, & Sackin H (1997) A conserved cytoplasmic region of ROMK modulates pH sensitivity, conductance, and gating. *Am J Physiol* **273**: F516-29

Chutkow WA, Pu J, Wheeler MT, Wada T, Makielski JC, Burant CF, & McNally EM (2002) Episodic coronary artery vasospasm and hypertension develop in the absence of Sur2 K(ATP) channels. *J Clin Invest* **110**: 203-208

Chutkow WA, Samuel V, Hansen PA, Pu J, Valdivia CR, Makielski JC, & Burant CF (2001) Disruption of Sur2-containing K(ATP) channels enhances insulin-stimulated glucose uptake in skeletal muscle. *Proc Natl Acad Sci U S A* **98**: 11760-11764

Chutkow WA, Simon MC, Le Beau MM, & Burant CF (1996) Cloning, tissue expression, and chromosomal localization of SUR2, the putative drug-binding subunit of cardiac, skeletal muscle, and vascular KATP channels. *Diabetes* **45**: 1439-1445

Clement JP, 4th, Kunjilwar K, Gonzalez G, Schwanstecher M, Panten U, Aguilar-Bryan L, & Bryan J (1997) Association and stoichiometry of K(ATP) channel subunits. *Neuron* **18**: 827-838

Conti LR, Radeke CM, Shyng SL, & Vandenberg CA (2001) Transmembrane topology of the sulfonylurea receptor SUR1. *J Biol Chem* **276**: 41270-41278

Conti LR, Radeke CM, & Vandenberg CA (2002) Membrane targeting of ATP-sensitive potassium channel. Effects of glycosylation on surface expression. *J Biol Chem* **277**: 25416-25422

Cook DL & Hales CN (1984) Intracellular ATP directly blocks K⁺ channels in pancreatic B-cells. *Nature* **311**: 271-273

Coronado R, Rosenberg RL, & Miller C (1980) Ionic selectivity, saturation, and block in a K⁺-selective channel from sarcoplasmic reticulum. *J Gen Physiol* **76**: 425-446

Crane A & Aguilar-Bryan L (2004) Assembly, maturation, and turnover of K(ATP) channel subunits. *J Biol Chem* **279**: 9080-9090

Croker B, Crozat K, Berger M, Xia Y, Sovath S, Schaffer L, Eleftherianos I, Imler JL, & Beutler B (2007) ATP-sensitive potassium channels mediate survival during infection in mammals and insects. *Nat Genet* **39**: 1453-1460

Cui N, Kang Y, He Y, Leung YM, Xie H, Pasyk EA, Gao X, Sheu L, Hansen JB, Wahl P, Tsushima RG, & Gaisano HY (2004) H3 domain of syntaxin 1A inhibits KATP channels by its actions on the sulfonylurea receptor 1 nucleotide-binding folds-1 and -2. *J Biol Chem* **279**: 53259-53265

Cui Y, GIBLIN JP, Clapp LH, & Tinker A (2001) A mechanism for ATP-sensitive potassium channel diversity: Functional coassembly of two pore-forming subunits. *Proc Natl Acad Sci U S A* **98**: 729-734

Cui Y, Wang W, & Fan Z (2002) Cytoplasmic vestibule of the weak inward rectifier Kir6.2 potassium channel. *J Biol Chem* **277**: 10523-10530

Cukras CA, Jeliaskova I, & Nichols CG (2002a) The role of NH₂-terminal positive charges in the activity of inward rectifier KATP channels. *J Gen Physiol* **120**: 437-446

Cukras CA, Jeliaskova I, & Nichols CG (2002b) Structural and functional determinants of conserved lipid interaction domains of inward rectifying Kir6.2 channels. *J Gen Physiol* **119**: 581-591

Czirjak G, Vuity D, & Enyedi P (2008) Phosphorylation-dependent binding of 14-3-3 proteins controls TRESK regulation. *J Biol Chem* **283**: 15672-15680

Dabrowski M, Tarasov A, & Ashcroft FM (2004) Mapping the architecture of the ATP-binding site of the KATP channel subunit Kir6.2. *J Physiol* **557**: 347-354

Daut J, Maier-Rudolph W, von Beckerath N, Mehrke G, Gunther K, & Goedel-Meinen L (1990) Hypoxic dilation of coronary arteries is mediated by ATP-sensitive potassium channels. *Science* **247**: 1341-1344

Diviani D, Abuin L, Cotecchia S, & Pansier L (2004) Anchoring of both PKA and 14-3-3 inhibits the Rho-GEF activity of the AKAP-Lbc signaling complex. *EMBO J* **23**: 2811-2820

Dougherty MK & Morrison DK (2004) Unlocking the code of 14-3-3. *J Cell Sci* **117**: 1875-1884

Doyle DA, Morais Cabral J, Pfuetzner RA, Kuo A, Gulbis JM, Cohen SL, Chait BT, & MacKinnon R (1998) The structure of the potassium channel: molecular basis of K⁺ conduction and selectivity. *Science* **280**: 69-77

Drain P, Geng X, & Li L (2004) Concerted gating mechanism underlying KATP channel inhibition by ATP. *Biophys J* **86**: 2101-2112

Dunne MJ & Petersen OH (1986) Intracellular ADP activates K⁺ channels that are inhibited by ATP in an insulin-secreting cell line. *FEBS Lett* **208**: 59-62

Eliasson L, Ma X, Renstrom E, Barg S, Berggren PO, Galvanovskis J, Gromada J, Jing X, Lundquist I, Salehi A, Sewing S, & Rorsman P (2003) SUR1 regulates PKA-independent cAMP-induced granule priming in mouse pancreatic B-cells. *J Gen Physiol* **121**: 181-197

Enkvetchakul D & Nichols CG (2003) Gating mechanism of KATP channels: function fits form. *J Gen Physiol* **122**: 471-480

Fakler B, Brandle U, Bond C, Glowatzki E, Konig C, Adelman JP, Zenner HP, & Ruppersberg JP (1994) A structural determinant of differential sensitivity of cloned inward rectifier K⁺ channels to intracellular spermine. *FEBS Lett* **356**: 199-203

Fan Z & Makielski JC (1999) Phosphoinositides decrease ATP sensitivity of the cardiac ATP-sensitive K(+) channel. A molecular probe for the mechanism of ATP-sensitive inhibition. *J Gen Physiol* **114**: 251-269

Fan Z & Makielski JC (1997) Anionic phospholipids activate ATP-sensitive potassium channels. *J Biol Chem* **272**: 5388-5395

Felsch H, Lange U, Hambrock A, Loffler-Walz C, Russ U, Carroll W, Gopalakrishnan M & Quast U (2004) Interaction of a novel dihydropyridine K⁺ channel opener, A-312110, with recombinant sulphonylurea receptors and KATP channels: comparison with the cyanoguanidine P1075. *Br J Pharmacol* **141**: 1098-1105

Findlay I (1987) The effects of magnesium upon adenosine triphosphate-sensitive potassium channels in a rat insulin-secreting cell line. *J Physiol* **391**: 611-629

Flagg TP, Kurata HT, Masia R, Caputa G, Magnuson MA, Lefer DJ, Coetzee WA, & Nichols CG (2008) Differential structure of atrial and ventricular KATP: atrial KATP channels require SUR1. *Circ Res* **103**: 1458-1465

Garlid KD, Paucek P, Yarov-Yarovoy V, Murray HN, Darbenzio RB, D'Alonzo AJ, Lodge NJ, Smith MA, & Grover GJ (1997) Cardioprotective effect of diazoxide and its interaction with mitochondrial ATP-sensitive K⁺ channels. Possible mechanism of cardioprotection. *Circ Res* **81**: 1072-1082

Giblin JP, Leaney JL, & Tinker A (1999) The molecular assembly of ATP-sensitive potassium channels. Determinants on the pore forming subunit. *J Biol Chem* **274**: 22652-22659

Goldin AL (2001) Resurgence of sodium channel research. *Annu Rev Physiol* **63**: 871-894

Goldstein SA, Bayliss DA, Kim D, Lesage F, Plant LD, & Rajan S (2005) International Union of Pharmacology. LV. Nomenclature and molecular relationships of two-P potassium channels. *Pharmacol Rev* **57**: 527-540

Goldstein SA, Bockenhauer D, O'Kelly I, & Zilberberg N (2001) Potassium leak channels and the KCNK family of two-P-domain subunits. *Nat Rev Neurosci* **2**: 175-184

Gribble FM, Tucker SJ, & Ashcroft FM (1997a) The essential role of the Walker A motifs of SUR1 in K-ATP channel activation by Mg-ADP and diazoxide. *EMBO J* **16**: 1145-1152

Gribble FM, Tucker SJ, & Ashcroft FM (1997b) The interaction of nucleotides with the tolbutamide block of cloned ATP-sensitive K⁺ channel currents expressed in *Xenopus* oocytes: a reinterpretation. *J Physiol* **504 (Pt 1)**: 35-45

Gribble FM, Tucker SJ, Haug T, & Ashcroft FM (1998a) MgATP activates the beta cell KATP channel by interaction with its SUR1 subunit. *Proc Natl Acad Sci U S A* **95**: 7185-7190

- Gribble FM, Tucker SJ, Seino S, & Ashcroft FM (1998b) Tissue specificity of sulfonylureas: studies on cloned cardiac and beta-cell K(ATP) channels. *Diabetes* **47**: 1412-1418
- Gromada J, Ma X, Hoy M, Bokvist K, Salehi A, Berggren PO, & Rorsman P (2004) ATP-sensitive K⁺ channel-dependent regulation of glucagon release and electrical activity by glucose in wild-type and SUR1^{-/-} mouse alpha-cells. *Diabetes* **53 Suppl 3**: S181-9
- Gross GJ & Auchampach JA (1992) Blockade of ATP-sensitive potassium channels prevents myocardial preconditioning in dogs. *Circ Res* **70**: 223-233
- Gutman GA, Chandy KG, Grissmer S, Lazdunski M, McKinnon D, Pardo LA, Robertson GA, Rudy B, Sanguinetti MC, Stuhmer W, & Wang X (2005) International Union of Pharmacology. LIII. Nomenclature and molecular relationships of voltage-gated potassium channels. *Pharmacol Rev* **57**: 473-508
- Haider S, Tarasov AI, Craig TJ, Sansom MS, & Ashcroft FM (2007) Identification of the PIP₂-binding site on Kir6.2 by molecular modelling and functional analysis. *EMBO J* **26**: 3749-3759
- Hambrock A, Loffler-Walz C, Russ U, Lange U, & Quast U (2001) Characterization of a mutant sulfonylurea receptor SUR2B with high affinity for sulfonylureas and openers: differences in the coupling to Kir6.x subtypes. *Mol Pharmacol* **60**: 190-199
- Hamill OP, Marty A, Neher E, Sakmann B, & Sigworth FJ (1981) Improved patch-clamp techniques for high-resolution current recording from cells and cell-free membrane patches. *Pflugers Arch* **391**: 85-100
- Hayabuchi Y, Davies NW, & Standen NB (2001) Angiotensin II inhibits rat arterial KATP channels by inhibiting steady-state protein kinase A activity and activating protein kinase C. *J Physiol* **530**: 193-205

Heusser K, Yuan H, Neagoe I, Tarasov AI, Ashcroft FM, & Schwappach B (2006) Scavenging of 14-3-3 proteins reveals their involvement in the cell-surface transport of ATP-sensitive K⁺ channels. *J Cell Sci* **119**: 4353-4363

Hille B (2001) *Ion channels of excitable membranes*. Sinauer Associates: Sunderland, Mass.

Ho K, Nichols CG, Lederer WJ, Lytton J, Vassilev PM, Kanazirska MV, & Hebert SC (1993) Cloning and expression of an inwardly rectifying ATP-regulated potassium channel. *Nature* **362**: 31-38

Hopkins WF, Fatherazi S, Peter-Riesch B, Corkey BE, & Cook DL (1992) Two sites for adenine-nucleotide regulation of ATP-sensitive potassium channels in mouse pancreatic beta-cells and HIT cells. *J Membr Biol* **129**: 287-295

Horie M, Irisawa H, & Noma A (1987) Voltage-dependent magnesium block of adenosine-triphosphate-sensitive potassium channel in guinea-pig ventricular cells. *J Physiol* **387**: 251-272

Hu K, Duan D, Li GR, & Nattel S (1996) Protein kinase C activates ATP-sensitive K⁺ current in human and rabbit ventricular myocytes. *Circ Res* **78**: 492-498

Hu K, Li GR, & Nattel S (1999) Adenosine-induced activation of ATP-sensitive K⁺ channels in excised membrane patches is mediated by PKC. *Am J Physiol* **276**: H488-95

Imamura Y, Tomoike H, Narishige T, Takahashi T, Kasuya H, & Takeshita A (1992) Glibenclamide decreases basal coronary blood flow in anesthetized dogs. *Am J Physiol* **263**: H399-404

Inagaki N, Gono T, Clement JP, 4th, Namba N, Inazawa J, Gonzalez G, Aguilar-Bryan L, Seino S, & Bryan J (1995b) Reconstitution of IKATP: an inward rectifier subunit plus the sulfonylurea receptor. *Science* **270**: 1166-1170

Inagaki N, Gono T, Clement JP, Wang CZ, Aguilar-Bryan L, Bryan J, & Seino S (1996) A family of sulfonylurea receptors determines the pharmacological properties of ATP-sensitive K⁺ channels. *Neuron* **16**: 1011-1017

Inagaki N, Gono T, & Seino S (1997) Subunit stoichiometry of the pancreatic beta-cell ATP-sensitive K⁺ channel. *FEBS Lett* **409**: 232-236

Inagaki N, Tsuura Y, Namba N, Masuda K, Gono T, Horie M, Seino Y, Mizuta M, & Seino S (1995a) Cloning and functional characterization of a novel ATP-sensitive potassium channel ubiquitously expressed in rat tissues, including pancreatic islets, pituitary, skeletal muscle, and heart. *J Biol Chem* **270**: 5691-5694

Isomoto S, Kondo C, Yamada M, Matsumoto S, Higashiguchi O, Horio Y, Matsuzawa Y, & Kurachi Y (1996) A novel sulfonylurea receptor forms with BIR (Kir6.2) a smooth muscle type ATP-sensitive K⁺ channel. *J Biol Chem* **271**: 24321-24324

Jiang Y, Lee A, Chen J, Cadene M, Chait BT, & MacKinnon R (2002a) Crystal structure and mechanism of a calcium-gated potassium channel. *Nature* **417**: 515-522

Jiang Y, Lee A, Chen J, Cadene M, Chait BT, & MacKinnon R (2002b) The open pore conformation of potassium channels. *Nature* **417**: 523-526

Jiang Y, Lee A, Chen J, Ruta V, Cadene M, Chait BT, & MacKinnon R (2003) X-ray structure of a voltage-dependent K⁺ channel. *Nature* **423**: 33-41

Jones PA, Tucker SJ, & Ashcroft FM (2001) Multiple sites of interaction between the intracellular domains of an inwardly rectifying potassium channel, Kir6.2. *FEBS Lett* **508**: 85-89

Kagan A, Melman YF, Krumerman A, & McDonald TV (2002) 14-3-3 amplifies and prolongs adrenergic stimulation of HERG K⁺ channel activity. *EMBO J* **21**: 1889-1898

Kakkar R, Ye B, Stoller DA, Smelley M, Shi NQ, Galles K, Hadhazy M, Makielski JC, & McNally EM (2006) Spontaneous coronary vasospasm in KATP mutant mice arises from a smooth muscle-extrinsic process. *Circ Res* **98**: 682-689

Kane GC, Lam CF, O'Coilain F, Hodgson DM, Reyes S, Liu XK, Miki T, Seino S, Katusic ZS, & Terzic A (2006) Gene knockout of the KCNJ8-encoded Kir6.1 K(ATP) channel imparts fatal susceptibility to endotoxemia. *FASEB J* **20**: 2271-2280

Kang G, Leech CA, Chepurny OG, Coetzee WA, & Holz GG (2008) Role of the cAMP sensor Epac as a determinant of KATP channel ATP sensitivity in human pancreatic beta-cells and rat INS-1 cells. *J Physiol* **586**: 1307-1319

Kang Y, Leung YM, Manning-Fox JE, Xia F, Xie H, Sheu L, Tsushima RG, Light PE, & Gaisano HY (2004) Syntaxin-1A inhibits cardiac KATP channels by its actions on nucleotide binding folds 1 and 2 of sulfonylurea receptor 2A. *J Biol Chem* **279**: 47125-47131

Kleppisch T & Nelson MT (1995) Adenosine activates ATP-sensitive potassium channels in arterial myocytes via A2 receptors and cAMP-dependent protein kinase. *Proc Natl Acad Sci U S A* **92**: 12441-12445

Kondo C, Repunte VP, Satoh E, Yamada M, Horio Y, Matsuzawa Y, Pott L, & Kurachi Y (1998) Chimeras of Kir6.1 and Kir6.2 reveal structural elements involved in spontaneous opening and unitary conductance of the ATP-sensitive K⁺ channels. *Receptors Channels* **6**: 129-140

Kono Y, Horie M, Takano M, Otani H, Xie LH, Akao M, Tsuji K, & Sasayama S (2000) The properties of the Kir6.1-6.2 tandem channel co-expressed with SUR2A. *Pflugers Arch* **440**: 692-698

Koster JC, Sha Q, & Nichols CG (1999a) Sulfonylurea and K(+) -channel opener sensitivity of K(ATP) channels. Functional coupling of Kir6.2 and SUR1 subunits. *J Gen Physiol* **114**: 203-213

- Koster JC, Sha Q, Shyng S, & Nichols CG (1999b) ATP inhibition of KATP channels: control of nucleotide sensitivity by the N-terminal domain of the Kir6.2 subunit. *J Physiol* **155**: 19-30
- Kovalev H, Quayle JM, Kamishima T, & Lodwick D (2004) Molecular analysis of the subtype-selective inhibition of cloned KATP channels by PNU-37883A. *Br J Pharmacol* **141**: 867-873
- Kozlowski RZ & Ashford ML (1990) ATP-sensitive K(+)-channel run-down is Mg²⁺ dependent. *Proc R Soc Lond B Biol Sci* **240**: 397-410
- Kubo M, Quayle JM, & Standen NB (1997) Angiotensin II inhibition of ATP-sensitive K⁺ currents in rat arterial smooth muscle cells through protein kinase C. *J Physiol* **503 (Pt 3)**: 489-496
- Kubo Y, Reuveny E, Slesinger PA, Jan YN, & Jan LY (1993) Primary structure and functional expression of a rat G-protein-coupled muscarinic potassium channel. *Nature* **364**: 802-806
- Kuo A, Gulbis JM, Antcliff JF, Rahman T, Lowe ED, Zimmer J, Cuthbertson J, Ashcroft FM, Ezaki T, & Doyle DA (2003) Crystal structure of the potassium channel KirBac1.1 in the closed state. *Science* **300**: 1922-1926
- Li Y, Wu Y, & Zhou Y (2006) Modulation of inactivation properties of CaV2.2 channels by 14-3-3 proteins. *Neuron* **51**: 755-771
- Liew CC, Hwang DM, Fung YW, Laurensen C, Cukerman E, Tsui S, & Lee CY (1994) A catalogue of genes in the cardiovascular system as identified by expressed sequence tags. *Proc Natl Acad Sci U S A* **91**: 10645-10649
- Light PE, Allen BG, Walsh MP, & French RJ (1995) Regulation of adenosine triphosphate-sensitive potassium channels from rabbit ventricular myocytes by protein kinase C and type 2A protein phosphatase. *Biochemistry* **34**: 7252-7257

Light PE, Bladen C, Winkfein RJ, Walsh MP, & French RJ (2000) Molecular basis of protein kinase C-induced activation of ATP-sensitive potassium channels. *Proc Natl Acad Sci U S A* **97**: 9058-9063

Light PE, Sabir AA, Allen BG, Walsh MP, & French RJ (1996) Protein kinase C-induced changes in the stoichiometry of ATP binding activate cardiac ATP-sensitive K⁺ channels. A possible mechanistic link to ischemic preconditioning. *Circ Res* **79**: 399-406

Lopatin AN, Makhina EN, & Nichols CG (1994) Potassium channel block by cytoplasmic polyamines as the mechanism of intrinsic rectification. *Nature* **372**: 366-369

Lopatin AN & Nichols CG (1996) [K⁺] dependence of open-channel conductance in cloned inward rectifier potassium channels (IRK1, Kir2.1). *Biophys J* **71**: 682-694

Lu Z & MacKinnon R (1994) Electrostatic tuning of Mg²⁺ affinity in an inward-rectifier K⁺ channel. *Nature* **371**: 243-246

Luhmann HJ & Heinemann U (1992) Hypoxia-induced functional alterations in adult rat neocortex. *J Neurophysiol* **67**: 798-811

Luk SC, Ngai SM, Tsui SK, Chan KK, Fung KP, Lee CY, & Waye MM (1998) Developmental regulation of 14-3-3 epsilon isoform in rat heart. *J Cell Biochem* **68**: 195-199

MacGregor GG, Dong K, Vanoye CG, Tang L, Giebisch G, & Hebert SC (2002) Nucleotides and phospholipids compete for binding to the C terminus of KATP channels. *Proc Natl Acad Sci U S A* **99**: 2726-2731

MacKinnon R (1991) Determination of the subunit stoichiometry of a voltage-activated potassium channel. *Nature* **350**: 232-235

Margail I, Miquet JM, Doble A, Blanchard JC, & Boireau A (1992) KATP channels modulate GABA release in hippocampal slices in the absence of glucose. *Fundam Clin Pharmacol* **6**: 295-300

Masia R, Enkvetchakul D, & Nichols CG (2005) Differential nucleotide regulation of KATP channels by SUR1 and SUR2A. *J Mol Cell Cardiol* **39**: 491-501

Matsuo M, Kimura Y, & Ueda K (2005) KATP channel interaction with adenine nucleotides. *J Mol Cell Cardiol* **38**: 907-916

Matsuo M, Kioka N, Amachi T, & Ueda K (1999) ATP binding properties of the nucleotide-binding folds of SUR1. *J Biol Chem* **274**: 37479-37482

Matsuo M, Tanabe K, Kioka N, Amachi T, & Ueda K (2000) Different binding properties and affinities for ATP and ADP among sulfonylurea receptor subtypes, SUR1, SUR2A, and SUR2B. *J Biol Chem* **275**: 28757-28763

Mauerer UR, Boulpaep EL, & Segal AS (1998) Regulation of an inwardly rectifying ATP-sensitive K⁺ channel in the basolateral membrane of renal proximal tubule. *J Gen Physiol* **111**: 161-180

McDonald TV, Yu Z, Ming Z, Palma E, Meyers MB, Wang KW, Goldstein SA, & Fishman GI (1997) A minK-HERG complex regulates the cardiac potassium current I(Kr). *Nature* **388**: 289-292

McKinsey TA, Zhang CL, & Olson EN (2000) Activation of the myocyte enhancer factor-2 transcription factor by calcium/calmodulin-dependent protein kinase-stimulated binding of 14-3-3 to histone deacetylase 5. *Proc Natl Acad Sci U S A* **97**: 14400-14405

Meisheri KD, Humphrey SJ, Khan SA, Cipkus-Dubray LA, Smith MP, & Jones AW (1993) 4-morpholinecarboximidine-N-1-adamantyl-N'-cyclohexylhydrochloride (U-37883A): pharmacological characterization of a novel antagonist of vascular ATP-sensitive K⁺ channel openers. *J Pharmacol Exp Ther* **266**: 655-665

Miller TR, Davis Taber R, Molinari EJ, Whiteaker KL, Monteggia LM, Scott VES, Brioni JD, Sullivan JP & Gopalakrishnan M (1999) Pharmacological and molecular characterization

of ATP-sensitive K⁺ channels in the TE671 human medulloblastoma cell line. *Eur J Pharmacol* **370**: 179-185

Mikhailov MV, Mikhailova EA, & Ashcroft SJ (2001) Molecular structure of the glibenclamide binding site of the beta-cell K(ATP) channel. *FEBS Lett* **499**: 154-160

Miki T, Iwanaga T, Nagashima K, Ihara Y, & Seino S (2001a) Roles of ATP-sensitive K⁺ channels in cell survival and differentiation in the endocrine pancreas. *Diabetes* **50 Suppl 1**: S48-51

Miki T, Liss B, Minami K, Shiuchi T, Saraya A, Kashima Y, Horiuchi M, Ashcroft F, Minokoshi Y, Roeper J, & Seino S (2001b) ATP-sensitive K⁺ channels in the hypothalamus are essential for the maintenance of glucose homeostasis. *Nat Neurosci* **4**: 507-512

Miki T, Nagashima K, Tashiro F, Kotake K, Yoshitomi H, Tamamoto A, Gono T, Iwanaga T, Miyazaki J, & Seino S (1998a) Defective insulin secretion and enhanced insulin action in KATP channel-deficient mice. *Proc Natl Acad Sci U S A* **95**: 10402-10406

Miki T, Suzuki M, Shibasaki T, Uemura H, Sato T, Yamaguchi K, Koseki H, Iwanaga T, Nakaya H, & Seino S (2002) Mouse model of Prinzmetal angina by disruption of the inward rectifier Kir6.1. *Nat Med* **8**: 466-472

Misler S, Barnett DW, Gillis KD, & Pressel DM (1992) Electrophysiology of stimulus-secretion coupling in human beta-cells. *Diabetes* **41**: 1221-1228

Miyoshi H & Nakaya Y (1995) Calcitonin gene-related peptide activates the K⁺ channels of vascular smooth muscle cells via adenylate cyclase. *Basic Res Cardiol* **90**: 332-336

Moreau C, Jacquet H, Prost AL, D'hahan N, & Vivaudou M (2000) The molecular basis of the specificity of action of K(ATP) channel openers. *EMBO J* **19**: 6644-6651

Murry CE, Jennings RB, & Reimer KA (1986) Preconditioning with ischemia: a delay of lethal cell injury in ischemic myocardium. *Circulation* **74**: 1124-1136

Mutafova-Yambolieva VN & Keef KD (1997) Adenosine-induced hyperpolarization in guinea pig coronary artery involves A2b receptors and KATP channels. *Am J Physiol* **273**: H2687-95

Nestorowicz A, Inagaki N, Gono T, Schoor KP, Wilson BA, Glaser B, Landau H, Stanley CA, Thornton PS, Seino S, & Permutt MA (1997) A nonsense mutation in the inward rectifier potassium channel gene, Kir6.2, is associated with familial hyperinsulinism. *Diabetes* **46**: 1743-1748

Nichols CG, Shyng SL, Nestorowicz A, Glaser B, Clement JP4, Gonzalez G, Aguilar-Bryan L, Permutt MA, & Bryan J (1996) Adenosine diphosphate as an intracellular regulator of insulin secretion. *Science* **272**: 1785-1787

Nishida M & MacKinnon R (2002) Structural basis of inward rectification: cytoplasmic pore of the G protein-gated inward rectifier GIRK1 at 1.8 Å resolution. *Cell* **111**: 957-965

Noma A (1983) ATP-regulated K⁺ channels in cardiac muscle. *Nature* **305**: 147-148

Ogihara T, Isobe T, Ichimura T, Taoka M, Funaki M, Sakoda H, Onishi Y, Inukai K, Anai M, Fukushima Y, Kikuchi M, Yazaki Y, Oka Y, & Asano T (1997) 14-3-3 Protein Binds to Insulin Receptor Substrate-1, One of the Binding Sites of which is in the Phosphotyrosine Binding Domain. *J Biol Chem* **272**: 25267-25274

O'Kelly I, Butler MH, Zilberberg N, & Goldstein SA (2002) Forward transport. 14-3-3 binding overcomes retention in endoplasmic reticulum by dibasic signals. *Cell* **111**: 577-588

Okuyama Y, Yamada M, Kondo C, Satoh E, Isomoto S, Shindo T, Horio Y, Kitakaze M, Hori M, & Kurachi Y (1998) The effects of nucleotides and potassium channel openers

on the SUR2A/Kir6.2 complex K⁺ channel expressed in a mammalian cell line, HEK293T cells. *Pflugers Arch* **435**: 595-603

Olsen RW & Sieghart W (2008) International Union of Pharmacology. LXX. Subtypes of gamma-aminobutyric acid(A) receptors: classification on the basis of subunit composition, pharmacology, and function. Update. *Pharmacol Rev* **60**: 243-260

Oomura Y, Ooyama H, Sugimori M, Nakamura T, & Yamada Y (1974) Glucose inhibition of the glucose-sensitive neurone in the rat lateral hypothalamus. *Nature* **247**: 284-286

Panksepp J & Reilly P (1975) Medial and lateral hypothalamic oxygen consumption as a function of age, starvation and glucose administration in rats. *Brain Res* **94**: 133-140

Park WS, Ko EA, Han J, Kim N, & Earm YE (2005) Endothelin-1 acts via protein kinase C to block KATP channels in rabbit coronary and pulmonary arterial smooth muscle cells. *J Cardiovasc Pharmacol* **45**: 99-108

Pasyk EA, Kang Y, Huang X, Cui N, Sheu L, & Gaisano HY (2004) Syntaxin-1A binds the nucleotide-binding folds of sulphonylurea receptor 1 to regulate the KATP channel. *J Biol Chem* **279**: 4234-4240

Price MP, Snyder PM, & Welsh MJ (1996) Cloning and expression of a novel human brain Na⁺ channel. *J Biol Chem* **271**: 7879-7882

Proks P, Capener CE, Jones P, & Ashcroft FM (2001) Mutations within the P-loop of Kir6.2 modulate the intraburst kinetics of the ATP-sensitive potassium channel. *J Gen Physiol* **118**: 341-353

Purves GI, Kamishima T, Davies LM, Quayle JM, & Dart C (2009) Exchange protein activated by cAMP (Epac) mediates cAMP-dependent but protein kinase A-insensitive modulation of vascular ATP-sensitive potassium channels. *J Physiol* **587**: 3639-3650

Quayle JM, Bonev AD, Brayden JE, & Nelson MT (1994) Calcitonin gene-related peptide activated ATP-sensitive K⁺ currents in rabbit arterial smooth muscle via protein kinase A. *J Physiol* **475**: 9-13

Quayle JM, Nelson MT, & Standen NB (1997) ATP-sensitive and inwardly rectifying potassium channels in smooth muscle. *Physiol Rev* **77**: 1165-1232

Quinn KV, Giblin JP, & Tinker A (2004) Multisite phosphorylation mechanism for protein kinase A activation of the smooth muscle ATP-sensitive K⁺ channel. *Circ Res* **94**: 1359-1366

Raab-Graham KF, Cirilo LJ, Boettcher AA, Radeke CM, & Vandenberg CA (1999) Membrane topology of the amino-terminal region of the sulfonylurea receptor. *J Biol Chem* **274**: 29122-29129

Rainbow RD, James M, Hudman D, Al Johi M, Singh H, Watson PJ, Ashmole I, Davies NW, Lodwick D, & Norman RI (2004) Proximal C-terminal domain of sulphonylurea receptor 2A interacts with pore-forming Kir6 subunits in KATP channels. *Biochem J* **379**: 173-181

Rajan S, Preisig-Muller R, Wischmeyer E, Nehring R, Hanley PJ, Renigunta V, Musset B, Schlichthorl G, Derst C, Karschin A, & Daut J (2002) Interaction with 14-3-3 proteins promotes functional expression of the potassium channels TASK-1 and TASK-3. *J Physiol* **545**: 13-26

Reimann F, Ryder TJ, Tucker SJ, & Ashcroft FM (1999) The role of lysine 185 in the kir6.2 subunit of the ATP-sensitive channel in channel inhibition by ATP. *J Physiol* **520**: 661-669

Repunte VP, Nakamura H, Fujita A, Horio Y, Findlay I, Pott L, & Kurachi Y (1999) Extracellular links in Kir subunits control the unitary conductance of SUR/Kir6.0 ion channels. *EMBO* **18**: 3317-3324

Ribalet B, John SA, & Weiss JN (2003) Molecular basis for Kir6.2 channel inhibition by adenine nucleotides. *Biophys J* **84**: 266-276

Ribalet B, John SA, & Weiss JN (2000) Regulation of cloned ATP-sensitive K channels by phosphorylation, MgADP, and phosphatidylinositol bisphosphate (PIP(2)): a study of channel rundown and reactivation. *J Gen Physiol* **116**: 391-410

Rychlik W & Rhoads RE (1989) A computer program for choosing optimal oligonucleotides for filter hybridization, sequencing and in vitro amplification of DNA. *Nucleic Acids Res* **17**: 8543-8551

Sakura H, Ammala C, Smith PA, Gribble FM, & Ashcroft FM (1995) Cloning and functional expression of the cDNA encoding a novel ATP-sensitive potassium channel subunit expressed in pancreatic beta-cells, brain, heart and skeletal muscle. *FEBS Lett* **377**: 338-344

Sakura H, Wat N, Horton V, Millns H, Turner RC, & Ashcroft FM (1996) Sequence variations in the human Kir6.2 gene, a subunit of the beta-cell ATP-sensitive K-channel: no association with NIDDM in white Caucasian subjects or evidence of abnormal function when expressed in vitro. *Diabetologia* **39**: 1233-1236

Sampson LJ, Davies LM, Barrett-Jolley R, Standen NB, & Dart C (2007) Angiotensin II-activated protein kinase C targets caveolae to inhibit aortic ATP-sensitive potassium channels. *Cardiovasc Res* **76**: 61-70

Schulze D, Krauter T, Fritzenschaft H, Soom M, & Baukrowitz T (2003) Phosphatidylinositol 4,5-bisphosphate (PIP2) modulation of ATP and pH sensitivity in Kir channels. A tale of an active and a silent PIP2 site in the N terminus. *J Biol Chem* **278**: 10500-10505

Schwanstecher C, Meyer U, & Schwanstecher M (2002a) K(IR)6.2 polymorphism predisposes to type 2 diabetes by inducing overactivity of pancreatic beta-cell ATP-sensitive K(+) channels. *Diabetes* **51**: 875-879

Schwanstecher C, Neugebauer B, Schulz M, & Schwanstecher M (2002b) The common single nucleotide polymorphism E23K in K(IR)6.2 sensitizes pancreatic beta-cell ATP-sensitive potassium channels toward activation through nucleoside diphosphates.

Diabetes **51 Suppl 3**: S363-7

Schwanstecher C & Schwanstecher M (2002) Nucleotide sensitivity of pancreatic ATP-sensitive potassium channels and type 2 diabetes. *Diabetes* **51 Suppl 3**: S358-62

Schwappach B, Zerangue N, Jan YN, & Jan LY (2000) Molecular basis for K(ATP) assembly: transmembrane interactions mediate association of a K⁺ channel with an ABC transporter. *Neuron* **26**: 155-167

Seghers V, Nakazaki M, DeMayo F, Aguilar-Bryan L, & Bryan J (2000) Sur1 knockout mice. A model for K(ATP) channel-independent regulation of insulin secretion. *J Biol Chem* **275**: 9270-9277

Seino S & Miki T (2003) Physiological and pathophysiological roles of ATP-sensitive K⁺ channels. *Prog Biophys Mol Biol* **81**: 133-176

Shi Y, Cui N, Shi W, & Jiang C (2008) A short motif in Kir6.1 consisting of four phosphorylation repeats underlies the vascular KATP channel inhibition by protein kinase C. *J Biol Chem* **283**: 2488-2494

Shi Y, Wu Z, Cui N, Shi W, Yang Y, Zhang X, Rojas A, Ha BT, & Jiang C (2007) PKA phosphorylation of SUR2B subunit underscores vascular KATP channel activation by beta-adrenergic receptors. *Am J Physiol Regul Integr Comp Physiol* **293**: R1205-14

Shimomura K, Girard CA, Proks P, Nazim J, Lippiat JD, Cerutti F, Lorini R, Ellard S, Hattersley AT, Barbetti F, & Ashcroft FM (2006) Mutations at the same residue (R50) of Kir6.2 (KCNJ11) that cause neonatal diabetes produce different functional effects.

Diabetes **55**: 1705-1712

Shiota C, Larsson O, Shelton KD, Shiota M, Efanov AM, Hoy M, Lindner J, Kooptiwut S, Juntti-Berggren L, Gromada J, Berggren PO, & Magnuson MA (2002) Sulfonylurea receptor type 1 knock-out mice have intact feeding-stimulated insulin secretion despite marked impairment in their response to glucose. *J Biol Chem* **277**: 37176-37183

Shuck ME, Piser TM, Bock JH, Slightom JL, Lee KS, & Bienkowski MJ (1997) Cloning and characterization of two K⁺ inward rectifier (Kir) 1.1 potassium channel homologs from human kidney (Kir1.2 and Kir1.3). *J Biol Chem* **272**: 586-593

Shyng SL, Cukras CA, Harwood J, & Nichols CG (2000) Structural determinants of PIP(2) regulation of inward rectifier K(ATP) channels. *J Gen Physiol* **116**: 599-608

Shyng SL & Nichols CG (1998) Membrane phospholipid control of nucleotide sensitivity of KATP channels. *Science* **282**: 1138-1141

Shyng S, Ferrigni T, & Nichols CG (1997a) Control of rectification and gating of cloned KATP channels by the Kir6.2 subunit. *J Gen Physiol* **110**: 141-153

Shyng S, Ferrigni T, & Nichols CG (1997b) Regulation of KATP channel activity by diazoxide and MgADP. Distinct functions of the two nucleotide binding folds of the sulfonylurea receptor. *J Gen Physiol* **110**: 643-654

Shyng S & Nichols CG (1997) Octameric stoichiometry of the KATP channel complex. *J Gen Physiol* **110**: 655-664

Spruce AE, Standen NB, & Stanfield PR (1985) Voltage-dependent ATP-sensitive potassium channels of skeletal muscle membrane. *Nature* **316**: 736-738

Standen NB, Quayle JM, Davies NW, Brayden JE, Huang Y, & Nelson MT (1989) Hyperpolarizing vasodilators activate ATP-sensitive K⁺ channels in arterial smooth muscle. *Science* **245**: 177-180

- Stanfield PR, Davies NW, Shelton PA, Sutcliffe MJ, Khan IA, Brammar WJ, & Conley EC (1994) A single aspartate residue is involved in both intrinsic gating and blockage by Mg²⁺ of the inward rectifier, IRK1. *J Physiol* **478 (Pt 1)**: 1-6
- Sturgess NC, Ashford ML, Cook DL, & Hales CN (1985) The sulphonylurea receptor may be an ATP-sensitive potassium channel. *Lancet* **2**: 474-475
- Surah-Narwal S, Xu SZ, McHugh D, McDonald RL, Hough E, Cheong A, Partridge C, Sivaprasadarao A, & Beech DJ (1999) Block of human aorta Kir6.1 by the vascular KATP channel inhibitor U37883A. *Br J Pharmacol* **128**: 667-672
- Suzuki M, Morita T, & Iwamoto T (2006) Diversity of Cl⁻ channels. *Cell Mol Life Sci* **63**: 12-24
- Taborsky GJ, Jr, Ahren B, & Havel PJ (1998) Autonomic mediation of glucagon secretion during hypoglycemia: implications for impaired alpha-cell responses in type 1 diabetes. *Diabetes* **47**: 995-1005
- Taglialatela M, Ficker E, Wible BA, & Brown AM (1995) C-terminus determinants for Mg²⁺ and polyamine block of the inward rectifier K⁺ channel IRK1. *EMBO J* **14**: 5532-5541
- Tamaro P & Ashcroft F (2007) The Kir6.2-F333I mutation differentially modulates KATP channels composed of SUR1 or SUR2 subunits. *J Physiol* **581**: 1259-1269
- Tanaka T, Ogiwara A, Uchiyama I, Takagi T, Yazaki Y, & Nakamura Y (1996) Construction of a normalized directionally cloned cDNA library from adult heart and analysis of 3040 clones by partial sequencing. *Genomics* **35**: 231-235
- Thomas PM, Cote GJ, Wohlk N, Haddad B, Mathew PM, Rabl W, Aguilar-Bryan L, Gagel RF, & Bryan J (1995) Mutations in the sulfonylurea receptor gene in familial persistent hyperinsulinemic hypoglycemia of infancy. *Science* **268**: 426-429

Thomas P, Ye Y, & Lightner E (1996) Mutation of the pancreatic islet inward rectifier Kir6.2 also leads to familial persistent hyperinsulinemic hypoglycemia of infancy. *Hum Mol Genet* **5**: 1809-1812

Thorneloe KS, Maruyama Y, Malcolm AT, Light PE, Walsh MP, & Cole WC (2002) Protein kinase C modulation of recombinant ATP-sensitive K(+) channels composed of Kir6.1 and/or Kir6.2 expressed with SUR2B. *J Physiol* **541**: 65-80

Trapp S, Haider S, Jones P, Sansom MS, & Ashcroft FM (2003) Identification of residues contributing to the ATP binding site of Kir6.2. *EMBO J* **22**: 2903-2912

Trapp S, Proks P, Tucker SJ, & Ashcroft FM (1998) Molecular analysis of ATP-sensitive K channel gating and implications for channel inhibition by ATP. *J Gen Physiol* **112**: 333-349

Trube G & Hescheler J (1984) Inward-rectifying channels in isolated patches of the heart cell membrane: ATP-dependence and comparison with cell-attached patches. *Pflugers Arch* **401**: 178-184

Tucker SJ, Gribble FM, Proks P, Trapp S, Ryder TJ, Haug T, Reimann F, & Ashcroft FM (1998) Molecular determinants of KATP channel inhibition by ATP. *EMBO J* **17**: 3290-3296

Tucker SJ, Gribble FM, Zhao C, Trapp S, & Ashcroft FM (1997) Truncation of Kir6.2 produces ATP-sensitive K⁺ channels in the absence of the sulphonylurea receptor. *Nature* **387**: 179-183

Tusnady GE, Bakos E, Varadi A, & Sarkadi B (1997) Membrane topology distinguishes a subfamily of the ATP-binding cassette (ABC) transporters. *FEBS Lett* **402**: 1-3

Ueda K, Inagaki N, & Seino S (1997) MgADP antagonism to Mg²⁺-independent ATP binding of the sulphonylurea receptor SUR1. *J Biol Chem* **272**: 22983-22986

- Ueda K, Komine J, Matsuo M, Seino S, & Amachi T (1999) Cooperative binding of ATP and MgADP in the sulfonylurea receptor is modulated by glibenclamide. *Proc Natl Acad Sci U S A* **96**: 1268-1272
- Vandenberg CA (1987) Inward rectification of a potassium channel in cardiac ventricular cells depends on internal magnesium ions. *Proc Natl Acad Sci U S A* **84**: 2560-2564
- Wang B, Yang H, Liu YC, Jelinek T, Zhang L, Ruoslahti E, & Fu H (1999) Isolation of high-affinity peptide antagonists of 14-3-3 proteins by phage display. *Biochemistry* **38**: 12499-12504
- Wang C, Wang K, Wang W, Cui Y, & Fan Z (2002) Compromised ATP binding as a mechanism of phosphoinositide modulation of ATP-sensitive K⁺ channels. *FEBS Lett* **532**: 177-182
- Wang XL, Lu T, Cao S, Shah VH, & Lee HC (2006) Inhibition of ATP binding to the carboxyl terminus of Kir6.2 by epoxyeicosatrienoic acids. *Biochim Biophys Acta* **1761**: 1041-1049
- Wei AD, Gutman GA, Aldrich R, Chandy KG, Grissmer S, & Wulff H (2005) International Union of Pharmacology. LII. Nomenclature and molecular relationships of calcium-activated potassium channels. *Pharmacol Rev* **57**: 463-472
- Wellman GC, Barrett-Jolley R, Koppel H, Everitt D, & Quayle JM (1999) Inhibition of vascular K(ATP) channels by U-37883A: a comparison with cardiac and skeletal muscle. *Br J Pharmacol* **128**: 909-916
- Wible BA, Taglialatela M, Ficker E, & Brown AM (1994) Gating of inwardly rectifying K⁺ channels localized to a single negatively charged residue. *Nature* **371**: 246-249

- Wickman KD, Iniguez-Lluhl JA, Davenport PA, Taussig R, Krapivinsky GB, Linder ME, Gilman AG, & Clapham DE (1994) Recombinant G-protein beta gamma-subunits activate the muscarinic-gated atrial potassium channel. *Nature* **368**: 255-257
- Xie LH, Takano M, Kakei M, Okamura M, & Noma A (1999) Wortmannin, an inhibitor of phosphatidylinositol kinases, blocks the MgATP-dependent recovery of Kir6.2/SUR2A channels. *J Physiol* **514 (Pt 3)**: 655-665
- Xu H, Cui N, Yang Z, Wu J, Giwa LR, Abdulkadir L, Sharma P, & Jiang C (2001) Direct activation of cloned K(atp) channels by intracellular acidosis. *J Biol Chem* **276**: 12898-12902
- Xu H, Yang Z, Cui N, Chanchevalap S, Valesky WW, & Jiang C (2000) A single residue contributes to the difference between Kir4.1 and Kir1.1 channels in pH sensitivity, rectification and single channel conductance. *J Physiol* **528 Pt 2**: 267-277
- Yamada M, Isomoto S, Matsumoto S, Kondo C, Shindo T, Horio Y, & Kurachi Y (1997) Sulphonylurea receptor 2B and Kir6.1 form a sulphonylurea-sensitive but ATP-insensitive K⁺ channel. *J Physiol* **499**: 715-720
- Yamada S, Kane GC, Behfar A, Liu XK, Dyer RB, Faustino RS, Miki T, Seino S, & Terzic A (2006) Protection conferred by myocardial ATP-sensitive K⁺ channels in pressure overload-induced congestive heart failure revealed in KCNJ11 Kir6.2-null mutant. *J Physiol* **577**: 1053-1065
- Yang J, Jan YN, & Jan LY (1995) Control of rectification and permeation by residues in two distinct domains in an inward rectifier K⁺ channel. *Neuron* **14**: 1047-1054
- Yang X, Lee WH, Sobott F, Papagrorgiou E, Robinson CV, Grossmann JG, Sundstrom M, Doyle DA, & Elkins JM (2006) Structural basis for protein-protein interactions in the 14-3-3 protein family. *Proc Natl Acad Sci U S A* **103**: 17237-17242

- Yang Z, Xu H, Cui N, Qu Z, Chanchevalap S, Shen W, & Jiang C (2000) Biophysical and molecular mechanisms underlying the modulation of heteromeric Kir4.1-Kir5.1 channels by CO₂ and pH. *J Gen Physiol* **116**: 33-45
- Yuan H, Michelsen K, & Schwappach B (2003) 14-3-3 dimers probe the assembly status of multimeric membrane proteins. *Curr Biol* **13**: 638-646
- Zerangue N, Schwappach B, Jan YN, & Jan LY (1999) A new ER trafficking signal regulates the subunit stoichiometry of plasma membrane K(ATP) channels. *Neuron* **22**: 537-548
- Zhang C, Miki T, Shibasaki T, Yokokura M, Saraya A, & Seino S (2006) Identification and characterization of a novel member of the ATP-sensitive K⁺ channel subunit family, Kir6.3, in zebrafish. *Physiol Genomics* **24**: 290-297
- Zhang YY, Robertson JL, Gray DA, & Palmer LG (2004) Carboxy-terminal determinants of conductance in inward-rectifier K channels. *J Gen Physiol* **124**: 729-739
- Zhou Y, Reddy S, Murrey H, Fei H, & Levitan IB (2003) Monomeric 14-3-3 protein is sufficient to modulate the activity of the Drosophila slowpoke calcium-dependent potassium channel. *J Biol Chem* **278**: 10073-10080
- Zhou Y, Schopperle WM, Murrey H, Jaramillo A, Dagan D, Griffith LC, & Levitan IB (1999) A dynamically regulated 14-3-3, Slob, and Slowpoke potassium channel complex in Drosophila presynaptic nerve terminals. *Neuron* **22**: 809-818
- Zuzarte M, Heusser K, Renigunta V, Schlichthorl G, Rinne S, Wischmeyer E, Daut J, Schwappach B, & Preisig-Muller R (2009) Intracellular traffic of the K⁺ channels TASK-1 and TASK-3: role of N- and C-terminal sorting signals and interaction with 14-3-3 proteins. *J Physiol* **587**: 929-952